NOTICE

AVIS

The quality of this microform is heavily dependent upon the quality of the original thesis submitted for microfilming. Every effort has been made to ensure the highest quality of reproduction possible.

If pages are missing, contact the university which granted the degree.

Some pages may have indistinct print especially if the original pages were typed with a poor typewriter ribbon or if the university sent us an inferior photocopy.

Reproduction in full or in part of this microform is governed by the Canadian Copyright Act, R.S.C. 1970, c. C-30, and subsequent amendments.

La qualité de cette microforme dépend grandement de la qualité de la thèse soumise au microfilmage. Nous avons tout fait pour assurer une qualité supérieure de reproduction.

S'il manque des pages, veuillez communiquer avec l'université qui a conféré le grade.

La qualité d'impression de certaines pages peut laisser à désirer, surtout si les pages originales ont été dactylographiées à l'aide d'un ruban usé ou si l'université nous a fait parvenir une photocopie de qualité inférieure.

La reproduction, même partielle, de cette microforme est soumise à la Loi canadienne sur le droit d'auteur, SRC 1970, c. C-30, et ses amendements subséquents.

Canadä

UNIVERSITY OF ALBERTA

GEOCHEMISTRY OF THE VAULT EPITHERMAL Au MINERALIZATION AND ITS ENVIRONS, OKANAGAN FALLS , SOUTHERN BRITISH COLUMBIA

by   Ⓒ

YONGLIANG XIONG

A thesis submitted to the Faculty of Graduate Studies and Research in partial fulfillment of the requirements for the degree of Master of Science

in

GEOLOGY

DEPARTMENT OF GEOLOGY
EDMONTON, ALBERTA
SPRING, 1993

Your file   Votre référence

Our file   Notre référence

The author has granted an irrevocable non-exclusive licence allowing the National Library of Canada to reproduce, loan, distribute or sell copies of his/her thesis by any means and in any form or format, making this thesis available to interested persons.

L'auteur a accordé une licence irrévocable et non exclusive permettant à la Bibliothèque nationale du Canada de reproduire, prêter, distribuer ou vendre des copies de sa thèse de quelque manière et sous quelque forme que ce soit pour mettre des exemplaires de cette thèse à la disposition des personnes intéressées.

The author retains ownership of the copyright in his/her thesis. Neither the thesis nor substantial extracts from it may be printed or otherwise reproduced without his/her permission.

L'auteur conserve la propriété du droit d'auteur qui protège sa thèse. Ni la thèse ni des extraits substantiels de celle-ci ne doivent être imprimés ou autrement reproduits sans son autorisation.

ISBN   0-315-82148-5

Canada

UNIVERSITY OF ALBERTA
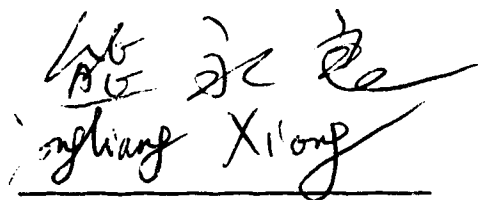
RELEASE FORM

NAME OF AUTHOR: YONGLIANG XIONG

TITLE OF THESIS: **GEOCHEMISTRY OF THE VAULT EPITHERMAL MINERALIZATION AND ITS ENVIRONS, OKANAGAN FALLS, SOUTHERN BRITISH COLUMBIA**

DEGREE: MASTER OF SCIENCE

YEAR THIS DEGREE GRANTED: SPRING, 1993
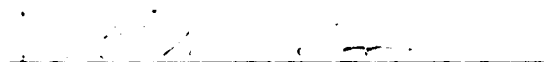
Department of Geology
China University of Geosciences
BEIJING, 100083
CHINA

April 16, 1993
Date
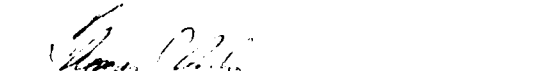
UNIVERSITY OF ALBERTA

FACULTY OF GRADUATE STUDIES AND RESEARCH

The undersigned certify that they have read, and recommend to the Faculty of Graduate Studies and Research for acceptance, a thesis entitled GEOCHEMISTRY OF THE VAULT EPITHERMAL GOLD MINERALIZATION AND ITS ENVIRONS, OKANAGAN FALLS, SOUTHERN BRITISH COLUMBIA submitted by YONGLIANG XIONG in partial fulfillment of the requirements for the degree of MASTER OF SCIENCE in GEOLOGY.

Bruce E. Nesbitt, supervisor

Karlis Muehlenbachs, committee member

Thomas Chacko, committee member

Douglas R. Schmitt, committee member

March 15, 1993
Date

ii

ABSTRACT

The Okanagan Falls area, located about 16 kilometers south of Penticton in southern British Columbia, hosts a number of occurrences of epithermal-type ore deposits. The Vault property is one of them. The primary objective of this study is to characterize mineralization on the Vault property using petrographic, fluid inclusion and stable isotope studies. The second objective is to evaluate stable isotope results in conjunction with fluid inclusion as an exploration tool for epithermal systems.

Located 3.0 km northwest of Okanagan Falls, southern B.C., the Vault property is an epithermal deposit of adularia-sericite type. Homogenization temperatures (Th) of primary inclusions range from 143 to 347°C. Pseudosecondary inclusions have a Th range from 120 to 186°C with an average Th of 146±15°C. Secondary inclusions have Th ranging from 93 to 144°C with an average of 119±17°C. According to Th from well preserved early stage inclusions, the deposit is likely to be formed around 270°C. Final ice melting temperatures (Tm$_{ice}$) of primary and pseudosecondary inclusions range from -2.0 to 0°C (corresponding to a salinity range of 0 to ~3.4 eq.wt.% NaCl). Two peak Tm$_{ice}$ are observed. One is at -0.1 to 0.0°C, and another one is at -0.8 to -0.6°C. Fluid inclusions in calcites with bladed textures have relatively lower Tm$_{ice}$ (-0.9±0.5°C), whereas fluid inclusions in minerals of non-bladed textures have relatively higher Tm$_{ice}$ (-0.1± 0.1°C). The relatively lower Tm$_{ice}$ for calcites with bladed texture were due to a boiling effect.

Stable isotope analyses of quartz samples from main stage quartz-calcite veins yield $\delta^{18}O$ values ranging from -0.2 to +6.6‰ (SMOW). $\delta^{18}O$ values of calcites range from -3.6 to +13.7‰. Calculated $\delta^{18}O_{fluid}$ values suggest that three types of fluids were involved in the formation of mineralization on the property. For the main stage of quartz-calcite veins, $\delta^{18}O_{fluid}$ values indicate two fluid reservoirs. One has $\delta^{18}O_{fluid}$ values ranging from +1.3 to +7.7‰. The other has $\delta^{18}O_{fluid}$ values ranging from -7.2 to

-4.0‰. For later calcite veins and fluorite-calcite veins, fluids with $\delta^{18}O$ values (~ -15 to ~ -10‰) close to those of pristine meteoric waters (-15 to -13‰) were involved. Carbon isotope data demonstrate that carbon reservoirs are strongly controlled by host rocks. For the carbonates hosted by mudstone, their $\delta^{13}C$ values may suggest an organic carbon signature. In contrast, the carbonate samples hosted by trachyte have an igneous carbon signature.

The $\delta^{18}O$ data of volcanic rocks on a regional scale in the Okanagan Falls area indicate that there are two ^{18}O depletion zones with mineralization and two ^{18}O depletion zones without mineralization. The ^{18}O depletion zones with mineralization are characterized by moderate depletions in ^{18}O (the lowest $\delta^{18}O_{whole-rock}$ values > -2‰) and moderate calculated water to rock ratios (1.5 to 2.5), whereas ^{18}O depletion zones without mineralization are characterized by extreme depletions in ^{18}O (the lowest $\delta^{18}O_{whole-rock}$ values < -6‰) and very high calculated water to rock ratio (up to 7.5).

ACKNOWLEDGEMENTS

TABLE OF CONTENTS

LIST OF TABLES

LIST OF FIGURES

LIST OF PLATES

I. INTRODUCTION

The Okanagan Falls area, located about 16 kilometers south of Penticton in southern British Columbia, hosts a number of occurrences of epithermal-type ore deposits. There are two epithermal Au-Ag deposits in the area, e.g., the Vault property, three kilometers northwest of the town of Okanagan Falls, and Dusty Mac, one and half kilometers east of Okanagan Falls (Fig. 1). From 1975 to 1977, 93,000 tonnes of ores (Minister of Mines and Petroleum Resources, B.C., 1975, 1976), with 19,483 oz of gold, and 339,283 oz of silver, were produced from the Dusty Mac deposit (Schroeter et al., 1989, p.35). The Vault property with an estimated gold reserve of 200,000 oz (Schroeter et al., 1989) is currently held by Inco Exploration and Technical Service Inc. and Seven Mile High Resources Inc.

Previous studies on epithermal deposits in this region focused on the Dusty Mac property. Church (1973, 1983) proposed a simple geological model for the Dusty Mac deposit. Firstly, dilations in major shears were developed. Then the dilations were filled with quartz accompanied by gold and silver. Tempelman-Kluit (1984) suggested a meteoric water circulation model for the deposit in which meteoric water, flowing through a detachment fault system, leached the metals from the country rock, and then deposited hydrothermal minerals when the fluid discharged. In 1986, Zhang conducted a stable isotope and fluid inclusion study on the Dusty Mac. He concluded that the Dusty Mac deposit was characterized by meteoric fluid with characteristics of low salinities, and relatively low homogenization temperatures (161°C - 303°C), which are typical of epithermal deposits (Zhang, 1986; Zhang et al., 1989)

Compared with other epithermal mining districts, the epithermal deposits in this area are not well known. This is partly due to the relatively small size of the presently discovered deposits in this area, in comparison with the giants of this style such as the Republic in neighboring Washington State (Muessig, 1967; Ivosevic, 1984) and the Creed

1
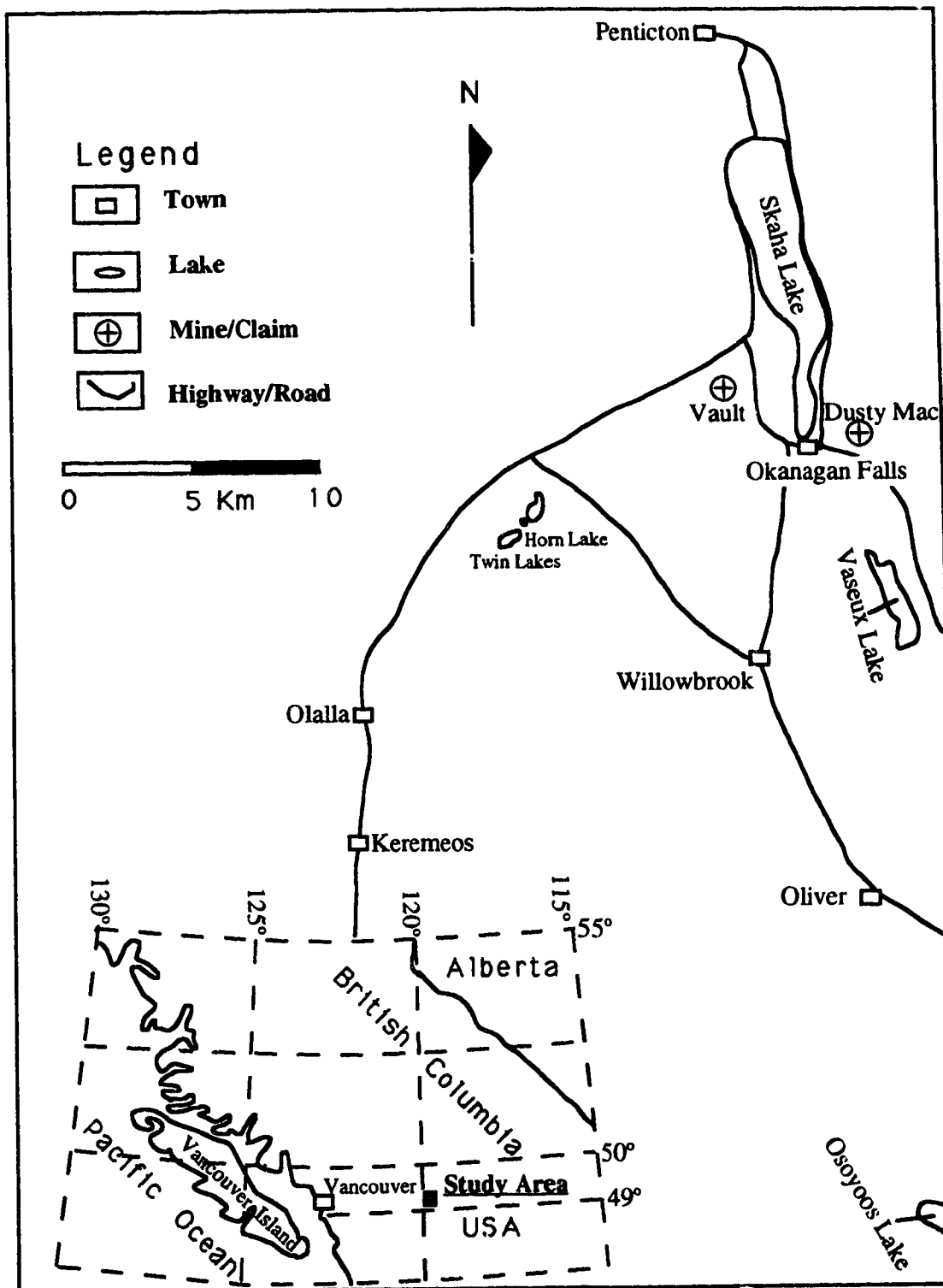
Fig. 1   Index map for the Okanagan Falls area

2

district in Colorado (Barton *et al.*, 1977), and partly due to the poor understanding of the epithermal systems in this region. This latter aspect points to a need for more detailed study on the epithermal systems in this area. In addition, epithermal systems in this area differ from those in Colorado such as Creede mine (Barton *et al.*, 1977) in that they are situated on the hangingwall side of a detachment fault, and consequently, the role of detachment faulting in formation of epithermal deposits needs to be explored.

The primary objective of this study is to characterize mineralization on the Vault property using petrographic, fluid inclusion and stable isotope studies. The second objective is to evaluate stable isotope results in conjunction with fluid inclusion as an exploration tool for epithermal systems. The third objective is to study calcite samples on a regional scale (both vein calcite and amygdaloid calcite in volcanic rocks) to determine the sources of carbon in hydrothermal fluids in this region.

II. REGIONAL GEOLOGY

Tectonic Setting

In order to understand the geological history and the generation of epithermal mineralization in the study area, it is helpful to summarize briefly the tectonic development of the Canadian Cordillera and to review the regional geology of the district.

The Canadian Cordillera is composed of five tectonic belts. From east to west, these are the Rocky Mountain, Omineca Crystalline, Intermontane, Coast Plutonic, and Insular Belts (Monger *et al.*, 1982; Gabrielse and Yorath, 1989) (Fig. 2). Generally speaking, the Rocky Mountain Belt is composed of autochthonous terrane (North American Terrane, i.e., ancestral North America). Autochthonous and pericratonic terranes comprise the Omineca Crystalline Belt. Other belts are composed of allochthonous terranes (Gabriels and Yorath, 1989). According to Gabriels and Yorath (1989), the present architecture of the Canadian Cordillera is the product of an evolution that spans an interval of about 1.7 Ga., and the tectonic history of the Canadian Cordillera could be outlined as follows. Gneissic Precambrian basement rocks mainly occur in the Omineca Belt and the southern part of the Rocky Mountain Belt. In the Middle Proterozoic, clastic and carbonate sequences of miogeoclinal character were developed in a passive margin setting. In the Late Proterozoic, thick, dominantly clastic strata were deposited throughout the full length of the Cordillera. From the Cambrian to Middle Devonian, a miogeocline in a passive margin setting occurred on the margin of ancestral North America. In contrast, in the allochthonous terranes, island arc environments prevailed. In the Late Devonian to Triassic, in ancestral North America, sediments were deposited on marine shelf in a miogeoclinal environment, whereas in allochthonous terranes, plutonism, volcanism and sedimentation took place in island arc environments. The Early Jurassic marked a transition from terrane-specific volcanism, plutonism and sedimentation to the development of overlap assemblages. In the Middle Jurassic, there was an important accretion event resulting in the formation of the Omineca Belt, and at the same time, the beginning of the development of the clastic wedge

4
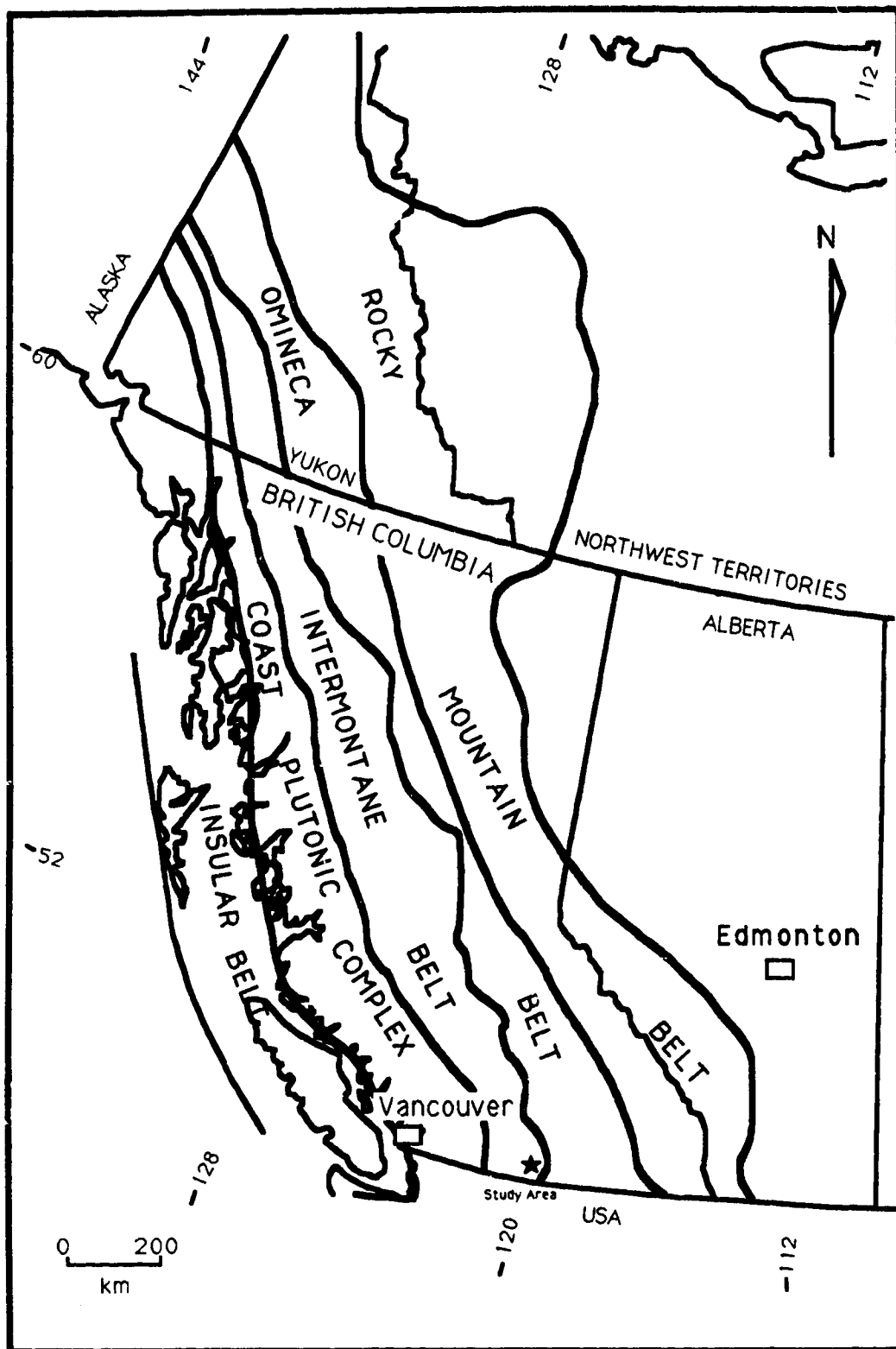
Fig. 2 Tectonic belts of the Canadian Cordillera (based on Monger *et al.*, 1982; Armstrong, 1988)

5

of the Rocky Mountain Belt Belt. By mid-Cretaceous, the Insular Superterrane collided with the Intermontane Superterrane. By the beginning of Late Cretaceous time, the Coast and Omineca belts were well established as uplifted metamorphic and plutonic welts. The latter, for the most part, had undergone renewed uplift, whereas the Coast Belt had just evolved from an island arc into a fully developed plutonic-metamorphic welt. In Late Cretaceous to Paleocene, throughout the Intermontane Belt, block faulting was associated with local plutonism and volcanism. In Eocene, a short-lived (55 to 45 Ma), intense and widespread phase of granitic magmatism and uplift in the Coast and Omineca belts (Armstrong, 1988) postdated the last main episode of contractional deformation and sedimentation east of the Insular Belt. In the Omineca Belt of south-central British Columbia, Eocene uplift was synchronous with volcanism and extension faulting.

Regional Geology

The Okanagan Valley is located in the southernmost part of the Quesnel terrane of the Intermontane Belt (Fig. 3). The regional geology is shown in Fig. 4.

Pre-Tertiary Geology

In the eastern part of the region, "Okanagan Gneisses" are exposed. They consist of massive, biotite granodiorite gneisses, which are Proterozoic to Paleozoic in age (Tempelman-Kluit, 1989). In the southern part of the region, the Carboniferous or older Kobau Group is exposed and composed of amphibolite, greenschist, quartzite, and mica schist (Little, 1961). Only a small portion of Knob Hill Group of Carboniferous or Permian age is exposed in the southeastern part. This group is characterized by massive 'chert' (largely silicified greenstone), greenstone and amphibolite (Tempelman-Kluit, 1989). The Old Tom and Shoemaker Groups of Ordovician to Upper Triassic age exist in the southwestern part. The main components of these groups are massive andesitic greenstone, greenstone breccia, and silicified volcanic rocks. A small portion of the Nicola Group of Upper Triassic/Lower Jurassic age is exposed in the western part of the region. This group mainly consists of greenstone, andesite, latite, and agglomerate. Most of the

6
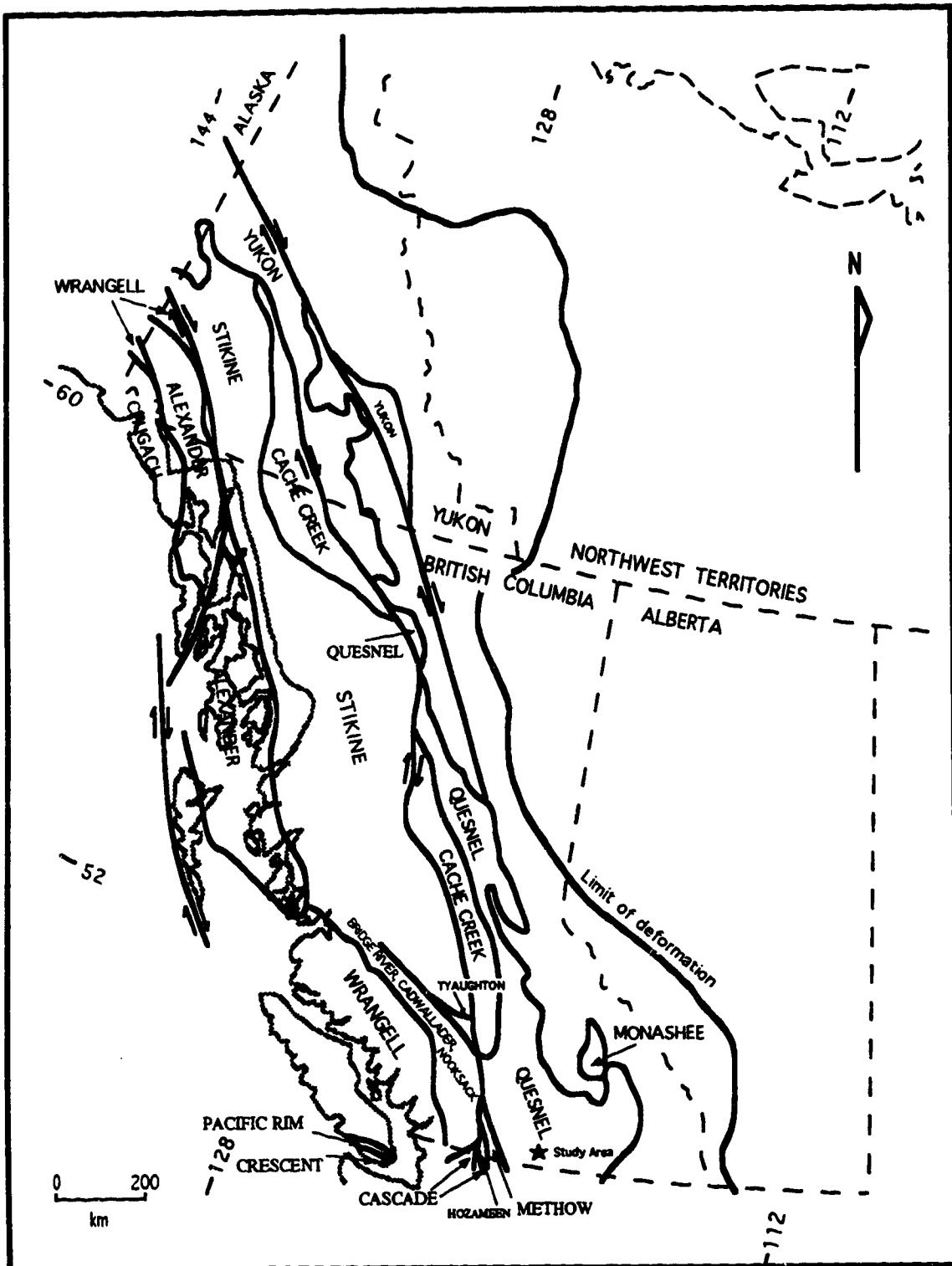
Fig. 3 Terrane map of the Canadian Cordillera (modified from Armstrong, 1988)

7
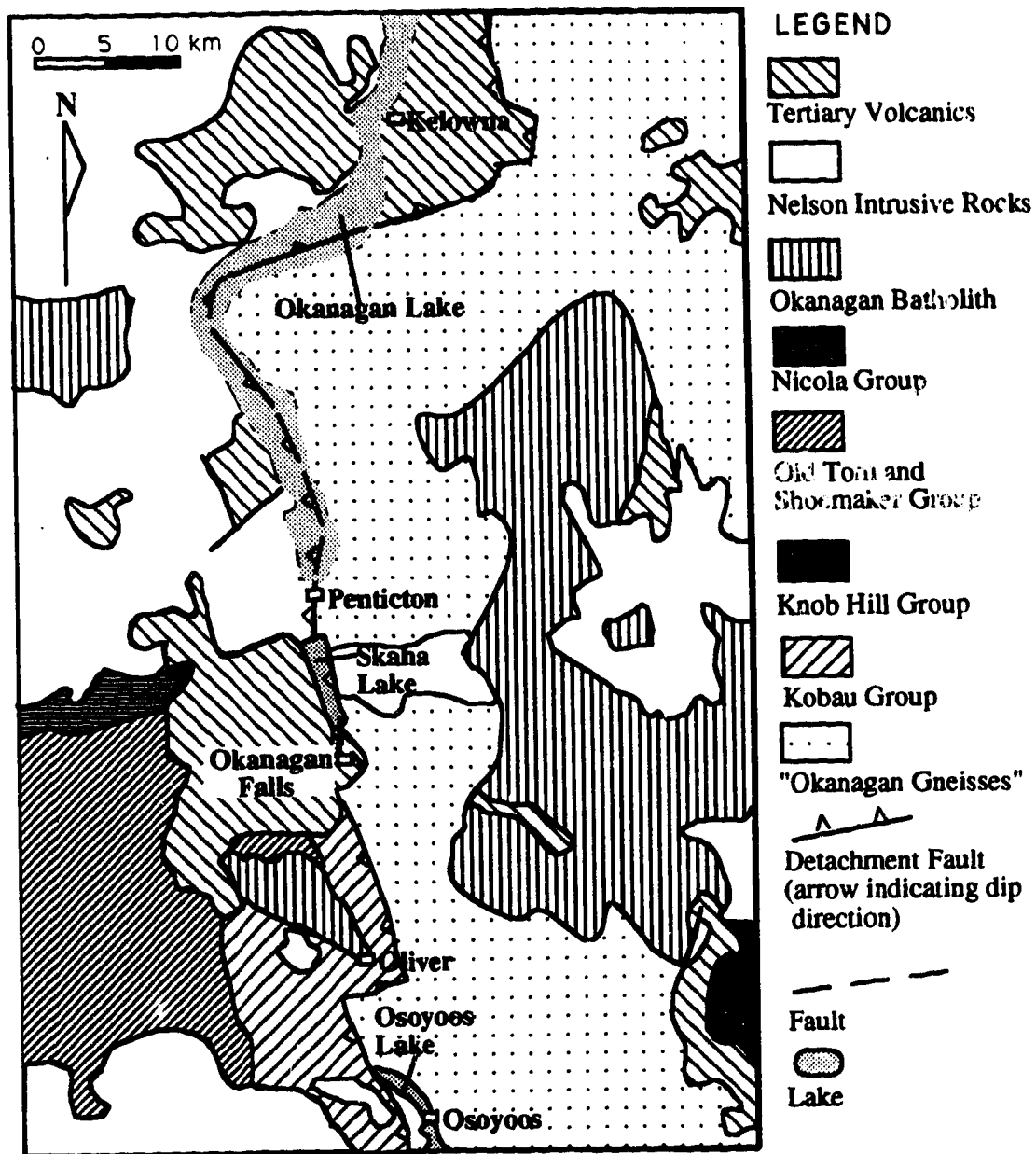
Fig. 4 Simplified regional geological map of the Okanagan Valley area (based on Little, 1961; Church, 1973; Tempelman-Kluit and Parkinson, 1986; Tempelman-Kluit, 1989)

west-central part of the region is occupied by the Nelson Intrusive Rocks, which are
Middle Jurassic in age (Tempelman-Kluit, 1989). The intrusions largely consist of
moderately foliated, hornblende biotite granodiorite, quartz diorite, and granite. In the
northwestern part of the region, a large portion of the Okanagan Batholith is exposed. This
intrusion is mainly composed of unfoliated to weakly foliated biotite granodiorite and
granite, and is Cretaceous-Jurassic in age (Tempelman-Kluit, 1989).

Tertiary Rocks

Subdivisions of Tertiary Rocks: Bostock (1941) made the first
comprehensive geological survey of the area. He divided the Tertiary rocks into a lower
sedimentary unit, the Springbrook Formation, overlain by a succession of lavas, the
Marron Formation, overlain in turn by volcanic rocks and fluvial and lacustrine
sedimentary rocks, the White Lake Formation, and an upper unnamed volcanic and
sedimentary unit. This division of the Tertiary rocks in the White Lake basin has largely
been followed in later studies (Church, 1973; Tempelman-Kluit, 1989) (Figs. 5 and 6).
Church (1973) further divided the Marron Formation into Yellow Lake Member, Kitly
Lake Member, Kearns Creek Member, Nimpit Lake Member, and Park Rill Member. In
addition, he added a new formation, the Skaha Formation, which overlies White Lake
Formation. Church (1983) proposed the Penticton Group which includes the Springbrook
Formation, Marron Formation, Marama Formation, White Lake Formation, and Skaha
Formation. He considered that the Olalla Rhyolite is the youngest rock in Penticton area.
He also tentatively correlated the Tertiary rocks in Okanagan Falls area with those in the
Hat Creek area near Cache Creek, the Terrace Mountain area near Vernon, the Kelowna
area, the Midway area close to the international border in British Columbia, and the
Republic area in Washington State (Fig. 6).

As shown in Fig. 5, the Tertiary rocks are surrounded by pre-Tertiary granitic
intrusions, greenstones and gneisses. The Springbrook Formation unconformably overlies
the pre-Tertiary rocks, and is exposed only in the southwestern part of the Okanagan Falls

9
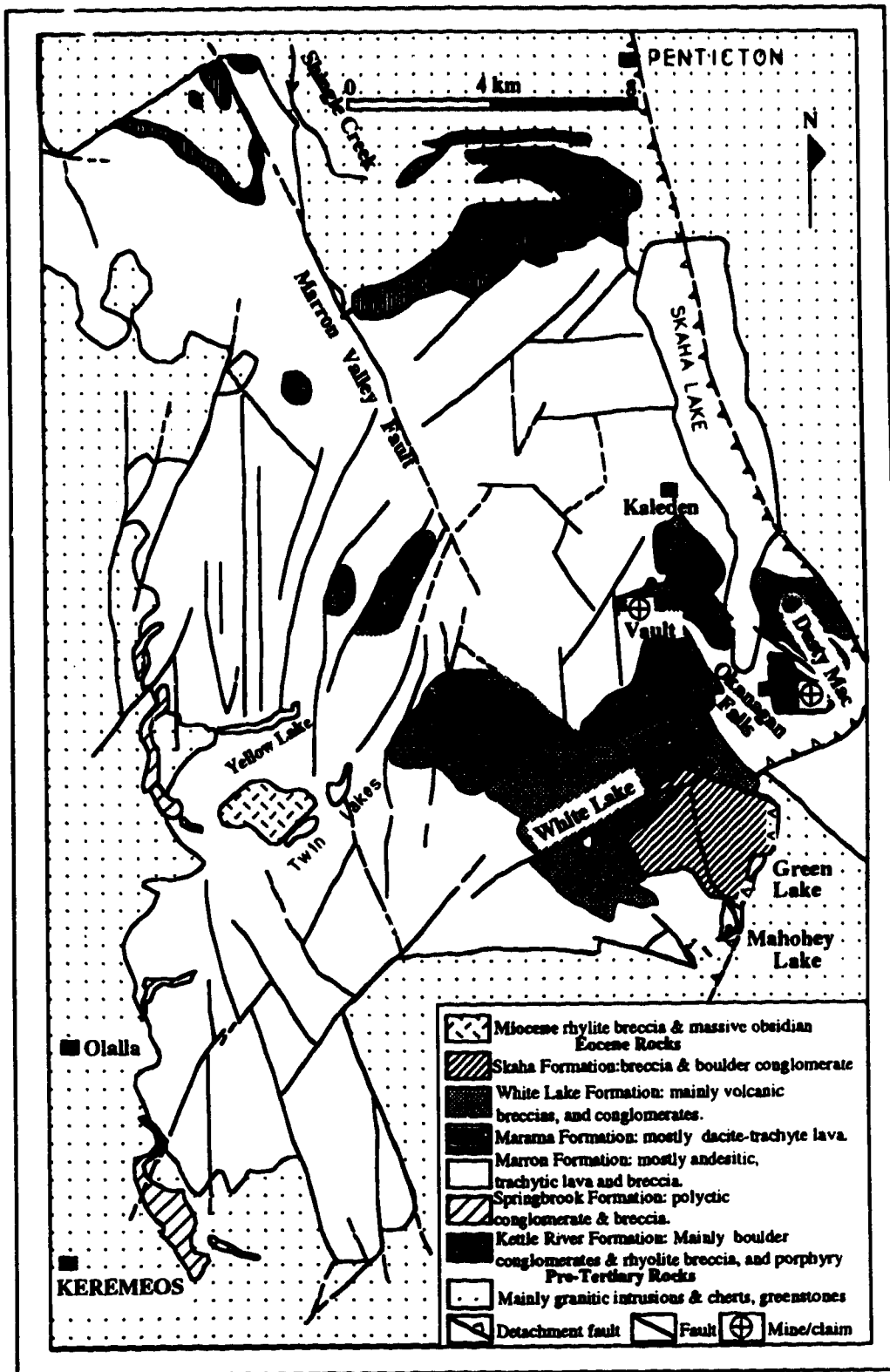
Fig. 5 Geological map of Okanagan Falls area (modified from Church, 1983; detachment fault based on Tempelman-Kluit and Parkinson, 1986, and Tempelman-Kluit, 1989)

10

Hat Creek Kelowna Penticton Midway Republic

Terrace
Mountain

Olalla Rhyolite

Miocene

Eocene

Basalt

Talaetkum
Basalt

Lambly
Creek
Basalt

Carrott
Mountain
Basalt

White
Lake
Formation

Slate Formation

Upper Member

Lower Memeber

White Lake
Formation

?

?

Naswhite
Creek
Formation

Marama
Formation

Marama
Formation

Kimolite Mountain Formation

Upper
Member

Middle
Member

Tom
Thumb
Tuff
Member

Kamloops Group

Finney Beds

Dacite

Rhyolite

Medicine Creek
Formation

Bouleau
Rhyolite

Marron
Formation

Marron Formation

Nimpit Lake
Member

Kitley Lake
Member

Penticton Group

Marron Formation

Park Rill
Member

Nimpit Lake
Member

Kearns Creek
Member

Kitley Lake
Member

Marron Formation

Park Rill
Member

Nimpit lake
Member

Kitley Lake
Member

Yellow lake
Memeber

Sanpoll Volcanics

Hat Creek Coal
Formation

Attenborough
Creek
Formation

Shatford Creek Member

Shatford
Creek
Member

Yellow Lake
Member

Kettle River
Formation

Cold-
water
Beds

Shorts
Creek
Fm

Kettle River
Formation

Kettle River Formation

Springbrook
Formation

Springbrook
Formation

O'Brien
Creek
Formation

Springbrook
Formation

Fig. 6 Correlation of the Tertairy rocks in Penticton with those in adjacent areas (modified from Church, 1983)

area. This formation is composed of polymictic conglomerates and breccias of which 90% of the fragments are from the Old Tom and Shoemaker Group. A Middle Eocene age was tentatively assigned to the Springbrook Formation by Church (1973). The Kettle River Formation, exposed in the north of the map area, is coeval with the Springbrook Formation. This is followed by the Marron Formation which is composed mainly of thick andesite, trachyte, and phonolitic lava flows exposed in a very large portion of the map-area. The Marron Formation is subdivided into five members as outlined in Fig. 6 (but not shown in Fig. 5). This formation having a K-Ar age of 51.6 ± 1.8 Ma (a biotite sample from the Kitley Lake Member) (Church, 1973) also belongs to Middle Eocene. The Marron Formation is unconformably overlain by dacitic domes of the Marama Formation, which is chiefly distributed in the central part of the map-area. Unconformably above the Marama Formation is the White Lake Formation composed of volcanic breccias, lacustrine and fluvial sediments rocks (such as mudstone), which is mainly located in the east-central part of the study area. Most of the clasts in the White Lake Formation sediments are products of erosion of earlier Tertiary volcanic rocks. The White Lake Formation is probably Eocene, but may be Oligocene in age. The Skaha Formation consisting of a landslide complex and fanglomerate beds is exposed in southeastern part of the map-area. The Skaha Formation overlies the White Lake Formation with minor unconformity, and is just slightly younger than the White Lake Formation (Church, 1973, 1983).

Okanagan Valley Detachment Fault

The Okanagan Valley follows a Tertiary, low-angle, west-dipping 8-25° detachment fault, which bounds the west side of a 170 km wide complex (Fig. 4; Fig. 5). This fault has been termed as the Okanagan Valley Detachment Fault (Tempelman-Kluit and Parkinson, 1986; Journeay and Brown, 1986; Carr et al., 1987, 1992; Parrish et al., 1988). This detachment fault, including the Eagle River detachment to the north, has a strike length of over 250 km (Carr and Brown, 1989). The detachment fault has been confirmed by geophysical studies (Cook et al., 1989, 1990). Structure contouring of the

12

fault surface in the Vernon area indicates that the fault is locally an irregular surface (Carr and Brown, 1990a, 1990b). The plastic-brittle Okanagan Valley fault is listric into a subhorizontally layered middle crust (Carr and Brown, 1990a, 1990b).

A detachment fault, as defined by Reynolds and Spencer (1985), is a fault that formed at a low angle, has significant displacement, and is of subregional scale. According to the crustal shear model of Wernicke and Burchfiel (1982), a detachment fault is composed of three elements, i.e., the lower plate, the detachment zone (shear zone), and the upper plate.

The upper plate of the Okanagan detachment fault is composed of various rocks, including Mesozoic granite, Mesozoic and Paleozoic metavolcanic and metasedimentary rocks, the Old Tom and Shoemaker Formations, and Eocene volcanic rocks whose K-Ar ages are between 55-45 Ma near Penticton and between 53-43 Ma near Kelowna (Church, 1973, 1983; Parkinson, 1985). A few of the pre-Eocene rocks (granodiorite and granite) have Eocene K-Ar ages because of Eocene thermal resetting (Tempelman-Kluit and Parkinson, 1986; Medford, 1975). The detachment zone consists of mylonitized ortho- and para-gneisses of middle to upper amphibolite grade, which yield Eocene K-Ar dates ranging from 60 to 40 Ma (Parkinson, 1985). The lower plate is composed of deformed Mesozoic granitic rocks and para-gneiss of uncertain age (Parrish et al., 1988). Intrusive rocks in the deformed lower plate range in age from Early Jurassic to Middle Eocene (Parkinson, 1985). The lower plate was ductilly deformed in the Okanagan Valley fault as late as 50 Ma (Parrish et al., 1988).

Based on regional geochronometry of minerals with different blocking temperatures, Parkinson (1985) invoked a large (10 km) and rapid (1 km/Ma; 1 mm/year) unroofing rate to bring the gneisses east of the fault to near surface temperatures in Eocene time, before the end of the volcanic episode. This unroofing rate is same as that suggested by Journeay and Brown (1986) based on the regional geochronometry of gneissic rocks

13

within the footwall of the fault. This also means that heat produced by detachment faulting would soon be dispersed by rapid unroofing processes.

Regarding the displacement of the fault, Tempelman-Kluit and Parkinson (1986) suggested an offset on the order of about 90 km based on the matching of the lower- and upper-plate rocks for the fault in the Middle Eocene. Bardoux (1985a, 1985b) suggested that minimum displacements on the fault would be on the order of 25 km in Eocene, if the denudation rate is at least as 1.5mm/year. Large displacements in post-Eocene time involving the shear zone can be ruled out due to the observation that dykes considered as feeders to nearby Eocene and Miocene volcanics have been found to cut and locally brecciated the mylonites (Bardoux, 1985a, 1985b).

III. GEOLOGICAL, STABLE ISOTOPE AND FLUID INCLUSION STUDIES ON THE VAULT PROPERTY

(I) Geology of the Vault Property

On the Vault property area, only the White Lake, Marama and Marron Formations are exposed (Fig. 7). The Marron Formation is at the base, and is overlain by the Marama Formation, which in turn is overlain by the White Lake Formation. These rocks are gently folded about northeasterly trending synclinal and anticlinal axes and offset by northwards and northeastward trending faults. Precious metal mineralization is related to an east-west fracture system confined largely to the lower Marama Formation and crossing the north-central part of the claim block (Meyers, 1989).

The section of Marron Formation on the property belongs to the Kitly Lake member described by Church (1973). It consists of purplish brown to grey, fine-grained plagioclase-porphyritic lavas of trachyte to trachyandesite composition. The upper contact of this unit is strongly weathered and may represent an eroded angular unconformity described by Church (1973).

The overlying Marama Formation is subdivided into upper and lower sections (Meyers, 1989). At the base of the lower Marama Formation is a coarse pyroclastic and /or epiclastic unit. Much of this section varies from lapilli to ash tuff, with coarse fragments and massive fine-grained trachyte porphyry flows intercalated with thinly laminated mudstone and sandstone. The upper Marama Formation is a massive, aphanitic dacite flow unit, with alkali feldspar, minor hornblende and biotite. Sheeted dacite feeder dykes of the Marama Formation, averaging about 1 meter in width, intrude the dacite in the central part of the property (Meyers, 1989).

At the top of the Vault property, the White Lake Formation consists of coarse agglomerate and laharic rocks interlayered with andesitic and trachytic flows,

15
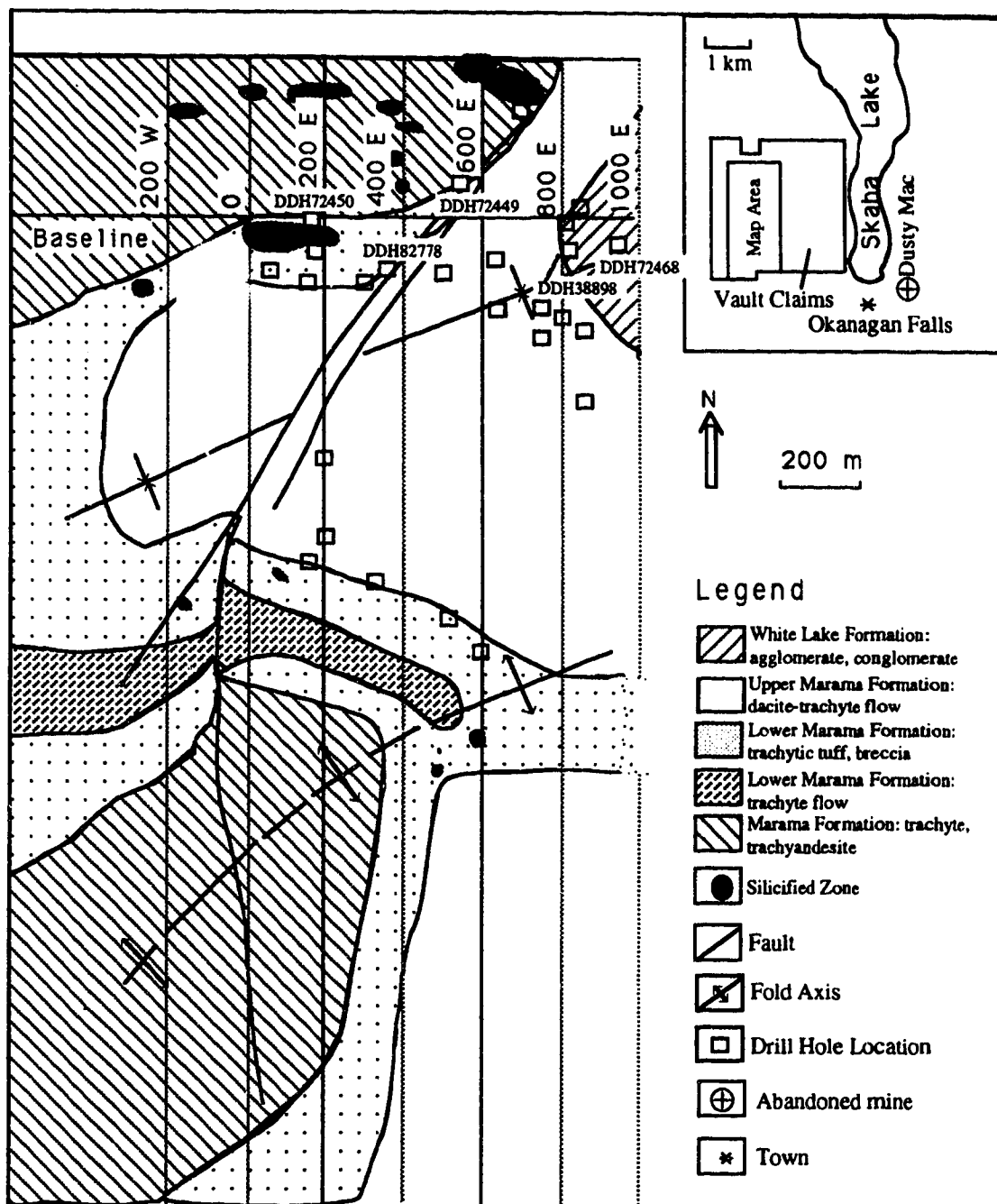
Fig. 7   Geological map on the Vault property (modified from Meyers, 1989)

16

conglomerates and carbonaceous mudstones. Church (1973) defined the unit as being

derived entirely from underlying Eocene rocks, with no pre-Tertiary components.

(II) Hydrothermal Alteration of the Wall Rocks on the Vault property

Numerous studies have been done on hydrothermal alteration of epithermal

deposits. Based on alteration styles of epithermal deposits, Heald *et al* . (1987) classified

epithermal deposits hosted by volcanic rocks into two types: acid-sulfate-type characterized

by the presence of enargite+pyrite±covellite and an argillic assemblage including abundant

hypogene alunite+major amounts of kaolinite, and adularia-sericite-type characterized by

the presence of adularia and sericite in or near the veins and by the absence of the

enargite+pyrite±covellite assemblage and hypogene alunite. Because of the presence of

adularia on the Vault property, the epithermal mineralization on the Vault property has been

considered to be an adularia-sericite-type deposit (Meyers, 1989).

According to Heald *et al.* (1987), sericitic alteration usually borders a silicified zone

near the vein in an adularia-sericite-type deposit. The sericitic zone typically grades into a

potassium metasomatized zone. An argillic zone is sometimes present . However, Heald *et*

al. (1987) also cautioned that in fact, the alteration "pattern" is so variable among the

adularia-sericite-type that generalization is impossible. Because alteration terminology is

often used inconsistently due to such problems as overlap of assemblages, metastability of

certain phases, this paper will follow the definition of alteration terminology of Heald *et al.*

(1987) (Table 1). In their model, the zonation pattern in an adularia-sericite-type deposit is:

silicified zone ⇒ sericitic ⇒ (argillic) ⇒ propylitic (or a potassium metasomatized zone)

with a sericitic cap formed over the orebody.

General Characteristics of the Alteration on the Vault property

On the Vault property, the groundmass volcanics typically have undergone

alteration to hydrothermal minerals such as quartz, adularia, calcite, dolomite, and clays.

Feldspar phenocrysts (plagioclase; sanidine) most commonly alter to calcite, adularia, or

clay; less commonly to clays + opaques, or opaques, or clay + minor chlorite ± quartz; and

17

Table 1 Alteration terminology used in this study (based on Meyer and Hemley, 1967, and Heald *et al*, 1987)

Alteration Terminology	Characteristics of Alteration Terminology	Notes
Silicic	Characterized by introduction of silica	Wall rock silicified; amethyst or chalcedony typically in veins
Sericitic	Consists of a mica-type mineral + quartz +pyrite; with addition of K-fel and/or biotite, alteration grades into possium silicate assemblage	
Sericitic-argillic	Consists of both white mica-type and kaolin-smectite-group minerals	
Argillic	Characterized by kaolin- and smectite-group minerasl; does not typically include mica-type minerals; K-feldspar may be present (metastably) and biotite may be partly recrystallized from chlorite.	Often zoned, with kaolinite nearer veins and montmo-rillonite farther from veins
Advanced argillic	Characterized by minerals representing extreme base leaching (e.g., kaolinite) and sulfate or halogen fixation (e.g., alunite, zunyite). Assemblage: dickite, kaolinite, pyrophyllite; usually sericite, quartz; frequently alunite, pyrite, tourmaline topaz, zynyite, amorphous clays.	
Propylityic	Characterized by chlorite, albite, epidote, charbonate ± pyrite, iron oxides, and minor sericite	Typically a regional alteration

18

rarely to quartz or chlorite + calcite + hematite. Ferromagnesian minerals (pyroxene, hornblende, biotite) most commonly alter to opaques; less commonly to clay or chlorite or chlorite + opaques ± calcite; and rarely to calcite, or chlorite + clay ± limonite. Other hydrothermal minerals seen include apatite (Plate 1), jarosite, sericite. In addition, according to the thin section descriptions of Groeneweg and Hunter's consulting report (1987), clay mineral montorillonite and trace tremolite were observed in their thin section examination.

The prime area of intense silicification and stockwork veining is in an elongate zone parallel to the east-west baseline (Meyers, 1989; Meyers and Hubner, 1991). It was originally traced on surface for 350 meters in the Discovery area and is coincident with geochemical and geophysical anomalies. Drill information indicates that the zone occurs above the Marron/lower Marama contact and the original zone is on the west side of the area currently being explored. Recent exploration has extended the zone of silicification and veining discontinuously for about 900 meters along strike (Meyers, 1989).

Zonation of the Hydrothermal Alteration

Lateral Zonation: In the mineralized areas such as the vein systems in the North trench from 550E to 425E of the property, argillic alteration is generally dominant. In order to determine the lateral variation of mineral assemblages in the argillic alteration zone, systematic samples have been collected. From observations of thin section and X-ray, it seems that even though chlorite and epidote, typical of propylitic alteration, are present in the eastern part of the property (550E), they become unstable and are completely destroyed westwards (from 525E to 425E)(Table 2, and also refer to Property Geological Map). This may mean that the area from 525E to 425E was the centre of hydrothermal system. If the alteration patterns in different drill holes in the depth of 300-450 m are compared, a lateral zonation appears to be present in a pattern of propylitic ⇒ sericitic ⇒ silicic ⇒ argillic, from 950E to 560E, and from 200E to 560E. This lateral zonation pattern is slightly

19
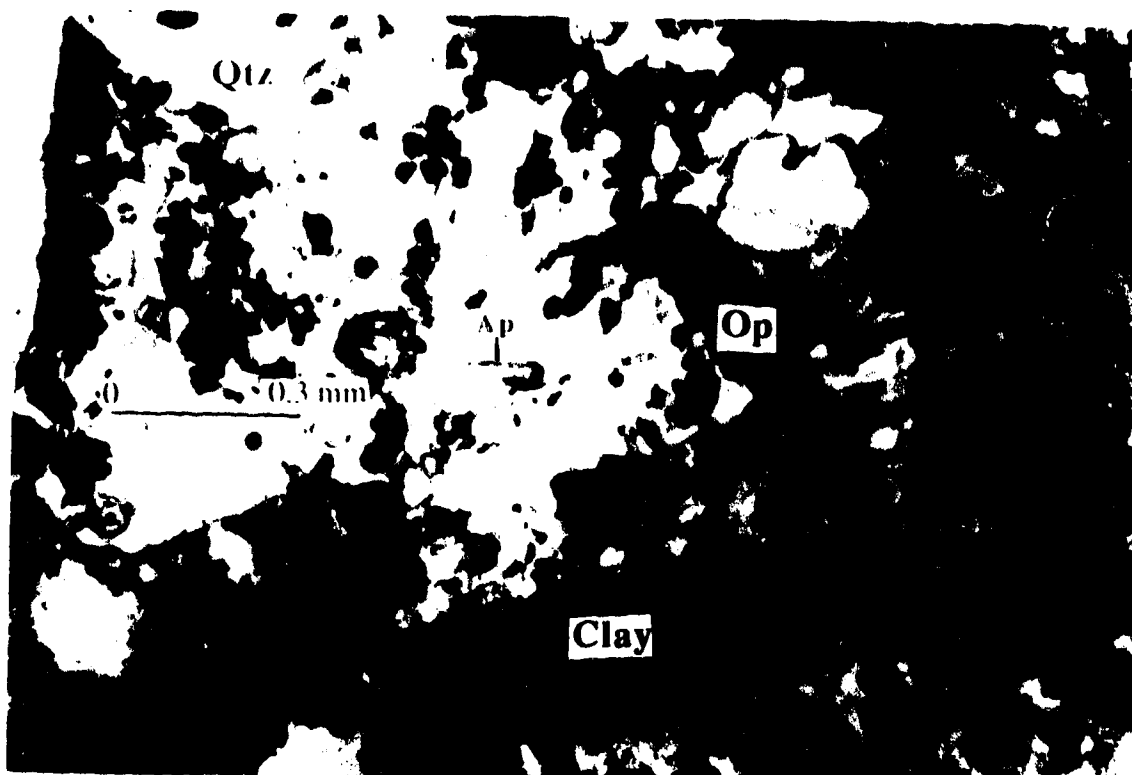
Plate 1 Hydrothermal apatite (AP) in silicic alteration zone in sample X-14. Cross polarized light. ×40. Qtz: quartz, Op: opaque.

Table 2 Mineral assemblage changes in the argillic zone of the North Trench of the Vault property

Drill Hole Line	Mineral Assemblage
550E	clay(ab)+chl(ab)+epi(mo)+alb*+adu* (mo)+hem(mi)+ser(mus*; mi)+vuggy qtz (mi)+jar*(mi)
525E	clay(kaol*)(ab)+adu(ab)+hem(mo)+vuggy qtz(mo) +cal(mi) +apt(tr) +goe*(mi, supergene)
500E	clay(ab)+chl(ab)+hem(ab)+cal+ser(ab)
425E	clay(ab)+adu(ab)+ser(mo)+hem(mi)+apt(mi)+chalcedony (mi)

abbreviation: ab-abundant; mo-moderate; mi-minor; tr-trace;adu-adularia; alb-albite, apt-apatite;cal-calcite; chl-chlorite; epi-epidote; goe-goethite;hem-hematite; jar-jarosite; kaol-kaolinite; mus-muscovite; ser-sericite.
* Identified by X-ray method

different from that proposed by Heald *et al.* (1987) for adularia-sericite type epithermal deposits in which an argillic zone is between a propylitic zone and a sericitic zone.

Vertical Zonation: On the property, the vertical zonation of hydrothermal alteration is more apparent. Alteration samples from different drill holes were collected to determine variations in alteration. At depth, the alteration assemblage is mainly composed of chlorite, epidote, calcite, pyrite, and quartz, typical of propylitic alteration. Near surface, the alteration assemblage typical of argillic alteration consists of clay (kaolinite, determined by X-ray), quartz, calcite, hematite, and chlorite. This argillic alteration was occasionally overprinted by silicic alteration which is mainly composed of quartz, calcite, and pyrite. Vertically, sericitic alteration chiefly occurred between argillic and propylitic alterations. Sericitic alteration is composed of sericite (sometimes muscovite), quartz, calcite, adularia, pyrite, and trace apatite. The results are listed in Table 3. Combined with X-ray identification, the systematic thin section descriptions in Table 3 reveal that from present-day surface to depth, the zonation sequence is from argillic (surface) ⟹ silicic (near surface to 290m) ⟹ argillic-sericitic (13m - 324m) ⟹ sericitic (143m - 415m) ⟹ propylitic (deepest). Silicic alteration is more pronounced in 560E-350E, which is the high grade mineralized area.

Variation of trace element contents with associated hydrothermal alteration implies that Au, Mo, and As were mainly introduced by silicic and sericitic alterations (see Fig. 8A, 8B, and 8C)(assay data from Inco Inc.). Argillic-sericitic and argillic alterations also introduced some As (Fig. 8B). The propylitic alteration introduced some Au and the least As (see Fig. 8A and 8B).

(III) Mineralization at the Vault property

There are two types of ores on the property (Meyers, 1989). One is stockwork ore characterized by disseminated sulfides. Sometimes sulfides congregate as massive sulfides. This type of mineralization is earlier than quartz-vein mineralization as indicated by cross

Table 3 Variation of alterations in selected drill holes on the Vault property

Drill Holes	Depth (meters)	Alteration Assemblage +Alteration Type	Grade (g/T)* Au	Ag	Trace Element (ppm)* As	Ba	Mo
DDH72468 (950E)	415	Sericitic: Ser+Py+Qtz+Chl+Kaol	0.93	1.9	65	44	316
	451	Propylitic: Chl+Py+Cal+Qtz with stock ore	1.37	2.1	15	23	2
DDH38898 (875E)	13.2	Argillic: Clay+Qtz+Lim+Hem+Chl	--	--	--	--	--
	287	Argillic-Sericitic: Clay+Ser+Cal +Hem+Qtz					
	324	Argillic-Sericitic: Clay+Ser+Cal +Qtz+Hem;	0.005	0.2	300	100	17
	375	Sericitic overprinting Silicic: Mus+ Ser+Qtz;	3.335	2.2	0.0	630	22
DDH72449	41	Argillic: Clay+Qtz+Cal	0.002	0.1	609	41	5
	225-226	Silicic: Qtz+Hem+Cal±Py±Apt	1.61	12.05	194	31.5	48
(560E)	269	Sericitic: Ser+Cal+Qtz+Py	0.523	1.8	175	57	36
	290	Silicic: Qtz+Cal	6.27	8.8	26	13	10
	319	Propylitic overprinted by Silicic: Chl+Epi+Qtz+Py+Rut	4.514	2.5	38	1458	
DDH82778	18	Silicic overprinted by Chloritic: Chl+Cal+(Qtz+Cal)+(Clay)	0.001	0.1	623	28	10
(350E)	49	Silicic: Qtz+Cal+Py	0.272	2.6	155	55	34
	53	Silicic: Qtz+Cal+(Chl+Epi)	0.42		380	58	214
	132	Silicic: Py+Qtz	5.81	15	174	22	437
DDH72450	18	Argillic overprinted by Silicic: Clay+Cal+(Qtz+Cal)	0.083	0.5	50	21	2
(200E)	123	Silicic: Qtz+Cal+Hem	0.238	0.88	170	27	11
	143	Sericitic: Ser+Qtz+Py+Apt	0.23	0.1	68	43	2
	150	Sericitic: Ser+Qtz+Adu+Cal	0.48	1.5	127	32	8
	370	Propylitic: Chl+Cal+Epi+Py	--	--	--	--	--
	378	Propylitic: Chl+Cal+Epi+Hem+Lim	--	--	--	--	--

Abbreviations: adu-adularia; apt-apatite; cal-calcite; chl-chlorite; epi-epidote; hem-hematite; kaol-kaolinite (identified by X-ray); lim-limonite; mus-muscovite; py-pyrite; qtz-quartz; rut-rutile; ser-sericite. 200E, 350E, etc., are drill hole lines (refer to Property Geology Map).
*Analysis data for Au, Ag, As, Ba, and Mo are from the core loggings of Inco Inc.

Fig. 8   (A) Au, (B)As, and (C) Mo concentrations in different alteration zones on the Vault property (assay data from Inco Inc.)

24

cutting relations. The stockwork mineralization is mainly composed of sulfides, which have botryoidal textures (Plate 2), and a small amount of quartz and calcite. Sphalerite and pyrrhotite are earlier than pyrite, whereas chalcopyrite is later than pyrite. Pyrite has two forms. One is small in size (0.006-0.004 mm) and the other is larger (0.2-0.4 mm). Another characteristic of this type of mineralization is that it is related to propylitic alteration. This relation is demonstrated by high Au concentrations in propylitic zone (Fig. 8A).The parageneses of different mineralizations on the property are shown in Fig. 9.

The second type of ore is quartz-vein ore. In quartz-vein mineralization, quartz and calcite are the dominant phases. They intergrow with each other to form bladed textures (Plate 3), which are quite common near the present-day surface. Sericite is late; it usually replaces quartz (Plate 4). Adularia is present in some thin sections; it commonly accompanies quartz. Sulfides in quartz veins are usually low in abundance. The sulfides are disseminated in quartz veins, and rarely aggregate to massive sulfides. Pyrite, the most abundant sulfide, is euhedral and has growth textures (Plate 5). Pyrrhotite is minor; it intergrows with sphalerite. Sphalerite is anhedral, and is minor in abundance. Both pyrrhotite and sphalerite are later than pyrite. Native gold is observed in association with pyrrhotite (Plate 6). Some of the pyrrhotite is altered by late hematite.

In order to determine the relations between Mo and Au, between Ba and Au, and between As and Au, respectively, and the variations of Mo, Ba, As concentrations with depth, relevant diagrams are compiled (Fig. 10, Fig. 11, Fig. 12)(assay data base from loggings of Inco Inc.). In the eastern-most part of the property represented by DDH72468 (950E), where mineralization was weak, Mo shows no correlation with Au, whereas As shows negative correlation with depth (Fig. 10). In the east-central part of the property, represented by DDH38898 (875E), where mineralization is strong, Mo is positively correlated with Au, whereas As shows a weak negative correlation with Au. Both Mo and As concentrations decrease with depth. Ba seems to not vary with the depth (Fig. 11). In the western part of the property represented by DDH72450 (200E), where mineralization

25
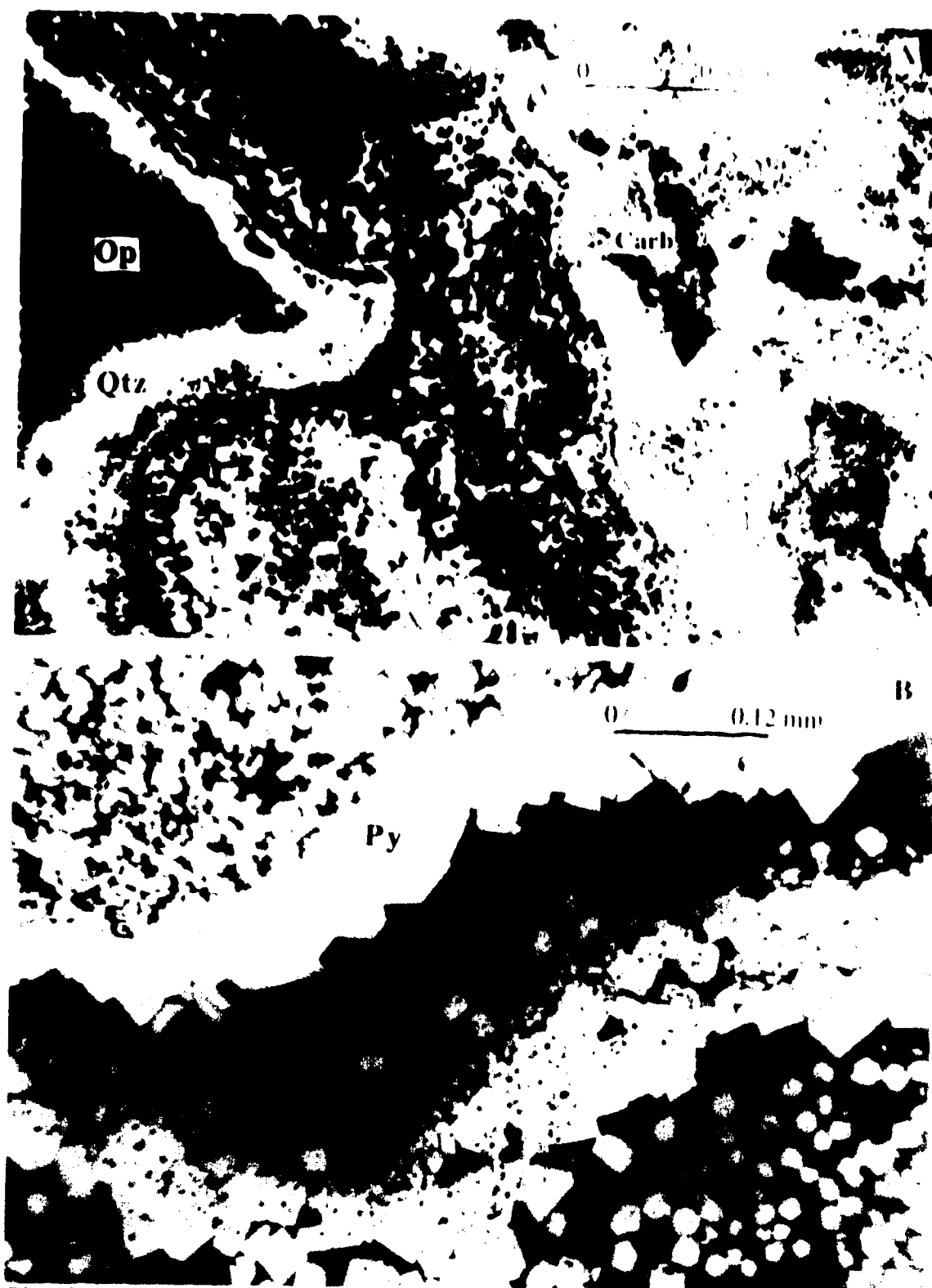
Plate 2 Botryoidal texture in stockwork ores in sample X.49.3 under (A) cross polarized light (10x4), and under (B) reflected light (10x10). Carb, carbonates, Qtz, quartz, Op, opaques, Py, pyrite.
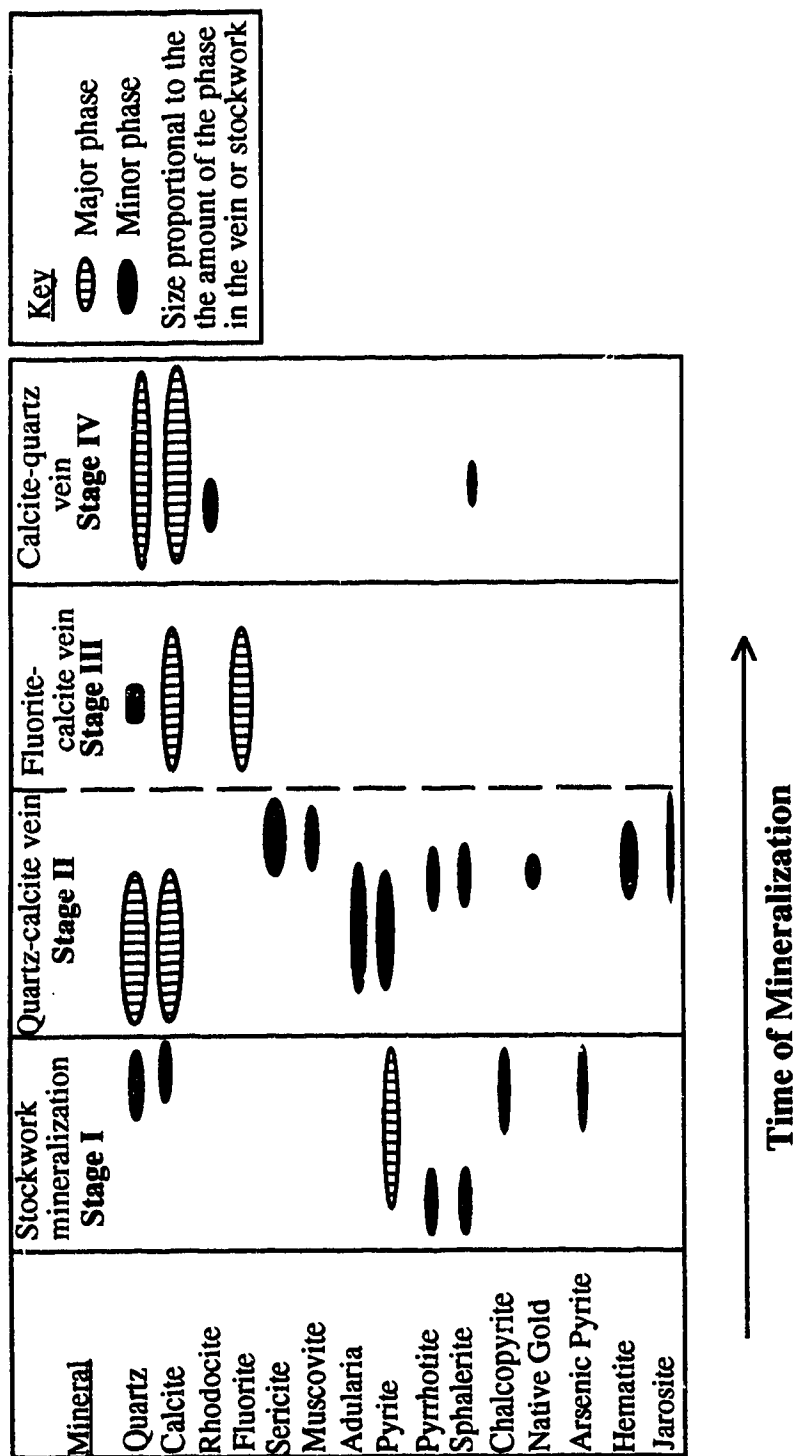
Fig. 9   Paragenesis sequences of mineralizations on the Vault property
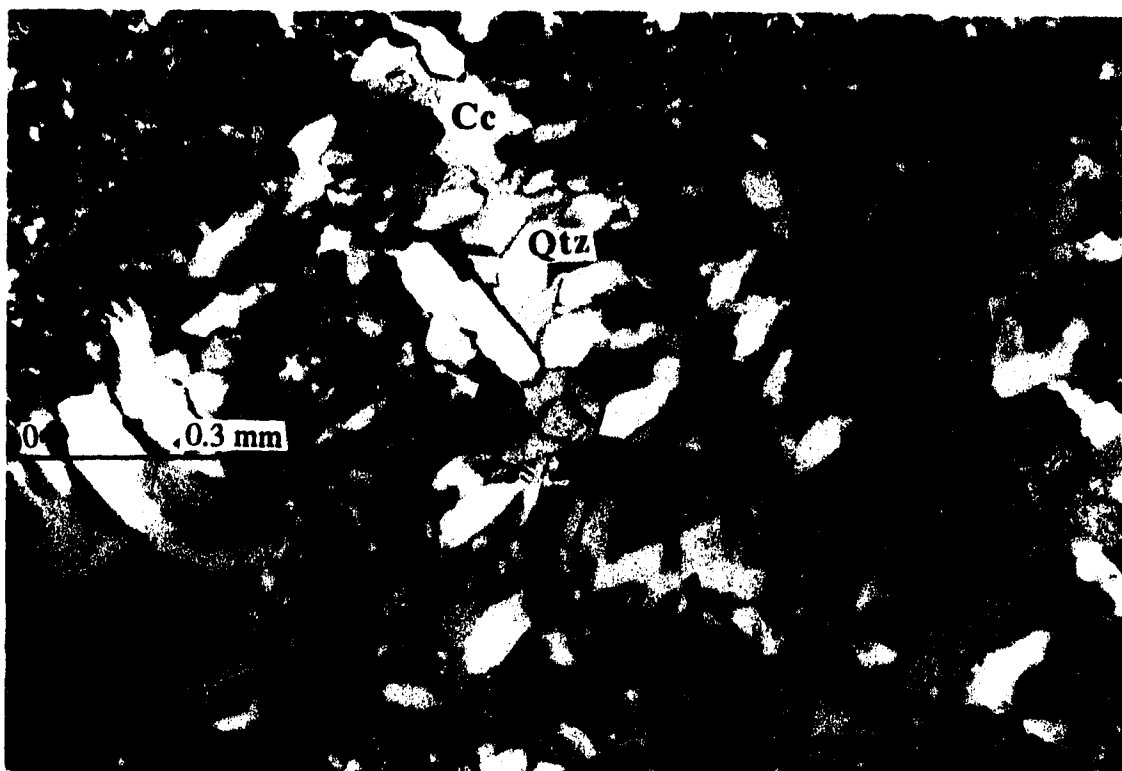
Plate 3   Bladed texture in main stage quartz-calcite vein in sample X68-6. (cross polarized light). (10x4). Cc-Calcite
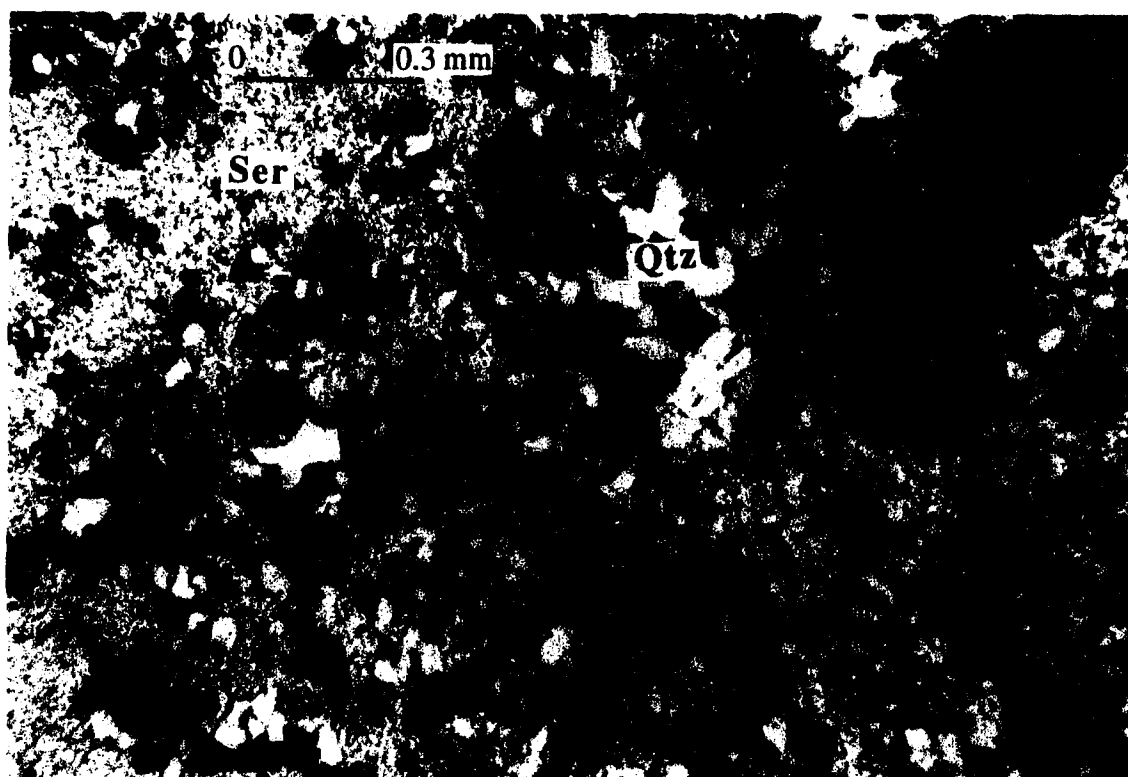
Plate 4   Quartz in main stage quartz-calcite vein was altered to sericite in sample X98-10. (cross polarized light) (10x4). Ser-sericite

Plate 5   Growth texture of pyrite in sample X778-14 under reflected light (10x10)
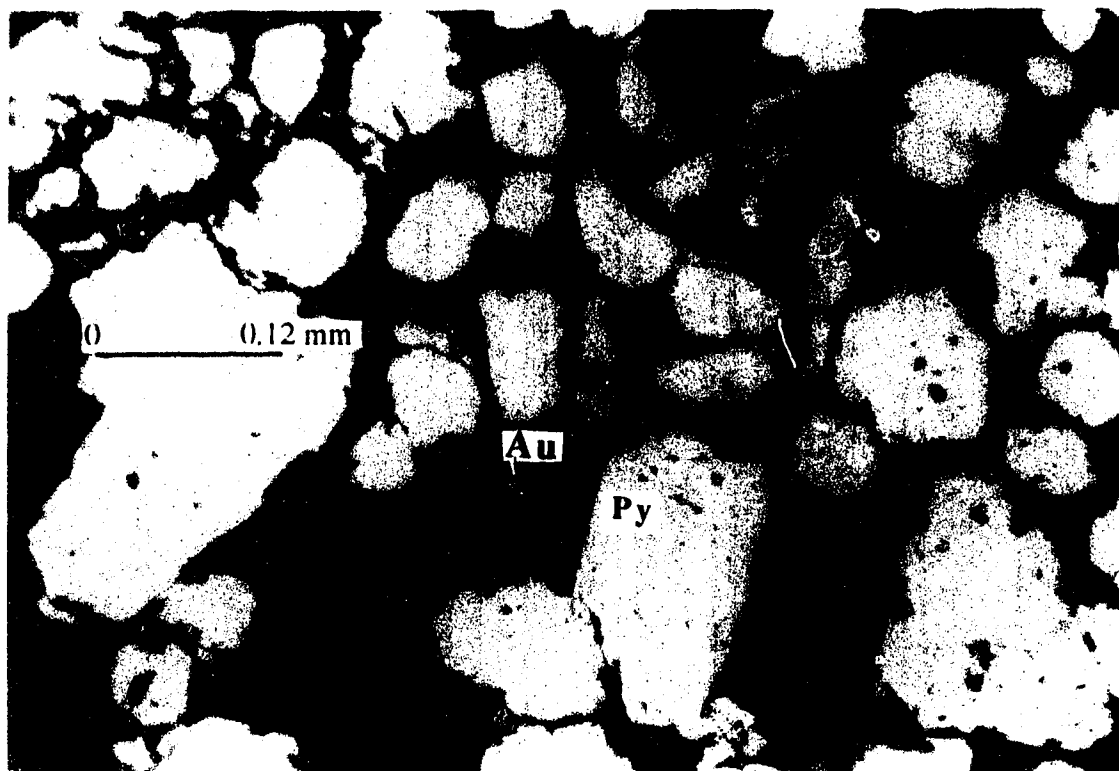
Plate 6   Native gold in stockwork ores in sample X98-3, (reflected light) (10x10). Py pyrite, Au native gold.
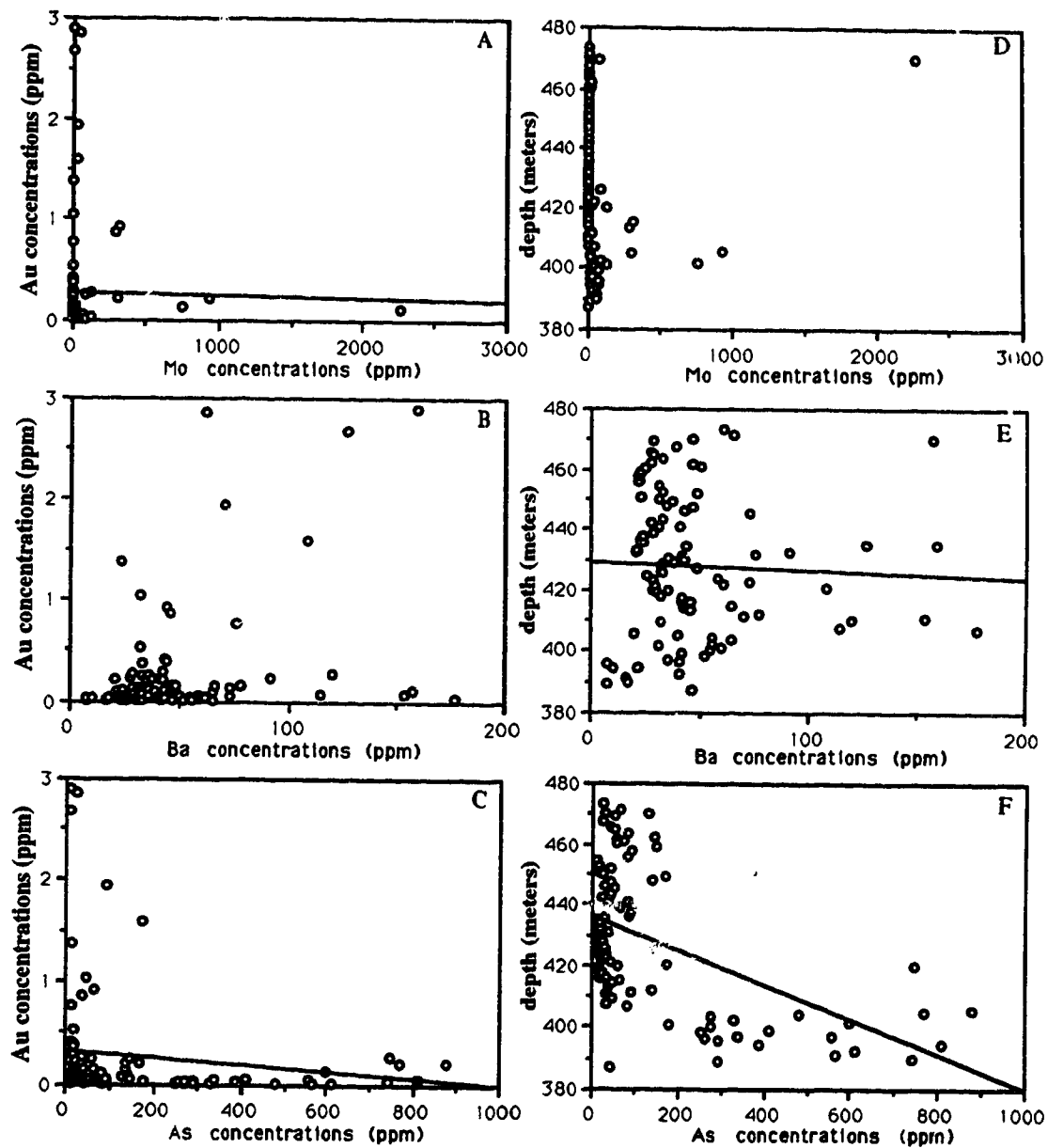
Fig. 10   Correlations (A) between Au and Mo, (B) between Au and Ba, and (C) between Au and As, and variations of (D) Mo with depth, (E) Ba with depth, and (F) As with depth in DDH72468 (assay data from Inco Inc.)

30
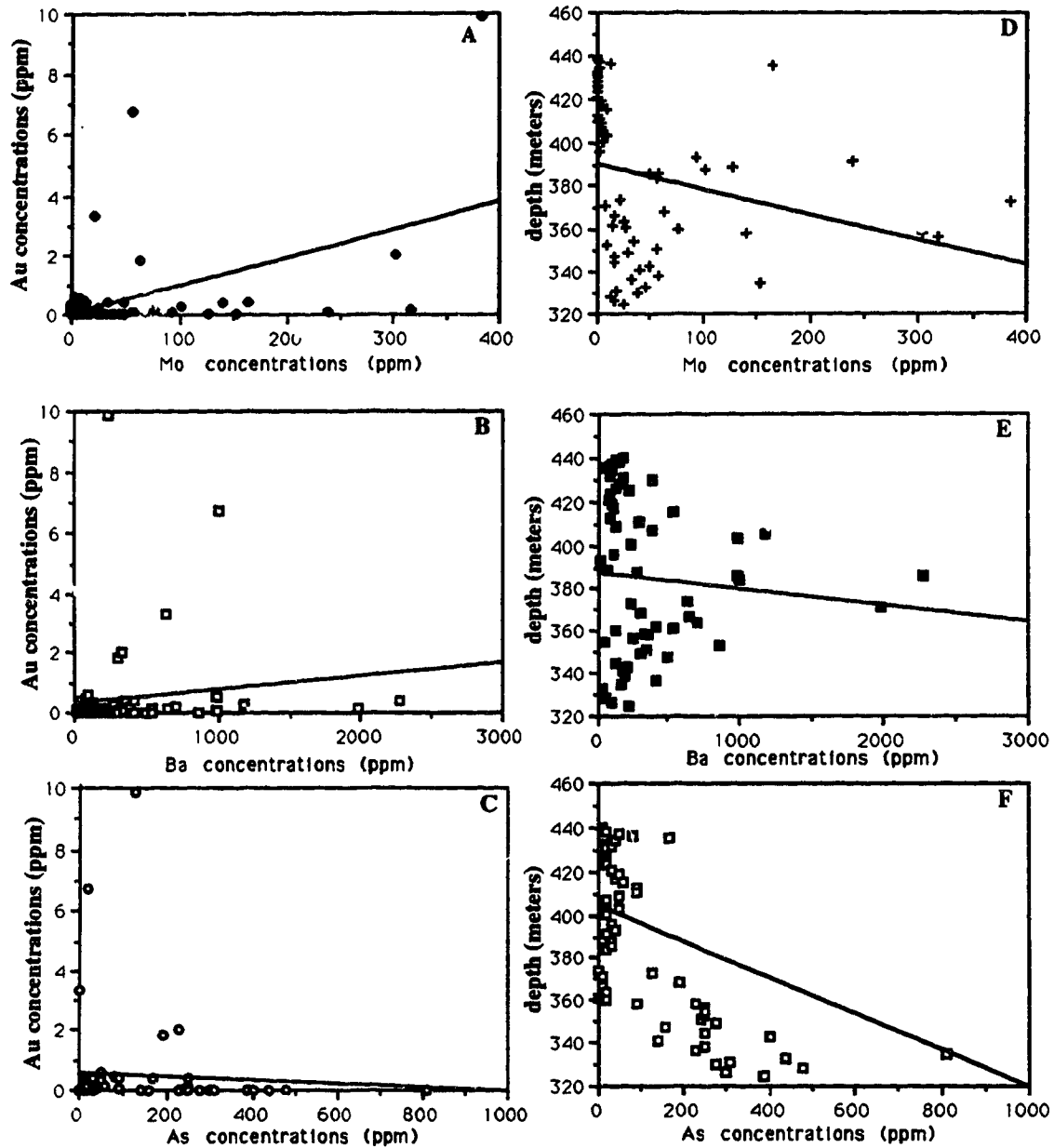
Fig. 11   Correlations (A) between Au and Mo, (B) between Au and Ba, and (C) between Au and As, and variations of (D) Mo with depth, (E) Ba with depth, and (F) As with depth in DDH38898 (assay data from Inco Inc.)

31
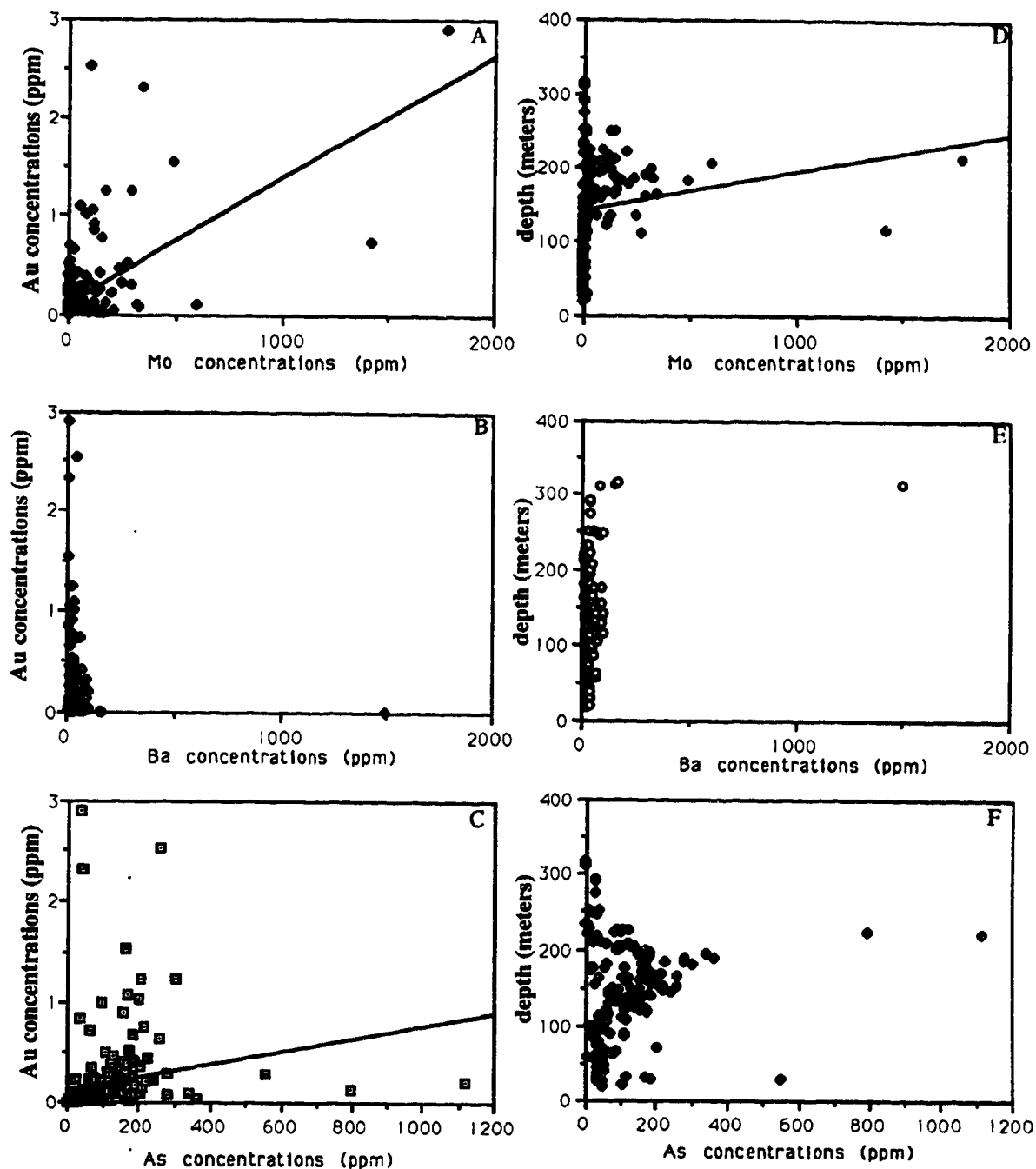
Fig. 12   Correlations (A) between Au and Mo, (B) between Au and Ba, and (C) between Au and As, and variations of (D) Mo with depth, (E) Ba with depth, and (F) As with depth in DDH72450 (assay data from Inco Inc.)

was also weak, Mo did not show clear correlation with Au, neither Mo nor As show clear correlation with depth (Fig. 12). The above data demonstrate that gold positively correlates with Mo in mineralized areas, as suggested by Meyers (1989), and in strongly mineralized areas, Mo and As negatively correlate with depth. These results may imply that in strongly mineralized areas higher concentrations of As and Mo should be expected at shallower depths.

At least two stages of mineralization are later than the main quartz-calcite stage. The fluorite-calcite stage was only observed in a near surface sample (depth of 18 m) in DDH72450. The fluorite is intergrown with calcite. The inclusions from the fluorite-calcite stage have relatively low homogenization temperatures, indicating that the fluorite-calcite stage may be later than main quartz-calcite stage (see the following section). Both field observations and thin section examination demonstrate that the calcite-quartz stage (calcite veins containing small amount of quartz) was the latest vent. Its crosscutting relations with quartz-calcite vein are apparent both macroscopically and microscopically. These two late stage mineralizations are unimportant to concentrations of Au on the Vault property.

(IV) FLUID INCLUSION STUDIES

Fluid Inclusion Techniques

Calcite, quartz and fluorite samples were selected for fluid inclusion studies. On this property, quartz contains few workable inclusions, whereas calcite crystals do contain workable inclusions. Generally, the fluid inclusions studied were large (> 10 μm in diameter). The criteria for recognition of primary inclusions are that the inclusions were distributed individually or in random clusters (Roedder, 1984). Smaller inclusions, which were clustered along the healed fractures, were considered to be secondary in origin (Roedder, 1981). Possible pseudo-secondary inclusions were identified on the basis of their oriented pattern along healed fractures but these fractures terminated over a short distance.

Fluid inclusions were examined in thin (thickness= 0.3-0.6mm), doubly polished chips. Temperature determinations were made using a FLUID INC. adapted, U.S.G.S. gas-flow heating/freezing system with a Doric Trendicator 410A digital thermometric control system attached to a Leitz-Wetzlar microscope with 10 times periplan oculars and 4, 10, and 32 times objective lenses.The heating-freezing stage was calibrated using a distilled water (ice), pure CO_2 inclusions in Alpine vein quartz, liquid nitrogen, and Merck standards. Standard errors are ±0.2°C for freezing measurements and ±2.0°C for heating to 300°C.

The abbreviations used in this thesis are: Th-homogenization temperature of the inclusion, T_{fice}- formation temperature of the ice; and T_{mice}- final melting temperature of ice.

Description of Fluid Inclusions

All of the fluid inclusions observed on the Vault property are aqueous inclusions containing vapour and liquid. Primary inclusions are usually large (15-20 μm) in size, and equant in shape (Plate 7), whereas secondary inclusions are irregular in shape and

34
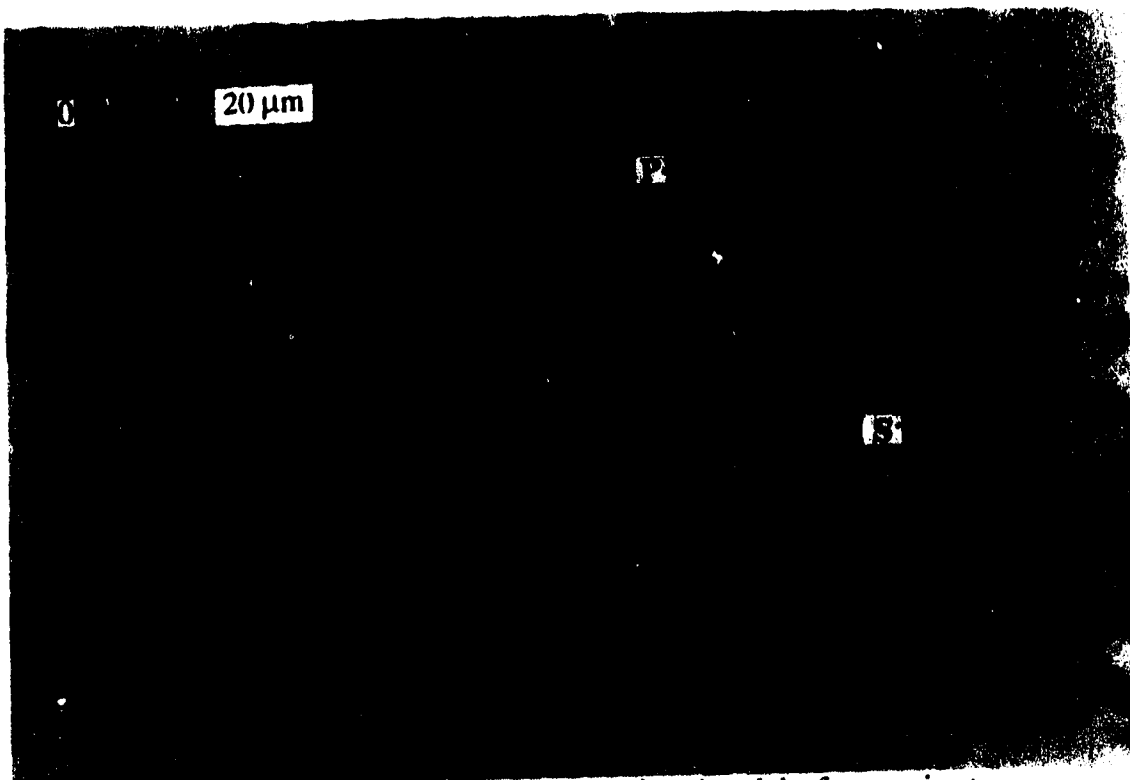
Plate 7 Primary (P) and secondary (S) fluid inclusions in calcite from main stage quartz-calcite vein in sample X-37. (Plane polarized light) (10x63)
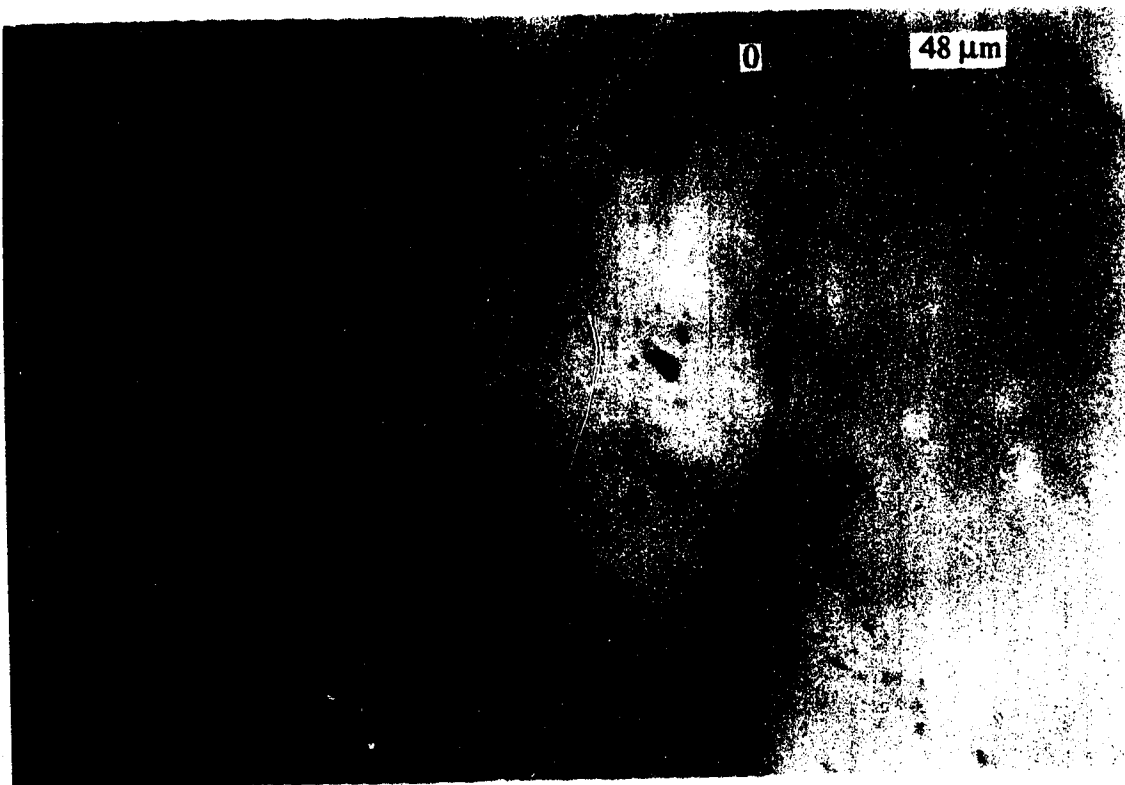
Plate 8   Fluid inclusions with a wide range of filling ratios in bladed calcite in sample X-16B. (plane polarized light) (10x25)

35

distributed along healed fractures. The size of secondary fluid inclusions varies from 6 μm to 30μm (Table 4).

The bubble percentages of inclusions range from less than 5 to 80% volume. Most of vapour bubbles occupy 10-15% volume. Fluid inclusions in fluorite and quartz have relatively narrow ranges of vapour percentages (10-35%), whereas inclusions in calcite have a wide range of vapour percentages (5-80%) (Table 4).

Temperature Measurements

Three temperatures: final ice melting temperature, ice formation temperature, and homogenization temperature of an inclusion, were measured in this study. The data are summarized in Table 4. Salinity determinations were based on freezing point depressions of ice in the system of $NaCl-H_2O$ (Potter *et al.*, 1978) for aqueous inclusions:

$$eq. \ wt.\% \ NaCl = 1.76958T + (4.2384 \times 10^{-2})T^2 + (5.2778 \times 10^{-4})T^3 (°C)$$

where T is freezing point depression, i.e., final melting temperature of ice.

Homogenization temperatures for primary inclusions range from 143° to 347°C. Two populations can be grouped in the histogram of homogenization temperatures for primary/pseudosecondary inclusions (Fig. 13). The first population has a homogenization temperature range from 110°C to 210°C, whereas the second population has a homogenization temperature range from 220°C to 347°C. The majority of measurements for primary inclusions falls into the first population with a peak at 150°-160°C. Homogenization temperatures of probable pseudosecondary inclusions range from 110° to 190°C. The peak temperature of homogenization temperatures of pseudosecondary inclusions is 140°-150°C (Fig. 13), whereas the average temperature of 26 inclusions is 146 ±15°C. Secondary inclusions have homogenization temperatures ranging from 93° to 144°C. The average temperature of 8 secondary inclusions is 119°±17°C. Note that there is an overlap in terms of homogenization temperatures for primary/pseudosecondary inclusions in the temperature range of 140°C to 150°C (Fig. 13). Because the pressure is low for the Vault property and boiling was observed for fluid inclusions homogenized at

Table 4 Fluid Inclusion Data in the Okanagan Falls Area

Sample/Host Mineral	Origin	Inc. Size	Bub Diam.	Phase Assem.	Vol% H2O	Tf ice	Tm ice	Th	Eq. wt. % NaCl
				Regional Samples					
V-5/Quartz	prim.	30	9	LV	70	-40.4	-0.2	209	0.35
	prim.	24	6	LV	75	--	-0.2	207	0.35
	prim.	18	6	LV	80	-37.7	-0.1	212.3	0.18
	prim	24	6	LV	85	-39.3	-0.2	--	0.35
	sec	15	6	LV	85	--	--	94.8	
	prim.	6	3	LV	90	--	--	191	
	prim.	6	3	LV	90	--	--	207	
	prim.	4.5	1	LV	90	--	--	210.6	
O-1/Calcite	prim	15	1.5	LV	90	-37.5	0.0	--	0
	prim	15	1.5	LV	90	-37.3	0.0	162.6	0
	prim	9	1	LV	95	-35.0	0.0	--	0
	prim	9	1	LV	95	-35.6	0.0	153.9	0
	sec?	4	0.5	LV	95			147.0	
	sec?	4	0.5	LV	95			150.4	
	sec?	6	0.5	LV	90			150.4	
	sec?	15	0.5	LV	90			174.4	
	prim	15	3	LV	85			174.4	
	prim	12	1.5	LV	95			173.5	
O-3/Calcite	prim	15	1.5	LV	90	-34.4	0.0	--	0
	prim	9	1	LV	80	--	0.0	165.8	0
	prim	24	6	LV	75	-39.3	-0.1	167.4	0.18
	prim	6	1	LV	90	--	--	167.3	
	prim	12	2	LV	85	--	--	168.7	
V-4/Calcite	prim	3	0.1	LV	95	-35.7	-0.4	?	0.70
	Prim	6	0.3	LV	95	-34.8	-0.1	?	0.18
	prim	9	1	LV	85	-33.3	-0.2	?	0.35
	prim	6	0.5	LV	80	--	--	169	
	prim	12	1.5	LV	90	--	--	175	
	prim	6	0.5	LV	90	--	--	179	
T-1/Calcite	prim	9	1.5	LV	85	-33.0	-0.2	--	0.35
	prim	9	1.0	LV	90	-33.5	-0.2	--	0.35
	prim	6	1	LV	80	--	--	253	
	prim	15	3	LV	80	--	--	257.9	
	prim	12	2	LV	90	--	--	257	
	prim	9	1.5	LV	80	--	--	258.2	
	prim	9	1.5	LV	85	--	--	260.6	

37

XP-2								
prim	12	3	L-V	85	—	—	261.2	0.18
prim	15	3	L-V	70	-40.1	-0.1	—	0.18
prim	21	3	L-V	95	-38.9	-0.1	—	0.18
prim	6	0.5	L-V	95	—	-0.1	—	0.53
prim	9	3	L-V	90	—	-0.3	—	
prim	30	6	L-V	75	-31.6	0.0	220.2	0
prim	24	9	L-V	80	-32.9	0.0	217.7	0
prim	9	3	L-V	90	—	0.0	238.2	0
prim	15	3	L-V	85	—	0.0	238.1	0
prim	6	1.5	L-V	80	—	—	233.5	
prim	6	1.5	L-V	80	—	—	233.5	
prim	3	1	L-V	90	—	—	227.2	
prim	3	1	L-V	85	—	—	223.6	
prim	12	3	L-V	85	-35.5	0.0	211.6	0
prim	10	1.5	L-V	85	—	—	—	0
prim	9	3	L-V	90	—	0.0	231.1	0
prim	9	3	L-V	85	—	0.0	237.8	0
prim	9	3	L-V	75	—	0.0	228.7	
sec	5	0.5	L-V	95	—	—	167.6	
R-2/Calcite								
prim	9	1.5	L-V	90	-38.8	3.4	119	
prim	12	1.5	L-V	90	-38.8	3.4	125	
sec	9	0.5	L-V	>95	-32.6	3.8	98	
prim	30	3	L-V	90	-35.6	3.6	132	
X-16B/Calcite (with bladed texture)			*Samples on the Vault property*					
prim	24	12	L-V	40	-43.1	-2.0	discriptitated	3.37
prim	15	3	L-V	85	-45.8	-0.8	231	1.39
p.sec?	15	3	L-v	90	-45.7	-1.9	155	3.21
p.sec?	6	0.1	L-V	>95	—	-1.0	162	1.73
prim	9	3	L-V	70	—	-1.9	347	3.21
prim	6	1.5	L-V	85	-37.7	-1.0	—	1.73
p.sec?	21	3	L-V	90	-44.8	-1.0	156	1.73
p.sec?	12	3	L-V	90	-40.7	-0.7	147	1.22
p.sec?	15	3	L-V	90	-40.7	-0.7	145	1.22
p.sec?	12	3	L-V	90	—	—	149	
X-34B/Calcite (with bladed texture)								
prim	18	3	L-V	90	-46.1	-0.8	160	1.39
prim	14	3	L-V	85	-46.6	-0.6	—	1.05
ps. sec?	6	0.3	L-V	>95	-43.0	-0.7	124	1.22
prim	9	3	L-V	80	-45.4	-0.6	—	1.05
prim	15	4.5	L-V	85	-42.1	-0.8	208	1.39
ps. sec ?	9	1.5	L-V	90	—	—	144	
ps. sec?	9	1.5	L-V	90	—	—	147	

Sample									
	ps. sec?	15	1.5	L-V	>95	--	--	120	
	prim	6	0.5	L-V	90	--	--	154	
	prim	18	3	L-V	90	-39.0	-0.7	159	1.22
	prim	15	3	L-V	95	-43.0	--	--	
	ps. sec?	21	3	L-V	95	-36.8	-0.6	140	1.05
	prim	18	3	L-V	90	--	--	158	
	ps. sec?	12	0.1	L-V	90	--	--	140	
	ps. sec	3	3	L-V	90	--	--	141	
	prim	12	1.5	L-V	85	--	--	174	
	ps. sec	12	1.5	L-V	90	--	--	129	
	ps. sec?	12	0.5	L-V	90	--	--	129	
	ps. sec	12		L-V	90	--	--	123	
X-37/Calcite	prim	27	3	L-V	90	--	-0.1	155	0.18
	sec	24	3	L-V	90	-38.9	-0.1	113	0.18
	p. sec?	45	3	L-V	95	-36.0	-0.1	143	0.18
	prim	18	6	L-V	80	-36.2	-0.2	148	0.15
	sec?	30	6	L-V	90	-35.6	-0.1	117.8	0.18
	prim	27	6	L-V	95	-38.8	0.2	144.0	
	prim	6	0.5	L-V	>95	-40.0	0.0	168.1	0
	prim	9	0.5	L-V	>95	-40.0	0.0	168.0	0
	prim	21	3	L-V	90	-35.6	0.0	--	
	prim	24	3	L-V	85	-38.8	0.2	--	0
	prim	24	6	L-V	75	-38.0	0.0	--	
	prim	18	3	L-V	75	--	0.1	--	
	prim	15	3	L-V	65	-38.0	0.2	--	
	prim	45	3	L-V	45	-35.2	0.0	158	0
X-55B/Quartz	prim	6	0.5	L-V	90	--	--	297	
X83-3/Calcite	prim	42	6	L-V	85	-33.8	-0.2	167	0.35
	prim	36	9	L-V	90	-33.3	-0.2	159	0.35
	prim	12	3	L-V	90	-32.6	-0.2	--	0.35
	prim	12	3	L-V	95	--	-0.2	--	0.35
	prim	30	6	L-V	90	-35.6	-0.1	174	0.18
	prim	15	6	L-V	85	-33.6	-0.1	--	0.18
	prim	12	1.5	L-V	90	-33.4	-0.1	--	0.18
X83-6/Calcite (with bladed texture)	prim	27	18	L-V	70	-38.6	-0.4	269	0.70
	prim	18	6	L-V	85	-38.4	-0.5	230	0.87
	p.sec	30	6	L-V	90	-38.4	-0.2	186	0.35
	prim	27	6	L-V	90	-37.2	-0.4	231	0.70
	prim	27	24	L-V	20	--	--	268	
	p.sec?	9	0.5	L-V	95	--	--	156	
	prim	21	9	L-V	85	--	--	286	

	p.sec?	30	0.1	LV	>95	--	--	--	175	
X50-3/Fluorite										
	prim	27	6	LV	85	--	-39.2	-0.3	160	0.53
	prim	24	6	LV	90	--	-39.2	+0.5	154	
	prim	15	3	LV	90	--	-39.7	-0.6	159	1.05
	prim	21	3	LV	90	--	-38.9	0.0	--	0
	prim	18	3	LV	90	--	-38.5	0.0	143	0
	prim	15	3	LV	90	--	-38.9	-0.2	161	0.35
	prim	15	3	LV	90	--	-38.9	-0.2	159	0.35
	prim	30	6	LV	85	--	-38.2	+2.0	--	
	prim	30	6	LV	90	--	-38.5	0.0	155	0
	prim	18	1.5	LV	90	--	-38.5	+1.1	143	
	prim	12	3	LV	85	--	--	+4.5	164	
	prim	18	3	LV	80	--	--	--	166	
	prim	15	3	LV	90	--	--	--	163	
	prim	9	1.5	LV	90	--	--	--	157	
X49-12										
	sec	18	3	LV	95		-41.1	2.8	127	
	sec	15	3	LV	90		--	2.9	--	
	sec	12	3	LV	90		-41.7	6.7?	144	1.39
	sec	36	6	LV	90		-40.1	-0.8	121	0.70
	sec	30	3	LV	90		-40.8	-0.4	--	
	sec	24		LV	95		--	--	126	
	prim	30		LV	90		--	--	201	
	prim	60		LV	70		-40.0	0.0	--	
X98-12/Quartz										
	prim	33	3	LV	65		-31.6	-0.1	202	0.18
	p.sec?	18	3	LV	85		-34.7	0.9	140	
	p.sec?	30	6	LV	90		-37.3	-0.2	162	0.35
	prim	15	6	LV	85		-33.4	0.0	192	0
	prim	24	9	LV	90		-31.9	0.0	185	0
	prim	39	3	LV	85		--	--	195	
	p.sec?	15	3	LV	95		-33.6	1.2	142	
	p.sec?	12	3	LV	95		-39.8	0.2	149	
	sec	18	3	LV	95		-31.8	1.8	96	
	sec	30	1.5	LV	95		-30.8	1.2	93	
	p.sec?	9	3	LV	>95		--	--	134	
	p.sec	12	3	LV	95		--	--	160	
	p.sec	15	3	LV	95		--	--	160	

Abbreviations and Note: inc.-inclusion; bub-bubble; diam.-diameter; assem-assemblage; prim-primary inclusion; sec-secondary inclusion; p.s.-pseudosecondary inclusion; Tm_{ice}-Ice Melting Temperature; Th-Homogenization Temperature; Tf_{ice}-Ice Formation Temperature. L-liquid (water); V-vapour. Inclusions homogenized into liquid unless indicated by underlining V. which means that the inclusion homogenized into vapour.
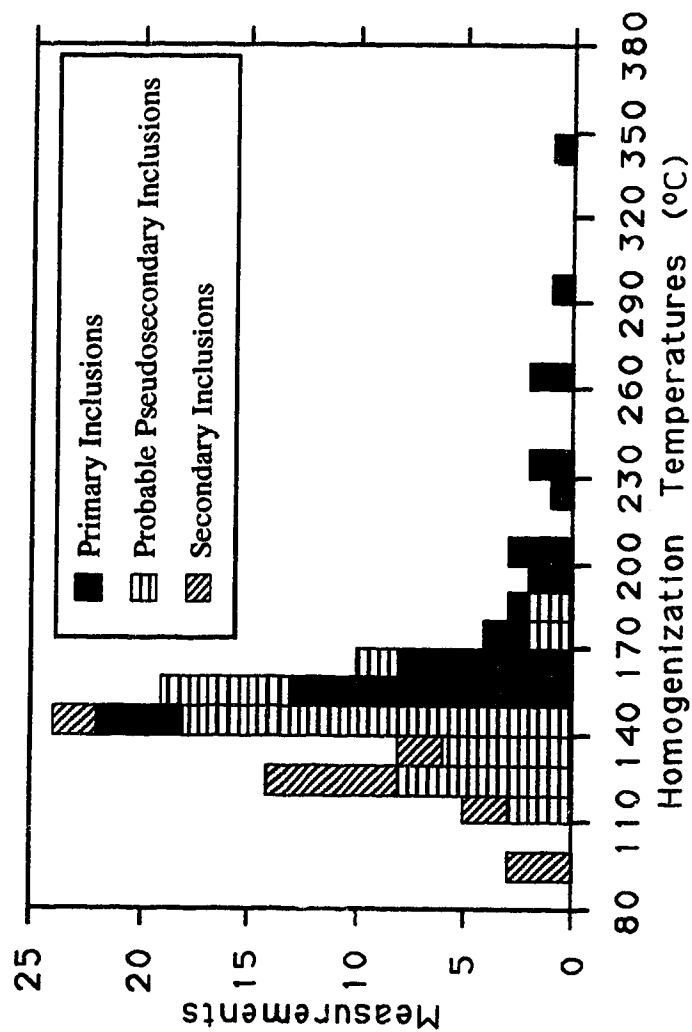
Fig. 13   Homogenization temperatures for samples on the Vault property. There is a peak at 150°C to 160°C for primary/pseudosecondary inclusions, whereas probable pseudosecondary inclusions have a peak at 140°C to 150°C. There is an overlap for primary/pseudo-secondary and secondary inclusions at the temperature range from 140°C to 150°C.

270°C (see following section), the pressure corrections will be so low that these homogenization temperatures are close to the temperatures of formation (Roedder, 1984).

Final melting temperatures of ice for primary and pseudosecondary inclusions range from -2.0° to 0°C, which corresponds to a salinity range of 0 to ~3.4 eq. wt.% NaCl. Two peaks in the final melting temperatures of ice are observed. One is at -0.1° to 0.0°C (corresponding to a salinity range of 0 to ~0.2 eq. wt.% NaCl), representing non-bladed samples, and the other one is at -0.8° to -0.6°C (corresponding to a salinity range of ~1.0 to ~1.4 eq. wt.% NaCl), representing calcite samples with bladed texture (Fig. 14). The average ice melting temperature of 33 primary and pseudosecondary inclusions is -0.4°±0.3°C, which corresponds to a salinity of ~0.8 eq. wt.% NaCl. The final ice melting temperature data for both primary and pseudosecondary inclusions indicate that the mineralizing fluids were very dilute in nature. In addition, a number of final melting temperatures of ice above 0°C (in the range of +0.1° to +6.7°C) have been observed (Table 4). They are most likely to be indicative of metastability (Roedder, 1981, 1984). As pointed out by Hollister et al. (1981), when a water-rich inclusions with a small vapour bubble at room temperature freezes, the vapour bubble can totally disappear. On warming, the ice can persist metastably in this vapour-free situation at least to +6.5°C. Since all of fluid inclusions on the property are water-rich, and all of the inclusions with final melting temperatures of ice higher than 0°C have high filling degrees (≥85% of liquid), it is likely that final melting temperatures of ice higher than 0°C indicate metastability.

Interpretation of Fluid Inclusion Data

1. Evidence of Boiling: When a homogeneous phase rises in a hydrothermal system, and if it experiences a decrease in pressure, boiling will occur (Reed and Spycher, 1985). Boiling induces a temperature decrease and a pH increase which causes minerals to precipitate (Reed and Spycher, 1985). Fluid inclusions trapped during a boiling process would have a wide range of filling ratios but the same or very close homogenization temperatures, and such fluid inclusions are strong evidence for boiling if observed

42
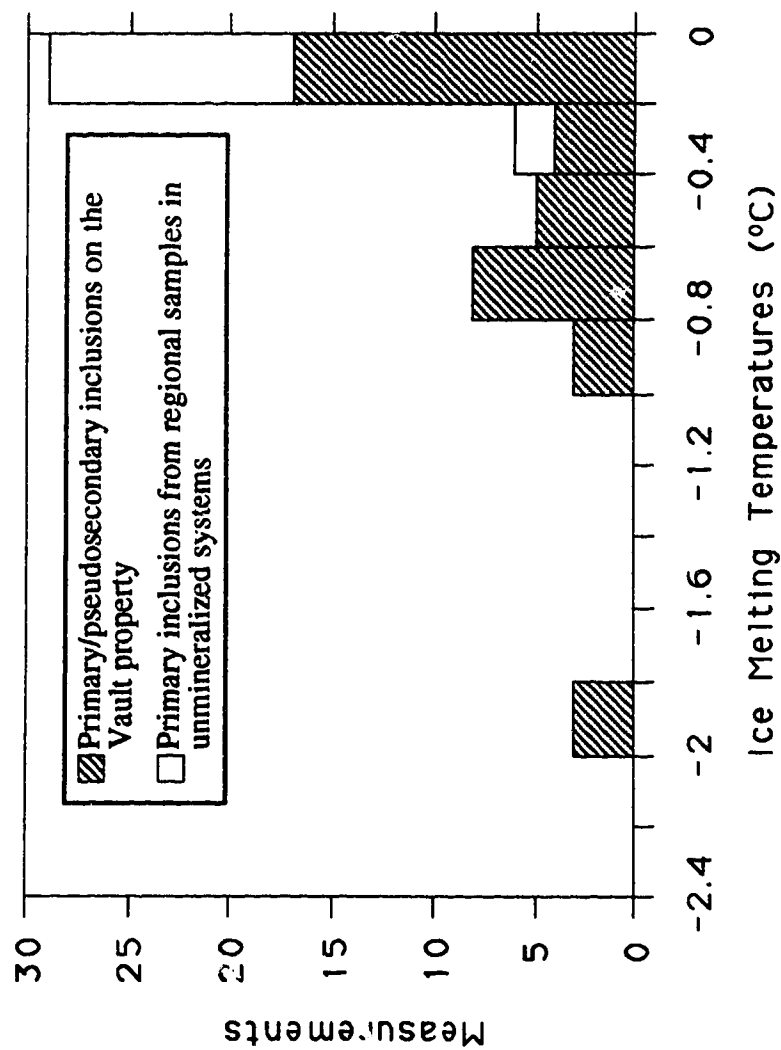
Fig. 14 Ice melting temperatures for samples on the Vault property and for regional samples from unmineralized systems

(Roedder, 1984). On the Vault property, fluid inclusions in samples X83-6 and X-16B

(Plate 8) have a wide range of filling ratios, but give very close homogenization

temperatures (refer to Table 4, X83-6), which is clearly indicative of a boiling process. In

addition, the boiling process is apparently suggested by the systematic trend, i.e., a boiling

trend in a homogenization temperature against salinity diagram (Fig. 15, Trend I).

According to Hedenquist and Henley (1985) and Shepherd et al. (1985), analysis of

systematic trends in homogenization temperatures and final melting temperatures of ice

(i.e., salinities) may yield evidence for the occurrence of boiling in a fossil hydrothermal

system, and in some instances may be more definitive than many of the observational

criteria often used. Such an analysis a¹⁻⁻ ⁻ ⁻. ⁻not rely upon the preservation of vapour-rich

inclusions. In Fig. 15, there is an obvious boiling trend for samples with bladed textures.

In this boiling trend, fluid inclusions having higher homogenization temperatures have

lower salinities (0.7 to 0.8 eq. wt.% NaCl), whereas fluid inclusions having lower

homogenization temperatures have higher salinities (1.0 to 1.5 eq. wt.% NaCl). This

difference implies that boiling may have slightly increased the salinity of the fluids.

2. Boiling Depth: According to Roedder (1984, p.273),

"if a boiling liquid and its coexisting vapour phase are trapped separately in a pair of

inclusions, these two inclusions will homogenize in the liquid and in the vapour phase,

respectively. These two homogenizations must be at the same temperature, and if the

boiling curve is known for that fluid, the pressure can be determined from this Th."

Fluid inclusions of X83-6 are just this case. The vapour-rich inclusion (~80 %

volume of vapour) homogenized to a vapour phase at 269°C and the liquid-rich inclusions

(~70% volume of liquid) homogenized to a liquid phase at 268°C (Table 4). The salinity

for this sample is about 0.7 eq. wt.% NaCl. Therefore, the fluid inclusion data from this

inclusion can be used to estimate the depth of boiling. According to Haas (1976), at the

temperature of 270°C, the pressure and density for fluids experiencing boiling with a

44
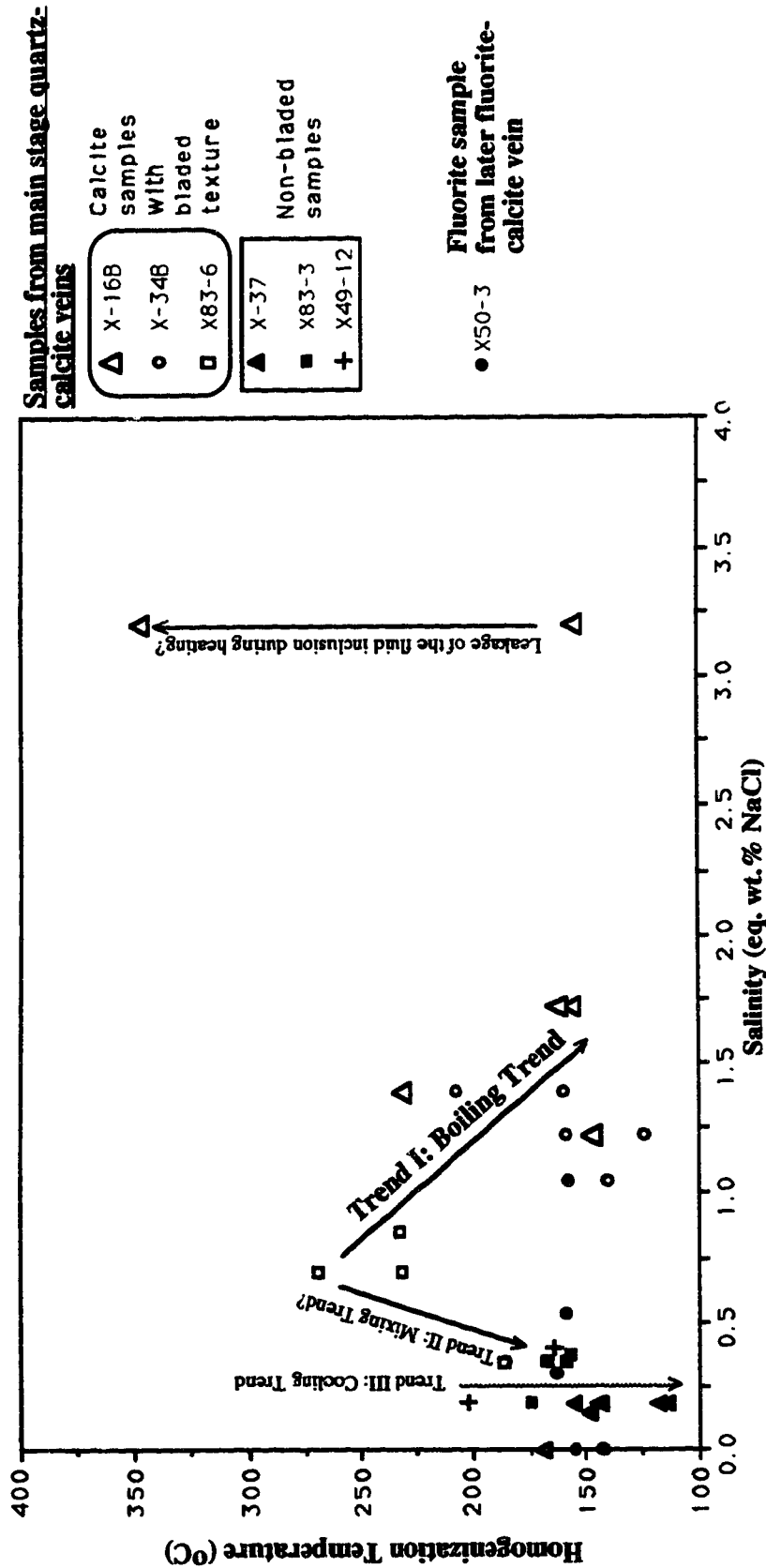
Fig. 15 Correlation between salinities and homogenization temperatures of fluid inclusions from bladed and non-bladed samples on the Vault property. Two trends are apparent. Trend I is a boiling trend. The starting fluid for boiling trend probably has a salinity of ~0.7 eq. wt.% NaCl at 270°C. The resultant fluid has a salinity of ~1.3 eq. wt.% NaCl. Trend II might be a mixing trend (according to Shepherd et al., 1985). This trend might represent a mixing process between an endmember with a salinity of ~0.7 eq. wt.% NaCl at ~270°C and the other endmember with a salinity close to zero at a temperature of ≤150°C. The simple cooling trend (Trend III) is not apparent for the fluid with a salinity of ~0.7 eq. wt.% NaCl at ~270°C, but is apparent for the fluid with lower salinities (~0.2 eq. wt.% NaCl).

45

salinity of 0.0 eq. wt.% NaCl, and with a salinity of 2.84 eq. wt.% NaCl, respectively, are

listed in Table 5.

Table 5 Pressure and density data for H_2O-NaCl solutions with salinities of 0.0 eq wt.% NaCl and 2.84 eq. wt. % NaCl at 270°C. respectively (Haas, 1976), and interpolated pressure and density data for a H_2O-NaCl solutions with a salinity of 0.7 eq. wt.% NaCl for fluids on the Vault property

Salinity	Pressure (bars)	Density (g/cm^3)
0.0	55.0	0.768
0.7	53.755	0.775
2.84	54	0.795

Based on the following equation (Shepherd *et al.*, 1985), the boiling depths for these two

fluids are calculated:

$$P = H \rho * 0.0981$$

where P is pressure in bars, H is boiling depth in meters, and ρ is density in 1000kg/m^3.

According to this equation, the boiling depths for the fluids with a salinity of 0.0 eq. wt.%

NaCl and a salinity of 2.84 eq. wt.% NaCl are ~730m and ~694m, respectively. By

interpolation, a fluid with a salinity of ~0.7 eq. wt.% NaCl taken as a representative of

fluids on the Vault property at a temperature of ~270°C would have a boiling depth of

~707m.

In addition, the fraction of water converted to steam (S) may be calculated from the

following formula (Drummond and Ohmoto, 1985; Lynch, 1989):

$$H^L_{T1} = (1-S) H^L_{T2} + SH^G_{T2}$$

where H^L and H^G are the enthalpy of H_2O^L and H_2O^G in saline solutions (Haas, 1976),

and $T1$ is the temperature at the beginning of boiling while $T2$ is the temperature at the end

of boiling. Assuming that the minimum temperature at beginning of boiling on the Vault

property is 270°C (salinity =0.7 eq. wt.% NaCl) and the temperature at the end of boiling

is 150°C (refer to Fig. 15) (salinity =1.5 eq. wt.% NaCl), the enthalpy data for such fluids

can be interpolated based the enthalpy data provided by Haas (1976) for fluids with 0.0 eq. wt% NaCl and 2.84 eq. wt.% NaCl (Table 6):

Table 6 Enthalpy data for H_2O^L at 270°C, H_2O^L and H_2O^G at 150°C at salinities of 0.0 and 2.84 eq. wt.% NaCl, respectively (Haas, 1976), and interpolated corresponding enthalpy data for fluids with salinities of 0.7 and 1.5 eq wt.% NaCl, respectively, on the property

Salinity	Temperature	H^L (J mol^{-1})	H^G (J. mol^{-1})
0.0	150°C	11370	49474
1.5	150°C	11357*	49481*
2.84	150°C	11345	49488
0.0	270°C	21405	
0.7	270°C	21378*	
2.84	270°C	21297	

* Interpolated data

According to the interpolated data, the calculated steam fraction S is equal to 26% for a fluid with a salinity of 0.7 eq wt.% NaCl at temperature of 270°C. Since the enthalpy data for a fluid with a salinity of 0.7 eq. wt. % NaCl at a temperature above 270°C are always larger than 21378 J. mole^{-1}, the steam fraction S on the Vault property should be $\geq 26\%$.

3. Deposition Mechanisms for Main Stage Quartz-Calcite Veins: As suggested by Fig. 15, there may be two processes responsible for the deposition of minerals:boiling and mixing. Boiling began with a fluid with a salinity of ~0.7 eq. wt.% NaCl, and was responsible for the formation of bladed textures. Because the boiling process tends to cause dramatic physicochemical changes for fluids (Reed and Spycher, 1985), it could be also responsible for the precipitation of gold.

Mixing process probably involved two endmembers of fluids. One endmember was characterized by a salinity close to zero and a temperature of $\leq$ 150°C. The other endmember was characterized by a salinity close to 0.7 eq. wt.% NaCl and a temperature of 270°C. Since a mixing process also results in large physicochemical changes, this

47

process may also be important for the deposition of gold. In addition, the calculated $\delta^{18}O_{fluid}$ values in the range of -3.8 to -0.1‰ may be indicative of a mixing (see isotope study section).

(V) Stable Isotope Studies

Over 20 samples of quartz and carbonate from the Vault property were analyzed in the stable isotope study. Quartz vein samples were crushed to -115 mesh size and were cleaned by first treating with hydrogen peroxide and nitric acid to remove any sulfides and then by boiling in aqua regia for about one hour. Calcite and whole rock samples were crushed and ground below -115 mesh size.

Isotope data are reported in the standard delta notation where δ is defined in units of per mil (‰) as:

$$\delta = [\frac{R_{sample}}{R_{standard}} - 1] \times 10^3$$

where R is the heavy/light isotope ratio. For oxygen,

$$R = \frac{^{18}O}{^{16}O}$$

whereas for carbon,

$$R = \frac{^{13}C}{^{12}C}$$

Isotopic fractionations between two phase are reported Δ_{AB}, defined as:

$$\Delta_{AB} = 1000 \ln \alpha_{AB}$$

where $\alpha_{AB} = \frac{R_A}{R_B}$.

Oxygen isotope analysis of silicate samples (and whole rock samples) was by the BrF_5 technique of Clayton and Mayeda (1963), where carbonate samples were analyzed by the standard technique of McCrea (1950). All samples were analyzed on a VG 602D mass spectrometer. All these analyses were carried out in the laboratory of Karlis Muehlenbachs at the University of Alberta. Oxygen isotope data are reported relative to the SMOW standard (Craig, 1961) and carbon isotope data are reported relative to the PDB standard (Craig, 1953). Analytical errors (2σ) are ±0.3 per mil for oxygen and ±0.05 per mil for carbon. The mass spectrometer was checked using NBS-28 standard at the beginning of experiment run and the result was +9.60‰ for oxygen isotope.

Carbonate Isotope Data

The isotopic data and sample types for carbonates are shown in Table 7 and Figure 16. The samples exhibit a wide range of $\delta^{18}O$ values, from -3.6 to 13.7 ‰. A wide range of $\delta^{13}C$ values is also exhibited, ranging from -4.6 to -12.5‰. Disseminated carbonate samples from propylitic trachyte have $\delta^{18}O$ values from -1.1 to +1.2‰ and $\delta^{13}C$ values from -10.2 to -4.6‰. Calcite samples from main stage quartz-calcite veins (Stage II) have $\delta^{18}O$ values ranging from +1.3 to +13.7‰ and $\delta^{13}C$ values ranging from -12.5 to -4.5‰. Calcite sample from a fluorite-calcite vein (Stage III) has a $\delta^{18}O$ value of +1.0‰ and a $\delta^{13}C$ value of -5.0‰. Carbonate samples from calcite-quartz veins (Stage IV) have $\delta^{18}O$ values ranging from -3.6 to +2.7‰ and $\delta^{13}C$ values ranging from -11.8 to -10.3‰. Because calcite on the Vault property has large grain size (up to ~10mm), and did not experience recrystallization, the original isotopic signatures of carbonates should be preserved, and should not be reset by later low temperature underground meteoric water (O'Neil, 1987).

Silicate Isotope Data

Six quartz samples from main stage quartz-calcite veins are analysed for $\delta^{18}O$. The $\delta^{18}O$ values range from -0.2‰ to +6.6‰. The $\delta^{18}O$ values of quartz samples do not show correlation with elevations, because the subsurface samples have $\delta^{18}O$ values ranging from +1.5 to +6.6‰, whereas the present-day surface samples have $\delta^{18}O$ values ranging from -0.2 to +3.8‰. Compared with $\delta^{18}O$ values of calcite samples from main stage quartz-calcite veins, $\delta^{18}O$ values of quartz samples are always lighter. Quartz samples from main stage quartz-calcite veins with bladed textures usually have lower $\delta^{18}O$ values (-0.2 to +3.8‰) than those from the same stage quartz-calcite veins without bladed textures (+4.0 to +6.6‰). The sample of vuggy quartz (X98-12) has the highest $\delta^{18}O$ values (+6.6‰).

Table 7 Stable Isotope Data for Samples from the Vault property

Sample Number	$\delta^{13}C_{Calcite}$ ‰	$\delta^{18}O_{Calcite}$ ‰	$\delta^{18}O_{water}$ ‰	Temperature	Location and sample description
X98-12	-10.3	-3.6 +6.6(Quartz)	~ -15 (for fluids from which calcite precipitated) -5.0 ((for fluids from which quartz precipitated)	155ºC[a] 200ºC[b]	DDH38898, depth at 328.6m. Calcite from carbonate vein cutting main stage quartz-calcite vein. Vuggy quartz is from main stage quartz-calcite vein. Host rock: mudstone.
X98-13	-11.8	+2.2	-9.5	155ºC[a]	DDH38898, depth at 324.0m. Rhodocite from carbonate vein. Mudstone as host rock.
XD-8	-4.9	+11.5	+5.5	270ºC[e]	DDH 38898, depth at 287.6m. Calcite from main stage quartz-calcite vein.Trachyte as host rock.
X778-8	-12.4	+2.7	-9.1	155ºC[a]	DDH 82778, depth at 53.8m. Calcite from calcite-quartz vein cutting main stage quartz-calcite vein. Mudstone as host rock.
X778-9	-10.3	+2.6	-9.2	155ºC[a]	DDH 82778, depth at 56.4m. The rest is the same as the above sample.
X50-3	-5.0	+1.0	-10.7	157ºC[c]	DDH 72450, depth at 18.4m. Calcite from fluorite-calcite vein. Trachyte as host rock.

51

					Description
X50-7	-6.9	+10.6 +4.0 (Quartz)	+4.5 (for fluids from which calcite precipitated)	270°C[e]	DDH 72450, depth at 123.95m. Calcite from main stage quartz-calcite vein. Trachyte as host rock.
X50-10	-6.3	+10.1	+4.0	270°C[e]	DDH 72450, depth at 150.9m. Main stage quartz-calcite vein. Trachyte as host rock.
X50-18	-4.6	+1.2	-10.6	155°C[a]	DDH 72450, depth at 378.5m. Disseminated calcite. Trachyte as host rock.
X49-6		+1.5 (Quartz)	-6.5 (for fluids from which calcite precipitated)	270°C[e]	DDH 72449, depth at 225.25m. Quartz from main stage quartz-calcite vein having bladed texture. Trachyte as host rock.
X49-17	-10.2	+8.4 +2.0 (Quartz)	+2.4 (for fluids from which calcite precipitated)	270°C[e]	DDH 72449, depth at 295.5m. Calcite from main stage quartz-calcite vein having bladed texture. Trachyte as host rock.
X49-31	-4.7	-1.1	-12.9	155°C[a]	DDH 72449, depth at 411.75m. Disseminated calcite. Trachyte as host rock.
X68-10	-12.5	+2.5	-3.5	270°C[e]	DDH 72468, depth at 415.9m. Calcite from main stage quartz-calcite vein. Mudstone as host rock.

Sample				Temp	Description
X83-5	-5.9	+13.7	+7.7	270°C[e]	DDH 82783, depth at 427.1 m. Calcite from main stage quartz-calcite vein with bladed texture. Trachyte dike as host rock.
X-55b	-4.6	+1.3(Calcite); -0.2 (Quartz)	-7.2 (for fluids from which quartz precipitated)	297°C[d]	Surface sample. Quartz and calcite from main stage quartz-calcite vein having bladed texture. Trachyte as host rock
X-118	-5.9	+5.9(Calcite); +3.8 (Quartz)	-0.1 (for fluids from which calcite precipitated)	270°C[e]	The same as the above.
X-19	-5.1	+7.4	+1.3	270°C[e]	The same as sample X-55b.
X-38B	-5.8	+4.0	-2.0	270°C[e]	The same as sample X-55b.
X-83	-6.7	+2.2	-3.8	270°C[e]	The same as sample X-55b.

Note: Calculations for calcite are based on the fractionation equation between calcite and water of O'Neil et al. (1969),
$1000 \ln \alpha_{CaCO3-H2O} = 2.78 \ (10^6 T^{-2}) - 3.39$; Calculations for quartz are based on the fractionation equation between quartz and water of Clayton et al. (1972), $1000 \ln \alpha_{SiO2-H2O} = 3.38 \ (10^6 T^{-2}) - 3.40$.

[a] The peak temperature of 155°C for the majority of late stage calcite-quartz veins.

[b] The homogenization temperature of ~200°C for quartz in X98-12.

[c] The homogenization temperature of 157±7.0°C for fluorite in co-existence with calcite in X50-3

[d] The homogenization temperature of 297°C for quartz of X-55b.

[e] The homogenization temperature of 270°C for the mineralizing fluid on the whole Vault property.

53
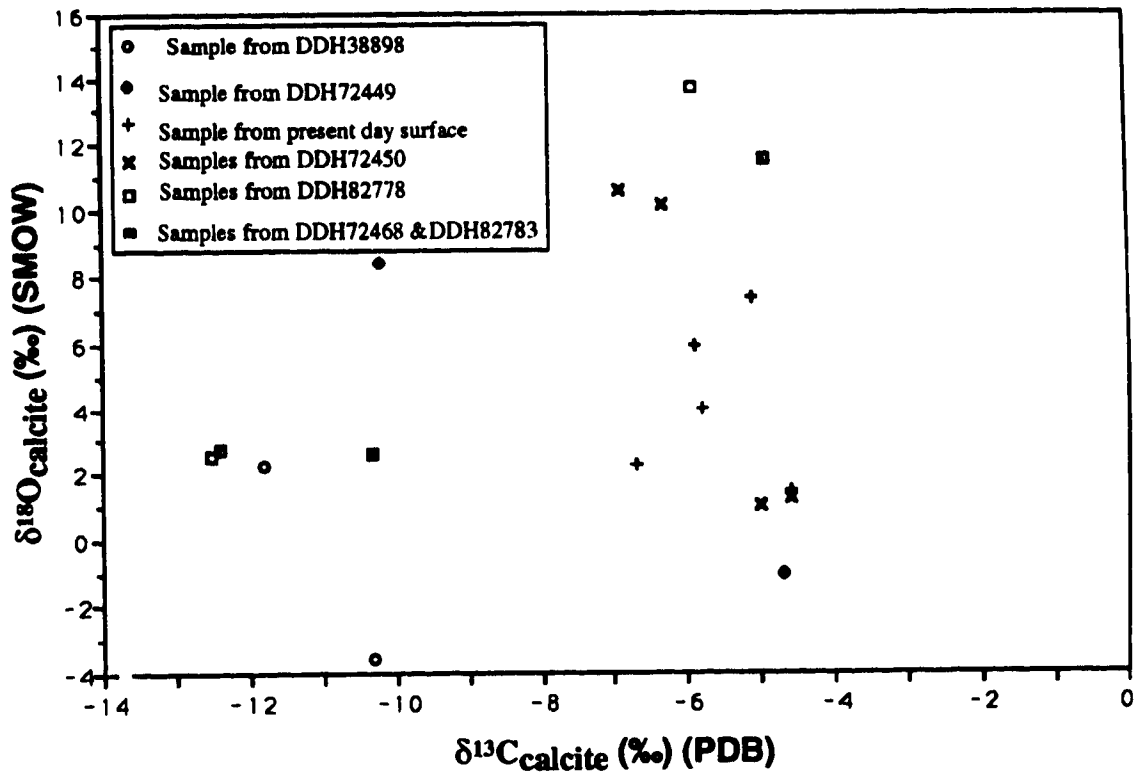
Fig. 16 Carbon and oxygen isotope data for calcite samples on the Vault property

Interpretation of Isotope Data

1. Reservoirs of Fluids

Based on isotopic fractionations between calcite and water in the temperature range of 0 to 500°C (O'Neil *et al.*, 1969), and between quartz and water in the temperature range of 250° to 500°C (Clayton *et al.*, 1972),

$$\Delta_{\text{calcite-water}} \approx 1000 \ln \alpha_{\text{calcite-water}} = 2.78 \ (10^6 T^{-2})\text{-}3.39$$

$$\Delta_{\text{quartz-water}} \approx 1000 \ln \alpha_{\text{quartz-water}} = 3.38 \ (10^6 T^{-2})\text{-}3.40$$

and homogenization temperatures, the isotopic compositions of fluids precipitating calcite and quartz were calculated (Table 8). Since on this property the temperature variation is about 100°C, this temperature change will only cause $\delta^{18}O$ variation by 5.0‰ for both calcite-water and quartz-water fractionation pairs. So the large variations (-3.6 to +13.7‰) in $\delta^{18}O$ for calcites on this property are probably due to different reservoirs of fluids or the same fluid at different water/rock ratios. The calculated fluid isotopic compositions suggest that fluids with wide range of $\delta^{18}O$ values (+7.7 to -15‰) interacted with rocks on the property.

Table 8 Calculated $\delta^{18}O_{\text{fluid}}$ Values for Mineralizations on the Vault property

Mineralization Type	Temperature	$\delta^{18}O_{\text{calcite}}$	$\delta^{18}O_{\text{quartz}}$	$\delta^{18}O_{\text{fluid}}$
Main Stage Quartz-calcite Vein (Stage II)	140°-300°C	-1.3 to +13.7	-0.2 to +6.6	-7.2 to +7.7
Fluorite-calcite vein (Stage III)	~157°C±7.0°C	+1.0		-10.7
Calcite-quartz Vein (Stage IV)	~155°C	-3.6 to +2.7		-15.0 to -9.1
Disseminated Calcite	~155°C	-1.1 to +1.2		-12.9 to -10.6

Note: Calculations for calcite are based on the fractionation equation between calcite and water of O'Neil *et al.* (1969), $1000 \ln \alpha_{\text{CaCO3-H2O}} = 2.78 \ (10^6 T^{-2})\text{-}3.39$; Calculations for quartz are based on the fractionation equation between quartz and water of Clayton *et al.* (1972), $1000 \ln \alpha_{\text{SiO2-H2O}} = 3.38 \ (10^6 T^{-2})\text{-}3.40$.

55

For samples formed at later calcite stage (Stage IV) (calcite-quartz vein in X98-12, X98-13, X778-8, X778-9), the $\delta^{18}O_{fluid}$ values are very light (from -15.4 to -9.1 ‰). These calculated values are similar to pristine or near pristine meteoric water of Tertiary-age in southern British Columbia ($\delta^{18}O_{fluid}$ = -13 ‰; Magaritz and Taylor, 1986). A calcite sample from fluorite-calcite vein (X50-3) (Stage III) also yields very ' ₁ ' $\delta^{18}O_{fluid}$ value ($\delta^{18}O_{fluid}$ = -10.7 ‰). For the samples formed at propylitic altera·' · ge as disseminated calcite (X50-18, X49-31), the $\delta^{18}O_{fluid}$ values are also very light, ranging from -12.9‰ to -10.6‰. These values only show slight shifts from meteoric water values (-15 to -13 ‰) at that time, suggesting that propylitic alteration was formed at high water to rock ratios. All of the samples mentioned above demonstrate the predominance of meteoric waters.

In contrast, samples from main stage quartz veins (Stage II) have a wide range of calculated $\delta^{18}O_{fluid}$ values from -7.2‰ to +7.7 ‰. They can be subdivided into three categories (Fig. 17). The first category is in the range of +1.3 to +7.7‰ such as XD-8, X50-7, X50-10 and X49-17. The second category is in the range of -3.8‰ to -0.1‰. This category includes all the surface samples. The third category has $\delta^{18}O_{fluid}$ value of -7.2‰ to -4.0‰. It is important to note that the calculated $\delta^{18}O_{fluid}$ values for quartz samples (X98-12, X-55b, and X49-6) (-7.2 to -4.0‰) are most reliable because quartz is resistant to oxygen isotope exchange below 450°C (Giletti and Yund, 1984) and homogenization temperatures used in the calculations of $\delta^{18}O_{fluid}$ values are obtained from X98-12 and X-55b.

Meteoric water having a $\delta^{18}O$ value of -13‰ can achieve the $\delta^{18}O_{fluid}$ values characteristic of the third category (-7.2 to -4.0‰) by interaction with volcanic rocks at temperature about 300°C at water to rock ratios (mass ratios) of ~1.00 to ~0.4 (Field and Fifarek, 1985), which is consistent with water/rock ratio calculations (see following Chapter). It is hard, however, to explain the fluids with $\delta^{18}O_{fluid}$ values of -3.8 to -0.1‰ by equilibration of meteoric water with volcanic rocks because those $\delta^{18}O_{fluid}$ values can only be achieved when water to rock ratio is low (~0.4 to ≤ 0.1) and temperature is above
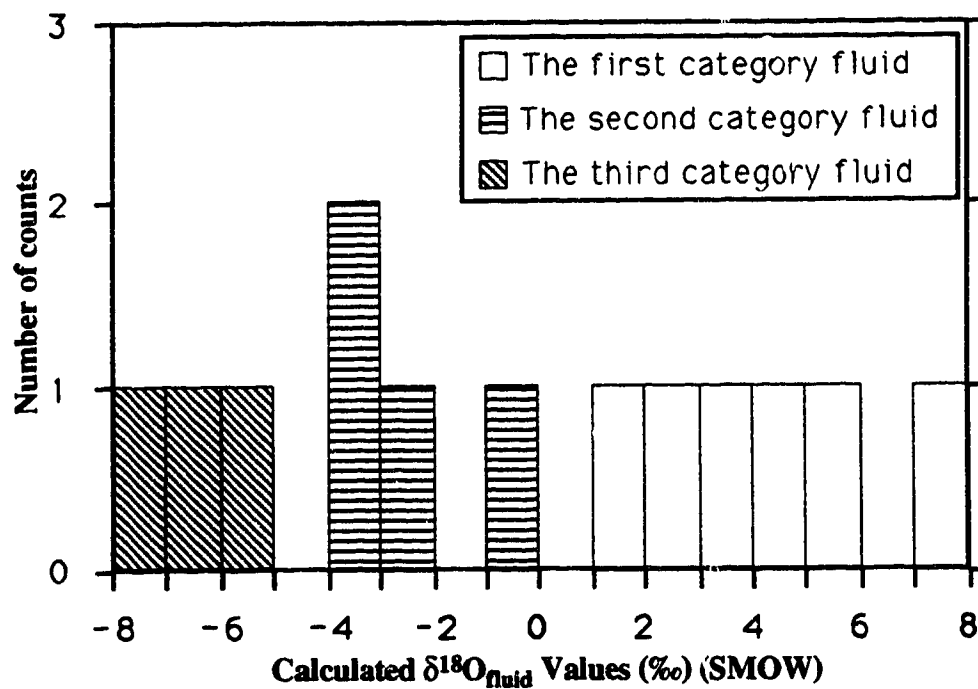
Fig. 17 Histogram showing three types of fluids for main stage quartz-calcite veins on the Vault property. The first and second types of fluids are calculated from the data for calcite samples. The third type of fluids is calculated from the data for quartz samples.

57

300^oC, which are inconsistent with both water to rock ratio calculations and temperature data from fluid inclusion studies. Similarly, it is even more difficult to invoke the equilibration mechanism to explain the $\delta^{18}O_{fluid}$ values of +1.3 to +7.7‰, since these $\delta^{18}O_{fluid}$ values requires a water to rock ratio of 0.01 or lower and a temperature of greater than 300^oC. One possible explanation is that the $\delta^{18}O$ values close to 0.0‰ are produced by boiling of fluids with $\delta^{18}O$ values of about -4.0‰ because boiling tends to result in increase in $\delta^{18}O$ values for fluids (Truesdell et al., 1977). For single-stage steam separation (boiling), the oxygen isotope composition difference between the final water (water experienced boiling) and the initial water (water did not experience boiling) is a function of initial temperature and steam separation temperature (Truesdell et al., 1977). According to Truesdell et al. (1977), for a fluid with the initial temperature about 300^oC and the boiling temperature about 250^oC, the $\delta^{18}O$ difference between the final water and initial water is only about 0.5‰; for a fluid with the same initial temperature as the above, but with a boiling temperature of 93^oC, the $\delta^{18}O$ difference is about 3‰. Since fluid inclusion data suggest that boiling probably occurred at around 270^oC, it is unlikely that boiling can produce a $\delta^{18}O$ difference of at least 8‰ between the initial water and final water required to account for the $\delta^{18}O$ differences between +1.3-+7.7‰ and -7.2 to -4.0‰, and between +1.3-+7.7‰ and -3.8‰ to -0.1‰. Instead, it is likely that fluids with $\delta^{18}O$ values ranging from +1.3 to +7.7‰ were contributed by a magma or a meteoric water source equilibrated with rocks equilibrated with rocks over long flow length. The latter is more likely since high salinity inclusions have not been observed. It is possible that meteoric water can have long equilibrium history with rocks by entering the detachment fault. The fluid with $\delta^{18}O$ values ranging from -3.8 to -0.1‰ may be a result of mixing process between a fluid with $\delta^{18}O$ values ranging from -7.2 to -4.0‰ equilibrated with volcanic rocks and fluid with $\delta^{18}O$ values ranging from +1.3 to +7.7‰.

However, the high $\delta^{18}O$ values of calcite samples used in calculations of the fluids of the first and second categories might be achieved when the calcites continued to be in

isotopic equilibrium with a fluid with $\delta^{18}O$ of -7.2 to -4.0‰ below 100°C. As mentioned

before, the temperature change on the property is no more than 120°C (270°C ⇒ 150°C)

(the temperature at beginning of boiling on the Vault property is 270°C, and the

temperature at the end of the boiling is 150°C; refer to Fig. 15). Therefore, it is not likely

that temperature by itself can account for the $\delta^{18}O$ variations (+1.3‰ ⇒ +13.7‰) for the

calcite samples.

2. Carbon Sources in Fluids

Carbon in hydrothermal fluids can be present in a number of forms but primarily as

CO_2 or CH_4. According to Ohmoto (1986), only the $\delta^{13}C$ value of ΣCO_2 may be

diagnostic of its source. Carbon-isotope compositions of hydrothermal carbonates are a

function of the T, Eh, and pH during precipitation, as well as the $\delta^{13}C_{\Sigma C}$ of the

hydrothermal fluids (see Ohmoto and Rye, 1979). The $\delta^{13}C$ value of ΣCO_2 can be

calculated from the $\delta^{13}C$ value of the carbonate mineral using (i) the fractionation factors

between the mineral, $H_2CO_{3apparent}$ ($CO_{2,aq}$ + H_2CO_3) or HCO_3^- , and between the

aqueous carbonate species, and (ii) the relative abundance of $H_2CO_{3apparent}$ and HCO_3^- in

the fluid (Ohmoto, 1972; Ohmoto and Rye, 1979). Because most homogenization

temperatures of fluid inclusions are above 150°C, the amount of HCO_3^- is negligible

compared to the amount of $H_2CO_{3apparent}$, therefore, the following approximation can be

made (Ohmoto, 1986):

$$^{13}C_{\Sigma CO2} = {}^{13}C_{carb.\ min.} - \Delta_{carb.\ min.-H2CO3\ apparent}$$

Since typical epithermal (geothermal) fluids usually exist at temperatures less than

those needed to establish isotopic and chemical equilibrium between CO_2 and CH_4

(Ohmoto, 1986), and the condition of f_{O2} is above CO_2-CH_4 and close to QFM (hematite

is observed in altered rocks on the Vault property), the $\delta^{13}C_{\Sigma CO2}$ is approximately equal to

$\delta^{13}C_{\Sigma C}$ (Ohmoto, 1986), and equal to $\delta^{13}C_{fluid}$. Carbon isotope fractionation factors,

$\Delta_{carb.min.-H2CO3\ apparent}$, for systems containing H_2CO_3, are not known, but this

species can probably be isotopically approximated by $CO_{2(gas)}$ (Ohmoto, 1986). Thus the

CaCO$_3$-CO$_2$ calculated carbon isotope fractionation factors of Bottinga (1969) can be used

to approximate CaCO$_3$-H$_2$CO$_3$ fractionation. Assuming that the homogenization

temperatures of 150-160°C is representative temperatures of trapping for the majority of

calcite samples, the fractionation between CO$_2$-CaCO$_3$ at 150-160°C is about -1.5‰

(interpolated from Fig. 6 of Chacko et al., 1991) for ^{13}C, which can be neglected.

Therefore, the following assumption is justified,

$$\delta^{13}C_{CaCO3}\approx\delta^{13}C_{H2CO3\ apparent}\approx\delta^{13}C_{\Sigma CO2}\approx\delta^{13}C_{fluid}$$

Based on the above assumption, half of δ^{13}C values fall into the probable range of

igneous carbon (-5‰ to -8‰, Taylor et al., 1967), and six samples cluster around -5‰,

the best average value for igneous carbon (Craig, 1953). Six samples fall into the range of

organic carbon area (δ^{13}C <-10‰, Ohmoto, 1986). Carbon isotope data demonstrated that

carbon reservoirs are strongly controlled by host rocks. For the carbonates hosted by

mudstone, such as X98-12, and X98-13, etc., their δ^{13}C values (-12.5 to -10.3‰) may

suggest an organic carbon signature (Table 7). Alternatively, these values might represent a

mixture of organic and igneous carbon sources or a mixture of organic and soil carbon

sources. However, because the hydrothermal activities in the study area immediately

followed the volcanism (see Chapter V), there would be little soil formed at the time of

mineralization, which would make the latest alternative unlikely. In contrast, the carbonate

samples hosted by trachyte have an igneous carbon signature. The igneous carbon for the

fluid can be contributed from interaction of the fluid with condensates of volcanic gas or

from interaction of the fluid with igneous carbon trapped in volcanic rocks in the form of

fluid inclusions, or from magmatic fluid from plutonic rocks. Only sample X49-17 is an

exception. It is hosted by trachyte, but has a δ^{13}C value of -10.2‰. This sample probably

represents a mixing of organic carbon and magmatic carbon. No samples fall into the

marine limestone carbon region. In addition, the relatively small range of δ^{13}C values for

samples in the magmatic carbon field and adjacent samples implies that the solution was

buffered such that the dominant carbonate species was H$_2$CO$_{3apparent}$, as suggested by

Golding and Wilson (1983) for the $\delta^{13}C$ values in Kalgoorilie, Western Australia. The conclusion that dominant carbonate species was $H_2CO_{3apparent}$, is also supported by the positive correlation between $\delta^{13}C$ and $\delta^{18}O$ values of calcites for the samples at the present-day surface (Fig. 16), because the positive correlation between $\delta^{13}C$ and $\delta^{18}O$ of carbonates is usually yielded by the precipitation of calcite from a H_2CO_3 fluid (Zheng, 1990). This conclusion also supports the assumption at the beginning of this paragraph.

Fig. 18 shows that most of samples did not show variations of $\delta^{13}C$ and $\delta^{18}O$ values with elevation. Only samples from DDH72449 shows a slight positive correlation between $\delta^{13}C$ and elevation, and between $\delta^{18}O$ and elevation. So the isotopic variations on the property are probably due to different source reservoirs, not due to elevation or temperature effect as observed in the Golden Cross, New Zealand (de Ronde and Blattner, 1988) or in San Juan Mountains, Colorado (Bethke and Rye, 1979).

3. Isotopic Disequilibrium

In sample X-55B, $\delta^{18}O$ values for quartz and calcite are $-0.2‰$ and $+1.3‰$, respectively. According to the fractionation relation between quartz and calcite (Clayton and Kieffer, 1991),

$$\Delta_{quartz\text{-}calcite} \approx 1000 \; ln\alpha_{quartz\text{-}calcite} = 0.335 \; (10^6T^{-2})+0.05 \; (10^6T^{-2})^2 - 0.0035 \; (10^6T^{-2})^3$$

at temperature of 300^oC (homogenization temperature for X-55b), the calculated $\delta^{18}O$ value for calcite should be $-1.58‰$. In comparison with its measured $\delta^{18}O$ value ($+1.3‰$), the difference is about 2.8 per mil, clearly indicating that quartz and calcite are not in isotopic equilibrium. This slight disequilibrium is also observed in the data set of X50-7 ($\delta^{18}O_{calcite} = +10.6‰$; $\delta^{18}O_{quartz} = +4.0‰$), X49-17 ($\delta^{18}O_{calcite} = +8.4‰$; $\delta^{18}O_{quartz} = +2.0‰$), and X-119 ($\delta^{18}O_{calcite} = +5.9$; $\delta^{18}O_{quartz} = +3.8‰$). This slight isotopic disequilibrium may mean that calcite samples might suffer retrograde process to some degrees. However, because the quartz and calcite pair is only in slight isotopic disequilibrium as indicated by sample X-55b, the calculated $\delta^{18}O_{fluid}$ values for calcite samples are still valid.

61
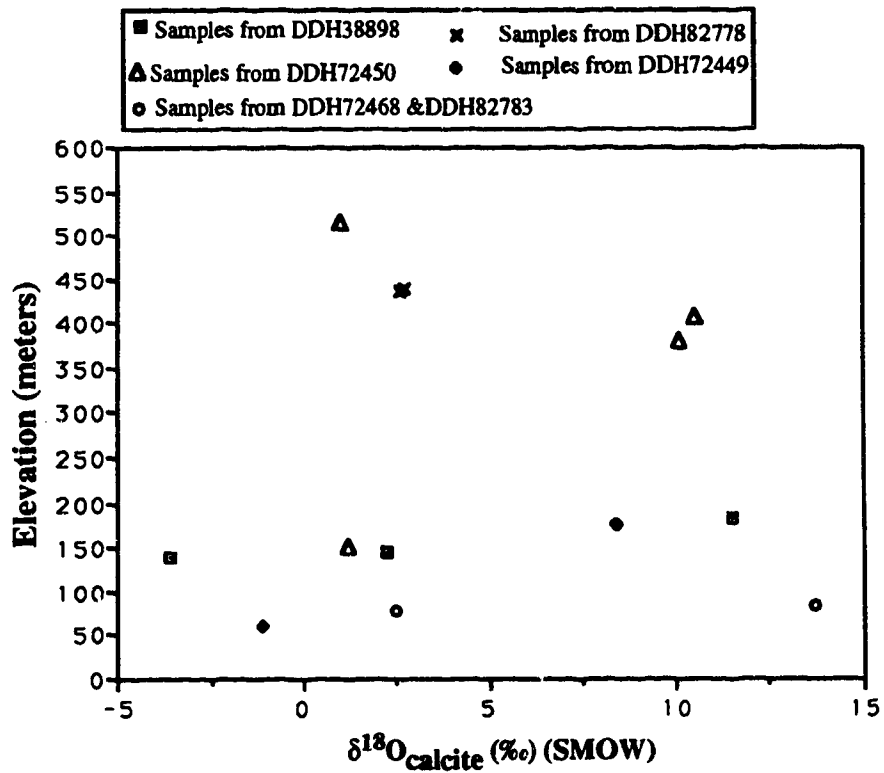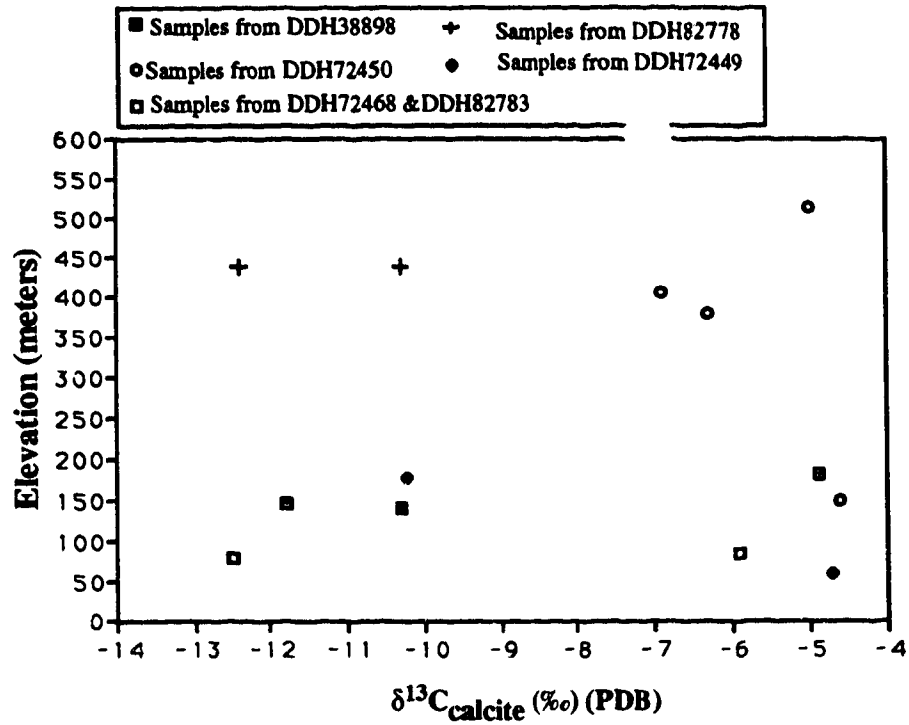
Fig. 18   Variations of $\delta^{13}C$ and $\delta^{18}O$ values of calcite samples with elevations on the Vault property

IV. STABLE ISOTOPE AND FLUID INCLUSION STUDIES ON REGIONAL HYDROTHERMAL SYSTEMS

Introduction

As pointed out by Criss and Champion (1991), oxygen isotope studies, especially on igneous whole rocks, have tremendous potential in deciphering the nature of hydrothermal processes on a regional scale, in part because the $\delta^{18}O$ values of unaltered rocks fall within rather narrow and well understood ranges. Deviations from these ranges produced by alteration are therefore readily apparent. Regarding fossil meteoric water-dominated systems, a number of studies have been made following two subparallel paths (Seal and Rye, 1992). One approach has been to study regional isotopic alteration patterns in country rocks surrounding shallow-level intrusions and interprets these patterns in terms of interactions with altering hydrothermal fluids (Criss and Taylor, 1986; Criss and Fleck, 1987; Criss and Champion, 1991; Soloman and Taylor, 1991; Larson and Zimmerman 1991). The other approach has been to study the isotopic evolution of ore fluids from specific ore deposits and interprets the evolution of ore fluids in terms of interactions between the hydrothermal solutions and country rocks (Taylor, 1979; Campbell et al., 1984). To date, however, few studies have united both lines of research (Seal and Rye, 1992).

Previously, the isotope studies on regional and ore deposit scale in the Okanagan Valley region had been conducted separately by Taylor and Magaritz (1978), Magaritz and Taylor (1986), and Zhang et al. (1989). As a part of their systematic regional stable isotope studies on plutonic rocks in the Canadian Cordillera, Taylor and Magaritz (1978) and Magaritz and Taylor (1986) studied the Okanagan and Nelson batholiths. Magaritz and Taylor (1986) found that most of the granitic rocks of Okanagan Batholith (185-150 Ma, Rb/Sr ages; Armstrong, 1988) in Okanagan Lake traverse were intensely chloritized and were depleted in ^{18}O (e.g., $\delta^{18}O_{feldspar}$ = -2.8 to +6.7 in samples collected along the edge of Okanagan Lake). Magaritz and Taylor (1986) concluded that hydrothermal systems

63

associated with the Tertiary porphyries are responsible for the ^{18}O depletions, because at a given locality, the dikes and porphyries consistently have lower $\delta^{18}O$ values than the granitic country rocks that they had intruded.

Zhang (1986) and Zhang *et al.* (1989) studied the Dusty Mac property. On an ore deposit scale, Zhang *et al.* (1989) concluded that the mineralization was formed by fluids with $\delta^{18}O$ values of -7 to -9‰. Based on these data in combination with fluid inclusion data, they proposed that meteoric water was responsible for the formation of epithermal mineralization on the Dusty Mac property.

The present study seeks to combine both approaches to help characterize the relationship between regional water-rock interactions and ore-forming processes. On the basis of the studies on the Vault property, the regional stable isotope study focuses on the Tertiary volcanic rocks, since epithermal systems in this region are hosted by the Tertiary volcanic rocks. In addition, the present study is also different from other regional isotope studies in that this study deals with a smaller scale area (about 340 km²) in comparison with similar studies which dealt with large scale regions (more than 5000 km²) (Criss and Taylor, 1986; Criss and Fleck, 1987; Criss and Champion, 1991). So the results from such a medium scale study may be more useful for exploration.

Data from This Study

In this study, about 50 whole rock volcanic samples plus 13 calcite samples were collected to analyze for oxygen and carbon isotope compositions. The results are listed in Table 9. The $\delta^{18}O_{whole-rock}$ values range from -6.8 to +9.9‰. The $\delta^{18}O_{calcite}$ values range from -3.8 to +15.5‰, and $\delta^{13}C_{calcite}$ values range from -15.0 to -4.3‰.

Data in Table 9 and Fig. 19 show that fresh felsic volcanic rocks in the area from Yellow Lake to Twin Lakes, and to the Marron Valley have $\delta^{18}O_{whole-rock}$ values ranging from +5.8 to +7.0‰. Such values are normal for felsic igneous rocks (Taylor, 1968). However, from the Marron Valley to Okanagan Falls, and to Penticton, $\delta^{18}O$ analyses of whole rock samples indicate mild to extreme depletions in ^{18}O (Fig. 19). Based on the

Table 9 Stable Isotope Data for Whole Rock and Calcite Samples in Okanagan Falls Area

Sample Number	$\delta^{18}O_{whole\ rock}$ ‰	$\delta^{13}C_{Calcite}$ ‰	$\delta^{18}O_{Calcite}$ ‰	$\delta^{18}O_{water}$ ‰	Rock Type	Sample description and Assemblage of alteration mineralogy for whole rocks, and distance away from the detachment fault (in meters)
					Samples in area from Yellow Lake to Twin Lake and to the Marron Valley	
RB-72	+9.9				Trachyte	Fresh pyroxene phenocrysts, very weakly altered plagioclase phenocryst. 14350m
XY-22	+6.9				Trachyte	Fresh sanidine phenocrysts, weakly altered plagioclase phenocrysts(altered by minor epidote and chlorite); groundmasses are weakly altered by epidote. 6450m
RB-73	+6.6				Dioritic porphyry	Weakly altered biotite phenocrysts; pyroxene and plagioclase phenocrysts were cut by sericite-veinlets. 12775m
XY-12	+6.6				Fresh biotite trachyte	Plagioclase phenocrysts are fresh. 8200m
XY-18	+6.5				Pyroxene trachyte	Most of pyroxene phenocrysts are fresh; a few of them were partially replaced by calcite. Plagioclase phenocrysts are fresh. 10800m
XY-19	+6.4				Trachyte	Most of plagioclase phenocrysts are fresh; a few of them were partially replaced by sericite. 10300m
XY-16	+5.9				Fresh hornblende trachyte	Hornblende phenocrysts are fresh. 11350m
XY-15	+5.8				Fresh trachyte	
XY-20	+5.0				Propylitic biotite trachyte	10700m
						Chl+Py replace both plagioclase phenocrysts and groundmasses. Most of biotite phenocrysts are fresh. Sanidine phenocrysts are fresh. The abundance of calcite is very low. 9250m
					Samples From Penticton to Kaledan (the Northern Hydrothermal System)	
XP-1	+3.9				Weakly silicic Trachyte	Propylitic alteration overprinted by silicic alteration: Qtz+Cal+Clay+Hem assemblage. Sanidine phenocrysts are fresh. 1100m
XP-2	-6.0	-3.6		-11.3[a]	Propylitic trachyte	Vein calcite
XP-3	-3.5				Strongly Propylitic phenocryst-rich trachyte	Cal+Py+Chl replace most of plagioclase phenocrysts. Calcite is abundant. 1875m

65

Sample		Rock type / alteration				Comments
XP-4	-6.1	Strongly Silicic trachyte				Propylitic alteration is overprinted by argillic alteration, which in turn is overprinted by silicic alteration. Chlorite and calcite replaced plagioclase phenocrysts; chlorite is replaced by clay minerals. Quartz replaces some of clay minerals. 2250m
T-1	-6.8	Strongly Propylitic trachyte	-6.6	1.0	-5.5[b]	Calcite wholly replaces most of plagioclase phenocrysts. Chlorite, hematite, and limonite replace some of plagioclase. Calcite for isotope analysis is in disseminated form. 1700m
		Samples near the Vault property (the Vault Epithermal System)				
XP-6	+2.5	Argillic trachyte				Propylitic alteration is overprinted by argillic alteration. 3750m
R-2	+4.1	Propylitic trachyte with carbonate veining	-5.3	+2.8	-11.4[c]	Calcite isotope analysis is from vein calcite. 6250m
X-46C	+3.4	Argillic trachyte				Clay minerals replace groundmass and plagioclase phenocrysts. Argillic alteration is overprinted by silicic alteration, which has assemblage of quartz+hematite. Some good crystals of quartz overgrew around chalcedony. 4500m
X-83	+3.4	Argillic trachyte	-6.7	+2.2	-3.8[h]	Vein calcite. 4500m
XP-7	+0.8	Silicic trachyte	-14.4	+2.7	-11.5[c]	Chlorite and calcite replace plagioclase phenocrysts. Propylitic alteration was overprinted by silicic alteration. Chlorite is partially replaced by quartz. Calcite isotope analysis is from disseminated calcite. 3300m
XY-25	+0.4	Argillic pyroclastics				Chlorite, pyrite and carbonate (small amounts) severely altered the groundmass, and partially altered plagioclase phenocrysts. Some of chlorite is replaced by clay mineral, pyrite is replaced by hematite. 3850m
XY-2	+0.3	Silicic trachyte				Quartz and pyrite as alteration assemblage. 4650m
R-4	+0.2	Propylitic trachyte porphyry				Chl+Cal+Py assemblage replaces plagioclase phenocrysts. 6250m

Sample		Rock type				Description
XY-1	+0.1	Propylitic trachyte				Carbonate and hematite severely altered the rock. Plagioclase phenocrysts are wholly or partially replaced by carbonate. No chlorite is observed. 4500m
XP-5	-1.8	Propylitic pyroxene trachyte				Propylitic alteration overprinted by silicic alteration, and sericitic alteration. Chl+ Cal+Py replace plagioclase and pyroxene phenocrysts. Calcite also replaces groundmass. 2950m
XY-3		Propylitic trachyte	-4.9	+7.0	-7.1c	Calcite isotope analysis is from disseminated calcite.

Samples in the area from the Vault to the Observatory (the Southern Hydrothermal System)

Sample		Rock type				Description
XY-7	+7.3	Weakly altered pyroxene-rich trachyte				Most of pyroxene phenocrysts are fresh. Only a few of them are replaced around the edge of the crystals by chlorite. 4850m
XY-4	+6.6	Fresh trachyte				Plagioclase phenocrysts are fresh. 5000m
XY-6	+3.8	Propylitic trachyte				4500m
XY-8	+3.7	Propylitic rhyolite				4500m
XY-5	+1.8	Argillic trachyte				Plagioclase phenocrysts are altered to clay minerals. 4600m

Samples from Green Lake to Willowbrook to Observatory

Sample		Rock type				Description
XY-9	+7.5	Fresh pyroclastics	-9.1	+6.8	-3.7d	Disseminated calcite for stable isotope analysis. 4300m
XW-2	+7.5	Silicified rhyolite?				750m
XY-10	+7.0	Fresh biotite tuff				Biotite phenocrysts are fresh. Small amounts of chlorite replaces groundmass. 6000m
X-7	+6.6	Propylitic breccias	-6.6	+5.4	-3.3e	Chl+Cal+Py+Qtz; fragments are strongly altered by calcite. Vein calcite for stable isotope analysis 300m
XW-5	-1.5	Silicic trachyte				Propylitic alteration is overprinted by silicic alteration. 600m
RB-BN-1*	-2.9	Chlorite breccia				Mahoney Lake
XW-1	-3.4	Chloritic gneiss				350m

67

Sample	Rock type				Notes
	Propylitic trachyte				
V-4		-3.6			calcite+chlorite+pyrite. Calcite veining. 3500m
V-4b	Silicic trachyte	-3.9	-8.0	-12.4d	Propylitic alteration is overprinted by silicic alteration assemblage. Chl+Cal+Qtz (veinlets). Chl+Cal mainly replaced plagioclase phenocrysts. Vein calcite for stable isotope analysis. 2700m
RB-BN-2*	Gneiss with quartz veinlets	-4.5			
					Mahoney Lake
V-53	Gneiss with calcite veinlets		-14.9±0.01	-5.0e	Mahoney Lake: Calcite isotope analysis is from vein calcite.
	Samples near the Dusty Mac (the Dusty Mac Epithermal System)				
XM-7	Argillic trachyte	+1.8	+3.8±0.03		Propylitic alteration is overprinted by argillic alteration. Some of the sanidine phenocrysts are still fresh. Most of plagioclase phenocrysts are replaced by carbonates. ...l+Chl (remains) +Clay +Hem. Most of chlorite are replaced by clay. 650m
XM-1	Silicic trachyte	+1.6			Quartz and calcite replace plagioclase phenocrysts. Biotite phenocrysts are replaced by calcite and hematite. 500m
XM-11	Silicic Trachyte	+1.6			Propylitic alteration is overprinted by silicic alteration. Cal+Qtz mainly replace plagioclase phenocrysts. Chlorite is replaced by calcite. 1750m
Ma-5	Argillic trachyte	-0.3			1350m
Ma-7	Argillic trachyte	-1.1			1300m
M-7	Argillic trachyte	-1.1			1000m
M-3	Argillic trachyte	-1.5			~1005m
M-4	Argillic trachyte	-1.5			~1009m
XM-10	propylitic trachyte	-1.8			Chlorite, calcite and pyrite replace plagioclase phenocrysts. 1600m
O-01	Strongly argillic trachyte	-6.1	-3.8	-15.3f	Vein calcite for stable isotope analysis. 1550m

O-3	Strongly argillic trachyte	-3.0	-5.1	+0.5	-10.4g	Most of plagioclase phenocrysts are replaced by clay minerals. Argillic alteration overprints propylitic alteration (some chlorite remains can be seen). Calcite isotope analysis is from vein calcite. 1550m
X-11	Propylitic trachyte	-4.0				Most of plagioclase phenocrysts are replaced by carbonates, pyroxene and biotite phenocrysts are altered by chlorite and pyrite, some of which is altered to hematite. 2500m
M-2	Argillic trachyte	-4.3		+15.5	+3.9g	Vein calcite for stable isotope analysis.

Note:
a Calculated at mean homogenization temperature of 229°±8°C (12) for XP-2
b Calculated at mean homogenization temperature of 257°±3°C (6) for T-1
c Calculated at mean homogenization temperature of 125°±5°C (3) for R-2
d Calculated at mean homogenization temperature of 174°±4°C (3) for V-4b
e Calculated at mean homogenization temperature of 206°±7°C (6) for V-53
f Calculated at mean homogenization temperature of 159°±11°C (7) for O-01
g Calculated at mean homogenization temperature of 167°±1°C (4) for O-3
h Calculated at mean homogenization temperature of 270°C for the Vault property.
* Unpublished data from Dr. Bruce E. Nesbitt.
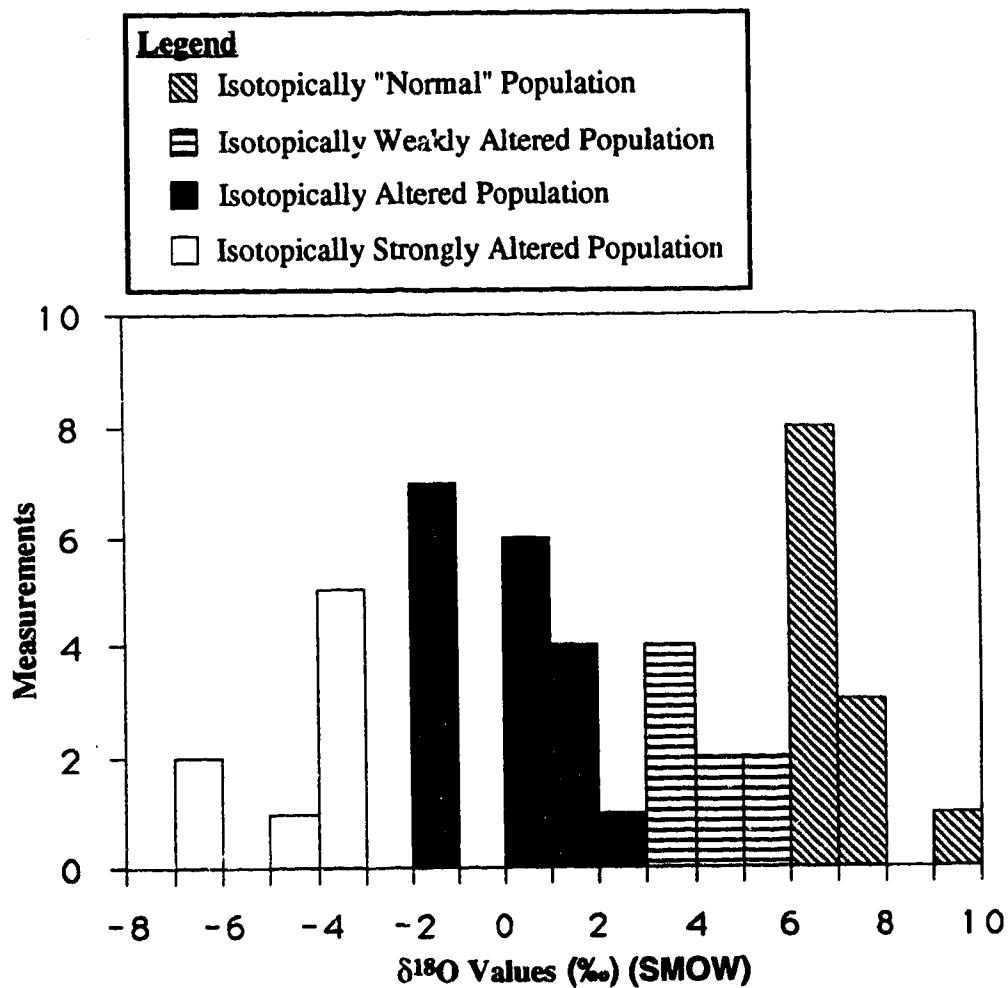
Fig. 19 Histogram of whole-rock $\delta^{18}O$ de_rminations for surface samples
from the Okanagan Falls area. The histogram displays a population of isotopically
"normal" rocks ($\delta^{18}O \geq$ +6), a population of weakly altered rocks (+3 < $\delta^{18}O$ < +6),
a population of altered rocks (-2 < $\delta^{18}O$ < +3), and a population of "strongly altered"
rocks ($\delta^{18}O$< -2) affected by exchange with significant volumes of low-^{18}O fluid.

$\delta^{18}O$ data on whole rocks, four depletion zones are defined: one around the Dusty Mac (the Dusty Mac Hydrothermal System, $\delta^{18}O_{whole-rock}$ values ranging from -4.0 to +1.8‰), one around the Vault property (the Vault Hydrothermal System, $\delta^{18}O_{whole-rock}$ values ranging from about -1.8 to +4.1 ‰), one in the south, around Willowbrook (the Southern Hydrothermal System, $\delta^{18}O_{whole-rock}$ values ranging from -3.9 to +7.59 ‰), and one in the north, the Northern Hydrothermal System, $\delta^{18}O_{whole-rock}$ values ranging from -6.8 to +3.9 ‰) (Fig. 19, and also refer to Fig. 20, and Fig. 21).

Interpretation of the Whole Rock Oxygen Isotope Data

(1) The Relation Between Depletions in ^{18}O

and Alterations of Rocks

There are four populations of $\delta^{18}O_{whole-rock}$ values divided in Fig. 19 in terms of degrees of depletions in , i.e., one population of isotopically "normal" rocks ($\delta^{18}O \geq +6‰$), one population of weakly altered rocks ($+3.2‰ < \delta^{18}O < +6‰$), one population of altered rocks ($-2.2‰ < \delta^{18}O < +3.2‰$), and one population of extremely altered rocks ($\delta^{18}O < -2.2‰$).

The results shown in Fig. 19 in combination with petrographic data in Table 9 suggest that there is a correlation between depletion in $\delta^{18}O$ and the degree of mineralogical alteration of the rocks. In the area from Yellow Lake to Twin Lake to Marron Valley, the $\delta^{18}O_{whole-rock}$ values are typical of "normal" igneous rocks (Taylor, 1968). The normal $\delta^{18}O_{whole-rock}$ values correspond to fresh or only very weakly altered samples. In this group samples, only XY-20 has been propylitically altered. It has lower $\delta^{18}O_{whole-rock}$ value (+5.0‰) compared with the rest of samples in this group. In contrast, the samples in the area from Penticton to Kaledan have extremely low $\delta^{18}O_{whole-rock}$ values (ranging from -6.8 to +3.9‰). The rocks in this area are characterized by weak silicic alteration (XP-1, +3.9‰), strong silicic alteration (XP-4, -6.1‰), and strong propylitic alteration (T-1, -6.8‰). Thin section examination shows that T-1 is strongly altered to calcite. In the less altered area from Green Lake to Willowbrook, and to the Astrophysical Observatory, the

71

$\delta^{18}O_{whole-rock}$ values cluster into two populations, with one being characteristic of fresh rocks (+7.0 to +7.5‰) and the other being characteristic of strongly altered (-3.9‰) to weakly altered rocks (+6.5‰, metamorphic breccias). In the area from the Vault property to the Astrophysical Observatory, the $\delta^{18}O_{whole-rock}$ values range from +7.3 to +1.8‰. The rocks from this area are characterized by no alteration or weak alteration (propylitic alteration). The overprint of propylitic alteration by silicic or argillic alteration is not common. However, in mineralized areas, even though alteration was intense, a more narrow range of higher $\delta^{18}O_{whole-rock}$ values is observed compared with the extremely ^{18}O-depleted areas. The samples around the Vault property have a small range of $\delta^{18}O_{whole-rock}$ values from -1.8 to +4.1‰. In this area, the dominant alteration styles are argillic and silicic with propylitic alteration as a background alteration. The propylitic alteration is commonly overprinted by argillic or silicic alteration. Similarly, in the area around the Dusty Mac deposit, the $\delta^{18}O$ values also exhibit a small range for the majority of $\delta^{18}O_{whole-rock}$ values (-2.0 to +1.8‰). The propylitic alteration is also commonly overprinted by argillic or silicic alteration.

The above data show that in the mineralized areas overprint of propylitic alteration by argillic or silicic alteration is typical. It seems that this overprinting process tends to constrain the $\delta^{18}O_{whole-rock}$ values to a relatively narrow range, and to have relatively higher $\delta^{18}O_{whole-rock}$ compared with extremely ^{18}O-depleted areas. This implies that the mineralized fluids are evolved meteoric waters which are unlikely to produce extremely depleted $\delta^{18}O$ values. In contrast, extremely ^{18}O-depleted areas are unmineralized (see the Mineralization Model chapter).

(2) The Relation between Depletions in ^{18}O And the Distance away from the Detachment Fault

Figure 20 shows the relation between depletions in $\delta^{18}O_{whole-rock}$ and the distance away from the detachment fault. There is a negative correlation between the distance away from the detachment fault and the depletion in ^{18}O in whole rocks. For example, in the

72

Distance away from the Detachment F__lt (in Meters)
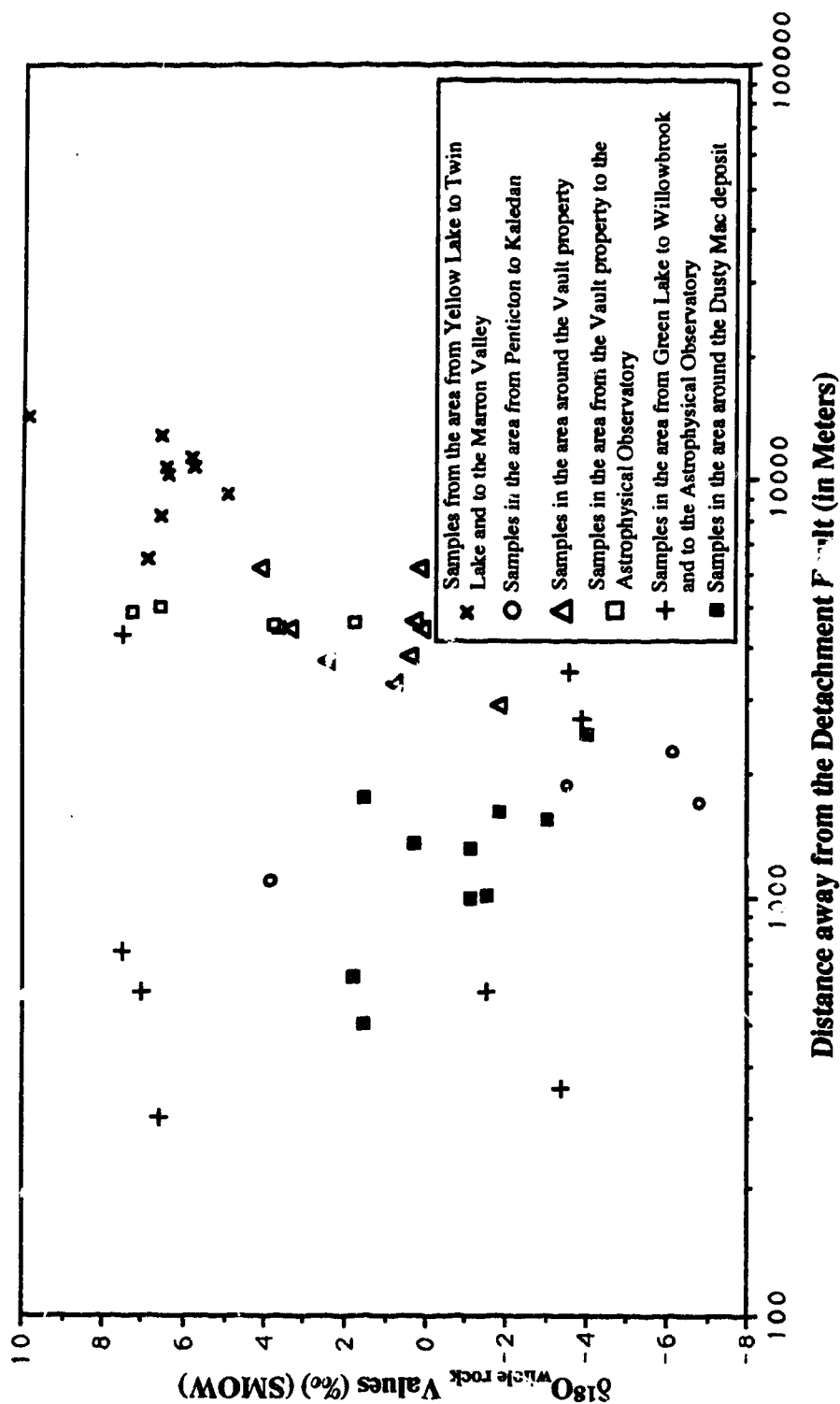
Fig. 20 A plot showing $\delta^{18}O_{whole-rock}$ values against the distance away from the detachment fault in the Okanagan Falls area. There is a tendency in which depletions in ^{18}O in whole rock samples increase with the decrease in the distance away from the detachment fault.

areas far away from the detachment fault such as in the Yellow Lake, normal $\delta^{18}O_{whole-rock}$ values are observed, whereas in areas close to the detachment fault such in the area from Penticton to Kaleden extremely depleted $\delta^{18}O_{whole-rock}$ values are observed.

This relation may imply that the detachment fault provided channelways for pristine meteoric waters to penetrate into volcanic rocks. As suggested by Criss and Champion (1991), the most direct and straightforward way to determine whether the fluid flow in a fossil hydrothermal system was channelized or pervasive is to examine lateral $\delta^{18}O_{whole-rock}$ variations on different scales. According to these workers, if the subsurface flow was dominantly channelized on a regional scale, then extremely sharp gradients in the $\delta^{18}O_{whole-rock}$ values should occur near the major structures, and rocks further away should all have normal values. If the flow was dominantly channelized b.)i a smaller scale, then different samples from individual outcrops should have high $\delta^{18}O_{whole-rock}$ values, depending on the proximi controlling minor structures such as small faults and joints. If, on other hand, the f ... minantly pervasive, the $\delta^{18}O_{whole-rock}$ values should exhibit smooth lat. variations on a large scale, and different samp' from single outcrops would have similar $\delta^{18}O_{whole-rock}$ values. Generally speaking, the results of this study demonstrate that the fossil hydrothermal systems in the Okanagan Falls area were channelized on a regional scale and pervasive on a small scale as shown by the sharp contrast in $\delta^{18}O_{whole-rock}$ values between th. Yellow Lake area (far away from the detachment fault) and Penticton-Kaleden area (close to the detachment fault), and similar $\delta^{18}O_{whole-rock}$ values in a mineralized hydrothermal system, respectively. This is different from the case in the Comstock Lode Mining District, Nevada (Criss and Champion, 1991), where the fossil hydrothermal systems were pervasive on a regional scale as suggested by uniform $\delta^{18}O$ values of rocks in the strongly altered zone whose permeability is dominantly controlled by micro-fractures.

74

(3) The Relation between Depletions in ^{18}O and Locations of Mineralization

To show the relation between depletions in ^{18}O in whole rocks and localities of mineralized hydrothermal system, a $\delta^{18}O_{whole-rock}$ value contour map is compiled (Fig. 21), since according to Criss and Champion (1991), contour maps of $\delta^{18}O$ values provide remarkably regular images of the integrated intensity of fluid circulation in fossil hydrothermal systems, and many different types of ore deposits are hosted in rocks with anomalous $\delta^{18}O$ values, with mineralization being particularly concentrated in zones where gradients are steepest.

The $\delta^{18}O_{whole-rock}$ value contour map shows that there are sharp isotopic gradients between the mineralized area(s) and non-mineralized area. In the neighborhood of the Dusty Mac deposit, $\delta^{18}O_{whole-rock}$ values sharply decrease from about +1.6 to -2.0 ‰ over a distance of less than 700 m. Similarly, in the neighborhood of the Vault property, $\delta^{18}O_{whole-rock}$ values also sharply decrease from about +2.5 to 0.0 ‰ over a distance of less than 850 m (Fig. 21). This phenomena may be partly due to higher density of sampling around the mineralized areas. In addition, in the neighborhood of Green Lake, where Skaha Formation, composed of gneissic fragments, occurs, the $\delta^{18}O$ analysis (+6.6‰) for a sample from a mineralized outcrop mapped by the author in 1991 in Skaha Formation also shows a depletion since normal $\delta^{18}O$ values for gneisses are usually larger than +10.0‰ (Valley, 1986). The conclusion that mineralization is associated with sharp $\delta^{18}O$ gradients but not associated with extremely ^{18}O-depleted areas may be of exploration significance.

Additionally, in the mineralized areas, such as the Vault property and the Dusty Mac deposit, one interesting feature is that $\delta^{18}O_{whole-rock}$ values are in a narrow range, which means that the mineralizing fluids were isotopically homogenized and that the mineralizing fluids are pervasive on a small scale. The pervasive nature of fluid flow on a small scale and the homogenization nature of the mineralizing fluids in terms of oxygen isotopes are

75
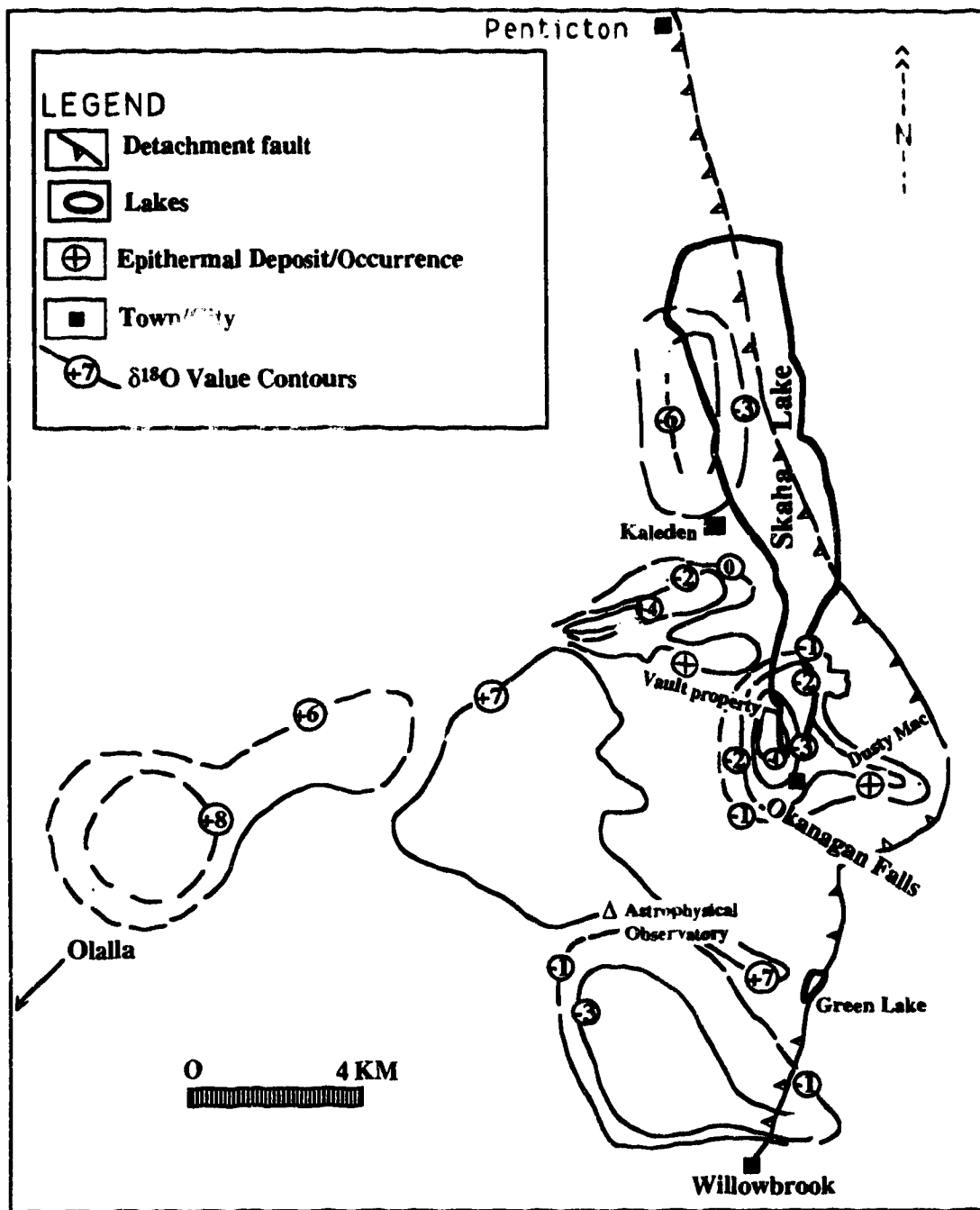
Fig. 21 $\delta^{18}O_{whole-rock}$ value contours and sample locations in the Okanagan Falls area

further indicated by a series of samples from the Dusty Mac deposit and the west of the Dusty Mac deposit. The $\delta^{18}O_{whole-rock}$ values of the samples from the Dusty Mac deposit (Ma-5, Ma-7) range from -1.1 to -0.1‰ (Table 9), which is very similar to the range of $\delta^{18}O$ values those samples (M-3, M-4, and M-7) from the west of the Dusty Mac deposit ($\delta^{18}O$ from -1.3 to -1.1‰). Samples from the Vault property are also indicative of the homogerization of mineralizing fluids with respect to oxygen isotopes as demonstrated by the $\delta^{18}O_{whole-rock}$ values of X-46c (+3.4‰) and X-83 (+3.4‰).

The isotopic data also show that meteoric water may have penetrated into pre-Tertiary units in this region. One sample from Old Tom and Shoemaker Formation in the neighborhood of Willowbrook, whose $\delta^{18}O$ value is -3.4‰ (XW-1), documents large depletion in ^{18}O. The implication of the depletion in ^{18}O in this sample is that meteoric water had penetrated into the pre-Tertiary unit.

(4) The Relations between Depletions in ^{18}O and Calculated Water to Rock Ratios

In order to know the difference between the hydrothermal systems in terms of water to rock ratios, water to rock ratios in a close system are calculated using the following equation (Taylor, 1974, 1979):

$$W/R = \frac{(\delta_w^f - \delta_r^i)}{(\delta_w^i - \delta_r^i + \Delta)}$$

where W is the atom percent water oxygen and R is the atom percent rock oxygen in the system, r stands for rock, w stands for water, f, and i are final $\delta^{18}O$ value and initial $\delta^{18}O$ value for rocks or waters, respectively, and $\Delta = f_r - f_w$. Assuming that the $\delta^{18}O$ value of plagioclase (An=30) is approximately equal to the $\delta^{18}O$ value at equilibrium (Taylor, 1974), and that δ_w^i for Tertiary meteoric waters is -13‰ (Magaritz and Taylor, 1986), then the oxygen isotope fractionation between plagioclase (An=30) and water (O'Neil and Taylor, 1967),

$$\delta^{18}O_{plag} - \delta^{18}O_{water} = 2.68 \ (\ 10^6 T^{-2}) - 3.53$$

can be used as Δ for calculating water to rock ratios. The water to rock ratios for selected

hyd:othermal systems are listed in Table 10.

Table 10 Calculated water to rock ratios for selected hydrothermal systems in the Okanagan
Falls area

Hydrothermal system	δ_r^f	δ_r^i	T°C	Δ	$(W/R)_{max}$	$(W/R)_{min}$
Area from Penticton to Kaledan	+3.9	+6.5	257	6.01	----	0.24
	-5.4	+6.5	257	6.01	7.48	-----
Area around the Vault property	+4.1	+6.5	270	5.56	-----	0.21
	-1.8	+6.5	270	5.56	1.47	-----
Area around the Dusty Mac	+1.8	+6.5	240	6.65	-----	0.57
	-2.0	+6.5	240	6.65	2.53	-----

Note: $(W/R)_{max}$ - maximum w/r ratio; $(W/R)_{min}$ - minimum w/r ratio;
$\Delta = \Delta_{plagioclase-water}$; Temperature for the area from Penticton to Kaledan based on Th of T-1; Temperature for the area around the Vault property based on the best Th for the property; Temperature for the area around the Dusty Mac deposit based on peak Th for the deposit (Zhang, 1986).

The calculated water to rock ratios suggest that in the extremely ^{18}O-depleted

area(s), the maximum water to rock ratios are very high (Table 10), whereas in the

mineralized areas where volcanic rocks are moderately depleted in ^{18}O, the maximum water

to rock ratios are larger than 1, but are smaller than those in the extremely ^{18}O-depleted

area.

The calculated water to rock ratios once again demonstrate that the detachment fault

provided pristine meteoric water with channelways as evidenced by the hydrothermal

systems close to the detachment such as the Northern Hydrothermal System which have

very high water to rock ratios.

Oxygen and Carbon Isotope Data of Regional Calcite Samples

Twelve regional calcite samples are analysed for oxygen and carbon isotopes. The data are presented in Table 9 and Fig. 22. In the area from Penticton to Kaleden, $\delta^{13}C_{calcite}$ and $\delta^{18}O_{calcite}$ values vary from -6.6 to -6.0‰ and from -3.6 to +1.0‰ , respectively (Table 9). Although there is not much difference in $\delta^{13}C_{calcite}$ value between the disseminated and vein calcites in propylitic trachyte, the disseminated calcite as an alteration product of plagioclase phenocrysts is heavier in ^{18}O than vein calcite. This difference implies that the fluid responsible for the propylitic alteration is more enriched in ^{18}O because these samples were formed under similar temperatures. In the area near the Vault property, $\delta^{13}C_{calcite}$ and $\delta^{18}O_{calcite}$ values range from -14.4 to -4.9‰, and from +2.2 to +7.0‰, respectively. There is no large difference in $\delta^{18}O_{calcite}$ value between vein and disseminated calcites. In the area from Green Lake to Willowbrook and to Astrophysical Observatory, $\delta^{13}C_{calcite}$ and $\delta^{18}O_{calcite}$ are in the ranges from -14.9 to -6.6‰ · -1.8 to +6.8‰, respectively. Disseminated calcite is again heavier in ^{18}O than vein calcites. In the area near the Dusty Mac deposit, $\delta^{13}C_{calcite}$ and $\delta^{18}O_{calcite}$ values range from -6.1 to -4.3‰ and from -3.8 to 15.5‰. In this area, all samples are vein calcites.

Interpretation

(1) The Relation between Depletions in ^{18}O in Whole Rocks and $\delta^{18}O$ Values for Calcite Separates

The $\delta^{18}O$ values for calcite separates of vein and disseminated forms show a weakly positive correlation with $\delta^{18}O_{whole-rock}$ in the same sample (Fig. 23). This may imply that fluids responsible for alteration are related to fluids responsible for precipitation of carbonates in vein and disseminated forms. For instance, extremely depleted $\delta^{18}O_{whole-rock}$ values correspond to very light $\delta^{18}O$ values for calcite separates. In addition, in the mineralized areas, around the periphery of the hydrothermal system, $\delta^{18}O$ values for calcite

79
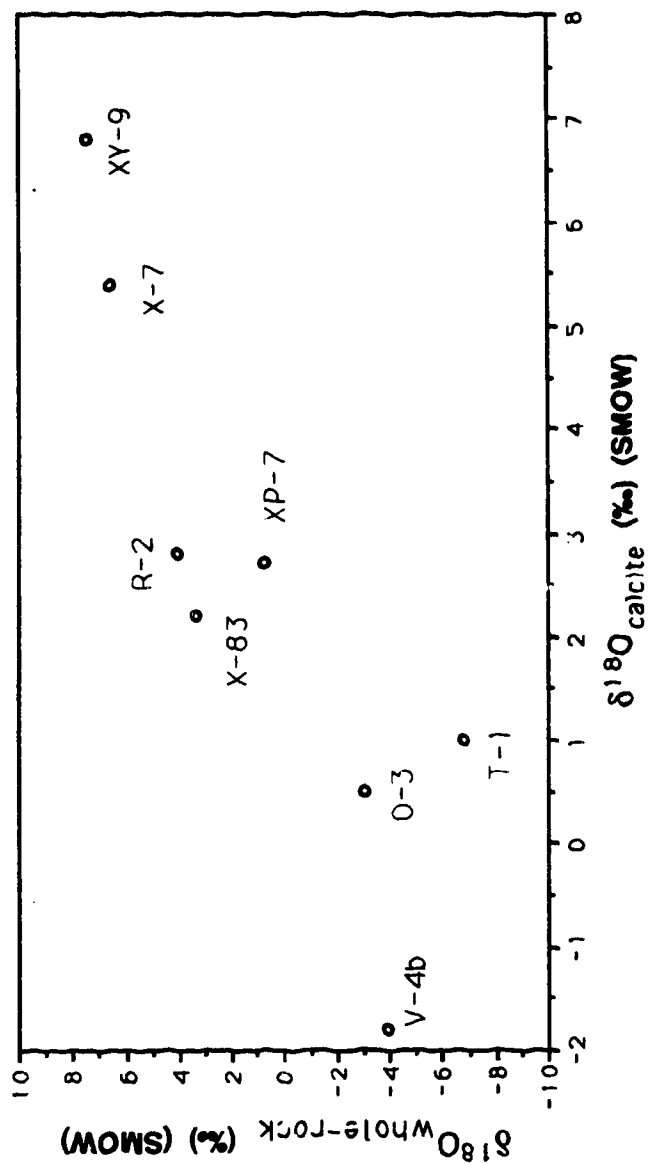
Fig. 22 $\delta^{18}O_{whole-rock}$ values against calculated $\delta^{18}O$ values for calcite samples (both whole-rock and calcite splits are from the same sample) in the Okanagan Falls area
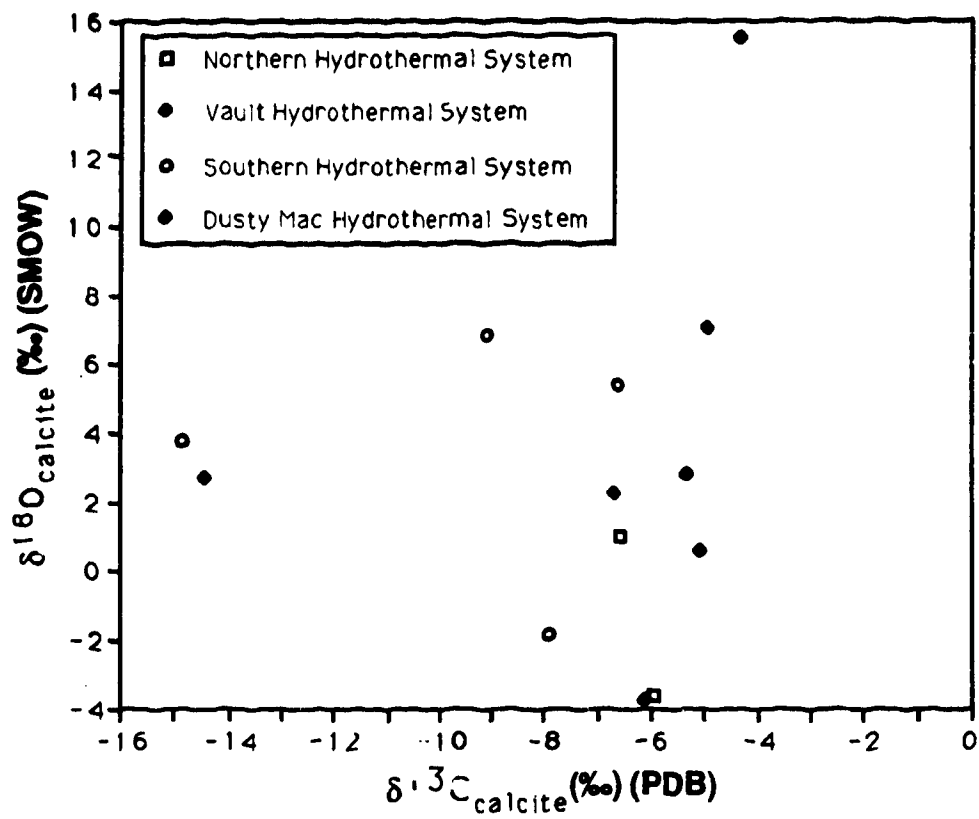
Fig. 23 $\delta^{13}C$ and $\delta^{18}O$ data for calcite samples from regional hydrothermal systems in the area of Okanagan Falls

separates are close to those at the center of the hydrothermal system (i.e., the Vault property). Because the temperatures in the periphery of the Vault property are lower than those at the center, These close d18O values for calcite separates may imply that the inflow fluids were more close to pristine meteoric fluids, while the outflow mineralizing fluids were ^{18}O-positively-shifted meteoric waters (Table 9).

(2) Carbon Sources for the Regional Hydrothermal Systems

In the area from Penticton to Kaledan, $\delta^{13}C_{calcite}$ values range from -6.6 to -6.0‰. Samples from the area around the Vault property have $\delta^{13}C_{calcite}$ values ranging from -14.4 to -5.3‰, a similar $\delta^{13}C_{calcite}$ range to values observed on the property. Samples from the area from Green Lake to Willowbrook and to the Astrophysical Observatory have $\delta^{13}C_{calcite}$ values ranging from -14.9 to -6.6‰, reflecting that at least two different carbon sources may have existed in the southern part of the study area. Samples around the Dusty Mac deposit have a narrow range of $\delta^{13}C_{calcite}$ values (-6.1 to -4.3‰), similar to the majority of $\delta^{13}C_{calcite}$ values observed on the Vault property.

The regional carbon isotope data demonstrate that $\delta^{13}C$ values of the fluids are strongly controlled by host rocks, similar to the conclusion on the Vault property. The majority of samples hosted by trachyte falls into the range of -7.0 to -4.5‰, probably indicating a magmatic carbon signature, while only two carbonate samples (-14.9‰ and -14.4‰) (one hosted by gneiss from the Southern Hydrothermal System and the other hosted by pyroclastic rock from the Vault Hydrothermal System) have an organic carbon signature (Fig. 22). A few samples (-10‰ < $\delta^{13}C_{calcite}$ < -7‰) may indicate mixing between a igneous carbon source and an organic carbon source.

Discussion

As mentioned in the introduction of this chapter, numerous stable isotope studies on whole rocks from hydrothermal systems have been conducted.The present study indicates that mineralization is not associated with extreme depletions in ^{18}O and extremely high water to rock ratios, which to some extent is opposite to the conclusion reached by Criss *et*

al (1983, 1985), Criss and Fleck (1987), and Criss and Champion (1991). Criss and

Fleck (1987) concluded that " an important corollary is that future exploration for Eocene

ore deposits in the Bitterroot lobe should be concentrated in the the relatively small areas of

intense meteoric-hydrothermal alteration which occur within and near areas having the

lowest $\delta^{18}O$ values". In 1983, Criss *et al.* (1983) observed that anomalies associated with

epithermal Ag-Au deposits at volcanic centers (e.g., Tonopah, Yankee Fork, Comstock,

Bohemia) are smaller (10 to 150 km), sharply bounded, and have central zones

characterized by very low-^{18}O host rocks, indicative of interaction with meteoric waters at

high water to rock ratios (>1). The highest-grade ore bodies are commonly associated with

the steepest gradients, just inside the perimeter of the anomaly. Subsequently, Criss *et al.*

(1985) reported that in the Yankee Fork mining district, Custer County, Idaho, two major

mines in this region, Sunbeam Mine and General Mine, are in very low contour area (zero

value area) (p. 1282, fig. 2). Recently, Criss and Champion (1991) found that in the

Comstock Lode Mining District, Nevada, extreme depletions occur in a 75 km^2 zone where

pervasive fluid-rock interactions resulted in regional propylitization and where

mineralization is present. This difference may result from the fact that in the Okanagan

Valley region the fluids channelized by the detachment fault may be dominant, whereas in

the regions studied by Criss and co-workers pervasive fluids are dominant.

This study, however, is similar to previous studies in that "bullseye" isotopic

anomalies exist (Fig. 21), even though the "bullseye" isotopic anomalies are smaller in

scale (~20km^2) in the present study compared with "bullseye" isotopic anomalies in other

regions. "Bullseye" meteoric-hydrothermal anomalies that are approximately 50 to 75 km^2

in areal extent have been found and studied in (1) the Miocene volcanic rocks of the

Western Cascades, particularly in the Bohemia mining district, Oregon (Taylor, 1971); (2)

Eocene rocks of the Challis volcanic fields, Yankee Fork mining district, Idaho (Criss *et*

al., 1985); (3) late Precambrian metavolcanic rocks of the Carolina Slate belt at Pilot

Mountain, North Carolina (Klein and Criss, 1988). All three of these areas are

characterized by thick sequences of andesitic rocks that include zones of propylitic or sericitic alteration associated with major zones of depletion. Associated with these altered areas in every case are anomalous concentrations of precious and base metals. According to Criss and Champion (1991), when volcanism is subaerial, it would be typically associated with meteoric groundwaters, and would logically be associated with symmetrical geologic features such as "bullseye" isotopic anomalies.

V. IMPLICATIONS, DISCUSSION AND MODEL FOR MINERALIZATION

Implications for Exploration

In comparison with known epithermal precious metal deposits, the homogenization temperatures of the Vault property fall into the known range (150°-300°C) of homogenization temperatures for such systems (Roedder, 1979). However, the homogenization temperatures of the majority of measurements on the property are lower than those of most epithermal deposits, e.g., 250°-300°C for stage I to IV mineralizations at Sunnyside, 250°-290°C for stage I to III mineralizations at Finlandia, 220°-300°C for main and later stage mineralizations at Mayflower, 190°-270°C for mineralizations at Creede, and 200°-300°C for gold-quartz-adularia vein deposits in Nevada (summarized by Spooner, 1981). It is possible that the representative temperatures for the mineralizing fluid at the Vault property is ~270°C as recorded by sample X83-6 (Fig. 15). The homogenization temperatures (~140° to 160°C) for the majority of measurements most likely reflect either the trapping temperatures when fluids experiencing boiling cooled down (Fig.15, Trend I), or reflect the homogenization temperatures for a mixing fluid between a low temperature endmember with a salinity of ~0.0 eq. wt.% at temperature of ≤150°C and the other endmember with a salinity of ~0.7 eq. wt.% at temperature of 270°C. The predominance of measurements around 165°C may imply that the host calcite samples were later in mineral paragenesis, i.e., the measurements are biased toward later stage mineralizations.

Compared with the calcite samples from unmineralized systems outside the Vault property, three populations of homogenization temperatures for all type of fluid inclusions from main stage quartz-calcite veins on the Vault property are grouped (Fig. 24). The first population is in the range of 90°C to 100°C, representing secondary fluid inclusions. The second population is in the range of 110°C to 210°C with a peak at about 150°-160°C. The third population is in the range of 220°C to 347°C. Similarly, three populations of homogenization temperatures are also divided for the samples outside the Vault property.
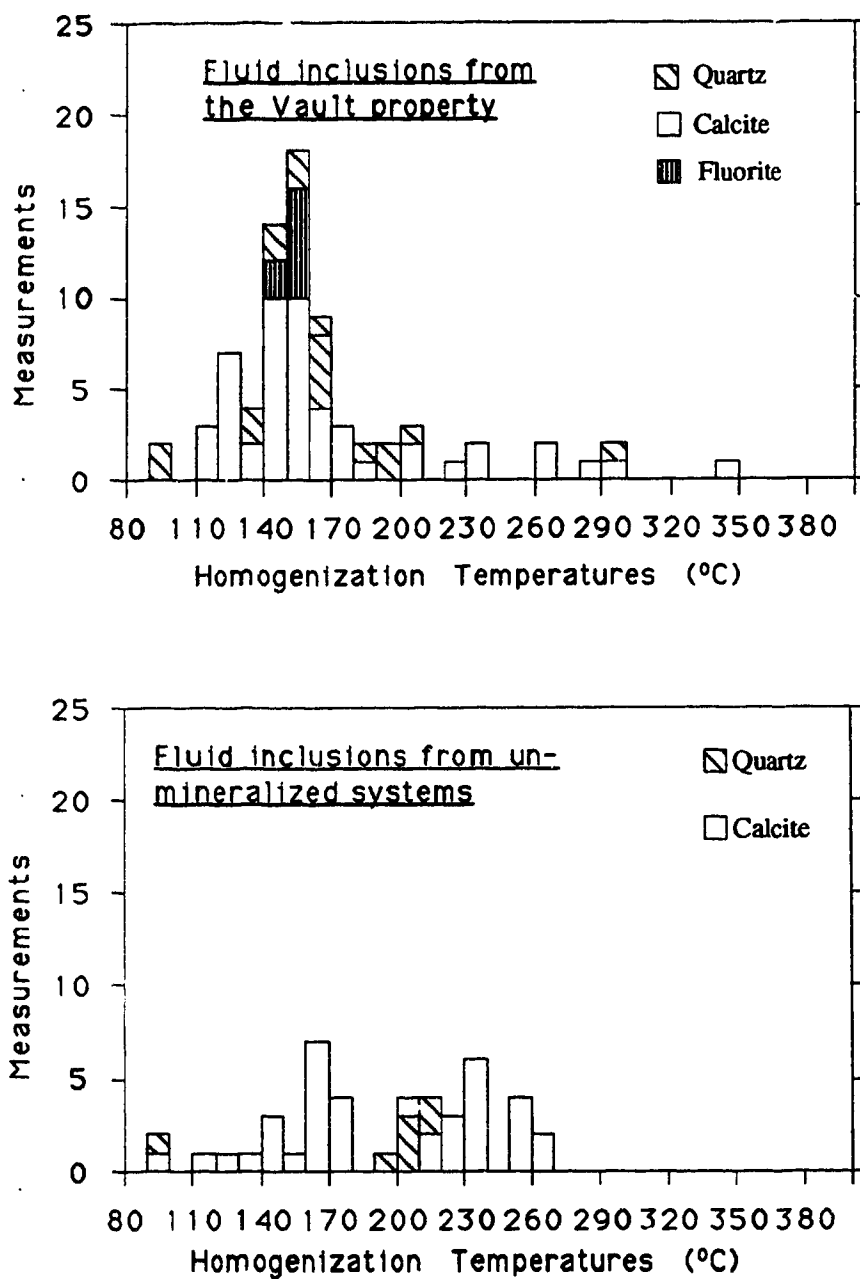
Fig. 24 Homogenization temperatures for samples on the Vault property versus those from un-mineralized systems in the Okanagan Falls area. It is obvious that three populations of homogenization temperatures can be subdivided for both cases. The very low temperature and low to moderate temperature populations of the regional samples are very similar to those of samples from the property. However, the relatively high temperature population for the samples on the property is in the range of 220°C to 347°C with several measurements higher than 270°C, whereas that population for the regional samples is in the range of 190°C to 270°C with no measurement above 270°C.

86

The first population is in the range of 90°C to 100°C, the same as that observed on the Vault property. The second population is in the range of 110°C to 180°C with a peak at 160°-170°C. The third population is in the range of 190°C to 270°C. It is obvious that the first and second populations on the property are similar to those for regional samples. The similarity between homogenization temperature measurements on the property and those on the regional scale points to that a low temperature (~100°C) fluid and a low to moderate temperature (~150-170°C) fluid are universal in this region. The difference between homogenization temperature measurements on the property and those on the regional scale lies in that the high temperature population for the samples on the property is in the range of 220°C to 347°C with several samples above 270°C, whereas the high temperature population for the measurements from regional samples is in the range of 190°C to 270°C with no measurements above 270°C. The high temperature population similar to that on the Vault property is also observed at the Dusty Mac deposit. The fluid inclusions from the Dusty Mac deposit have a peak homogenization temperature of 245°C with an average of 233°±31°C (Zhang, 1986). Therefore, the data from the Vault and the Dusty Mac properties may imply that fluids responsible for the formation of ores were hotter than most of the regional fluids.

In addition, final melting temperatures of ice on the property (averaging at -0.4°C) are relatively lower than those from the samples outside the property, even though some samples from the property also have ice melting temperatures close to 0°C (Fig.14). This may suggest that fluids on the property were slightly more saline (salinities averaging at ~0.8 eq. wt.% NaCl equivalent) compared with the pristine meteoric water on the regional scale.

The Timing of Mineralization

Even though precise dating of the mineralization is lacking, the timing of mineralization can be roughly constrained based on geological evidence and existing dating on the volcanic rocks. Since the volcanism in the Okanagan Falls area is Eocene in age

87

(Church, 1983; Tempelman-Kluit and Parkinson, 1986; Parrish *et al.*, 1988), and is broadly coeval with detachment faulting, the hydrothermal activities must also be Eocene in age because of lack of major thermal events after volcanism and detachment faulting. In other words, the hydrothermal activities should immediately follow volcanism, and be roughly contemporaneous with the detachment faulting.

The Heat Source for the Mineralization

Concerning the thermal history along the Okanagan Valley fault, Mathews (1981) suggested the following geothermal history based on K-Ar ages in the Okanagan Valley. About 60 Ma, temperatures greater than 500°C prevailed in the gneisses so that radiogenic argon could largely or completely escape from the system. Within a few million years, the temperatures fell below the blocking temperature (450°-500°C) of hornblende. After another 6-9 Ma later (i.e., about 50 Ma ago), the temperature fell below 250°C, the blocking temperature for biotite, and moreover, the 250°C isotherm would sink through the gneisses at rate of about 1 km in 5 Ma. By about 46 Ma ago, the upper part of the gneiss block was exposed by Eocene erosion. Within the next few million years, the gneisses were covered by a blanket of sedimentary and volcanic rocks at least 1.5 km thick. If this geothermal history is valid, it means that detachment faulting could provide heat for hydrothermal systems established since Eocene. The other possible heat source may be from the plutons. The other probable heat source is from possible plutonic bodies beneath.

The Mineralization Model

The characteristics of the hydrothermal fluids for the Vault property, the Dusty Mac, and the regional hydrothermal systems are tabulated in Table 11.

Table 11 Comparison of the characteristics of hydrothermal fluids responsible for veining on the Vault property with those on the Dusty Mac deposit, and with those in the area from Penticton to Kaledan

	the Vault property	Dusty Mac deposit*	Penticton-Kaleden
Temperature	~270°C	~240°C	~229 to ~257°C
Depth (meters)	~707 m	≥ 380 m	?
Salinity (eq. wt.% NaCl)	Two populations: ~0.0-0.2 and ~1.0-1.4	~0.5	~0.0
$\delta^{18}O_{fluid}$ SMOW	~Two reservoirs: +1.3 to +7.7 -7.2 to -4.0	-7 to -9	~-11.3
W/R	1.5	2.5	7.5

* Data from Zhang (1986)

Numerous studies in Tertiary epithermal precious metal deposits in the U.S. have demonstrated that in this type of deposit, the fluid inclusions usually have homogenization temperatures of 200°-300°C and low salinities. Stable isotope studies have suggested that meteoric water plays a dominant role in the formation of this type of deposit even though a few of deposits may have been involved in magmatic water such as in the Cortez gold deposit, Nevada (Rye et al., 1974). These observations provide the basis for the widely cited mineralization model involving the circulation of meteoric water in the formation of epithermal deposits (Bethke, 1988). A central part in this model is that volcanic rocks have access to meteoric waters because of the presence of cauldron craters and ring faults caused by volcanic activities.

The data from the Okanagan Falls area seem to offer a mineralization model (Fig. 25) slightly different from the model largely based on data from the western United States in that the detachment fault provided a major channel for meteoric water to penetrate the existing rocks in the Okanagan Falls area. This model is supported by several lines of evidence. Firstly, the systematic variations in calculated water to rock ratios (Table 11)

89
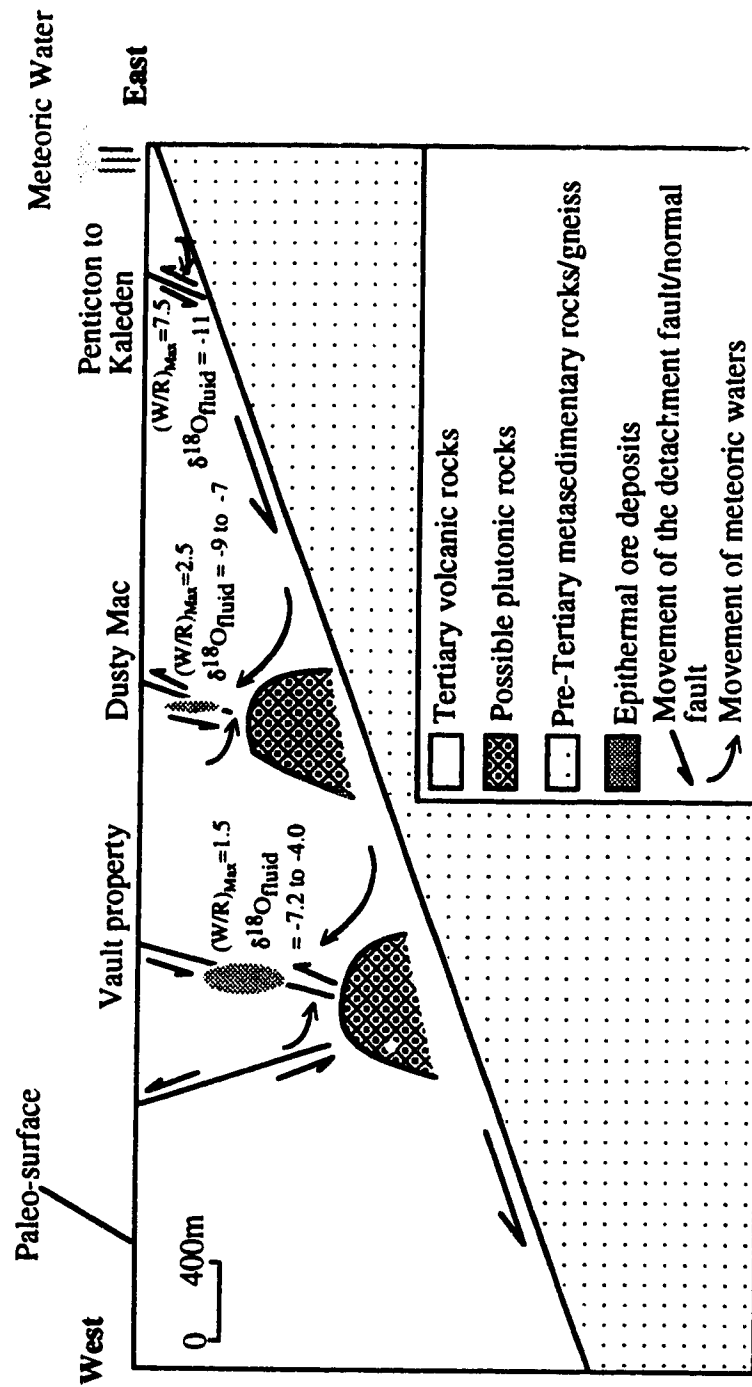
Fig. 25 A generalized mineralization model for epithermal deposits in the Okanagan Falls area. ⁓⁞ ⁝ ᵇᵢ⁚
model the detachment fault plays an important role to provide channelway for meteoric waters to
penetrate.

from Penticton-Kaleden (7.5), to Dusty Mac (2.5), and to the Vault property (1.5) seem to indicate that the closer a site is to the detachment fault, the closer the fluids were to pristine meteoric water. This implies that the fluid on the Vault property had the longest interaction history with volcanic rocks and the fluid at the site close to the detachment fault such as in the area around Penticton and Kaledan had the shortest interaction history. Secondly, altered volcanic rocks of the same alteration styles, i.e., argillic alteration, have quite different $\delta^{18}O$ values in the Vault property ($\delta^{18}O=\sim+3.4‰$) and in the Dusty Mac ($\delta^{18}O=\sim-1.0‰$ to $-2.0‰$) Thirdly, two peaks of salinities are observed on the Vault property. One peak corresponding to the samples with bladed texture is in the range of 1.0 to 1.4 eq. wt.% NaCl. This peak salinities is higher than the peak salinity observed on the Dusty Mac deposit (~0.5 eq. wt.% NaCl, Zhang, 1986). Since the fluid temperature in these two properties are similar ($\sim270°C$ at the Vault property, $\sim240°C$ at the Dusty Mac deposit), the differences in $\delta^{18}O$ value in altered rocks and in salinity in mineralizing fluids between the Vault property and Dusty Mac deposit may reflect the fact that the mineralizing fluids on the Vault property were more enriched in ^{18}O and were in longer interaction history with host rocks than those on the Dusty Mac property. So the oxygen isotope and salinity data suggest that the mineralizing fluids on the Vault property are more evolved than those on the Dusty Mac property. This is consistent with the observation that the Vault property is farther away from the detachment fault than the Dusty Mac deposit. Meteoric waters entering the detachment fault would reach the Dusty Mac earlier than they would reach the Vault property and hence would be less evolved. This model also explains that why the relationship between the $\delta^{18}O$ anomalies and mineralization is different from those observed in the western United States.

Tempelman-Kluit (1984) proposed a mineralization model similar to the above model. In his model, he considered that meteoric waters flowed from west to east. If this model was correct, meteoric water would become heavier in ^{18}O westwards. Clearly, his model is not consistent with the isotope and salinity data presented above.

91

SUMMARY

The Okanagan Valley is tectonically situated in the southernmost part of the Quesnel

terrane of the Intermontane Belt. The valley follows a low angle detachment fault, wh: ͺ

was active in ductile deformation in Mesozoic (and possibly until Early Eocene) and in

br'ttle deformation until Middle Eocene. The conservative estimate of the displacement of

the detachment fault is on the order of 25 km in Eocene (Bardoux, 1985). The denudation

rate is in the range of ~1.5 mm/year.

The Vault property is on the upper plate of the detachment fault. There are two

types of Au-Ag mineralization on the property. One is quartz-vein ore of adularia-sericite

type. The other is stockwork ore characterized by disseminated sulfides. The lateral

hydrothermal alteration seems to be zoned towards the center of alteration in a pattern of

propylitic $\Rightarrow$ sericitic $\Rightarrow$ argillic $\Rightarrow$ silicic. Similarly, the alteration is also vertically zoned

from depth to surface in a pattern of propylitic $\Rightarrow$ sericitic $\Rightarrow$ argillic-sericitic $\Rightarrow$ silicic $\Rightarrow$

argillic. Au, As and Mo are strongly associated with silicic alteration, and As is most likely

to be introduced during argillic-sericitic and argillic alterations.

Workable fluid inclusions on the Vault property are mainly hosted by calcite. The

mineralizing fluids were likely to have temperatures around 270°C, even though the

majority of homogenization temperature data is biased to temperatures around 160°C,

which may reflect relatively late stage mineralization(s). Salinity data indicate that the

mineralizing fluids were very dilute (0 to ~3.4 eq. wt.% NaCl). Boiling of such fluids was

evidenced by a wide range of filling ratios and systematic trends in salinity and

homogenization temperature data.

There are three populations of $\delta^{18}O_{fluid}$ values for main stage mineralization at the

Vault property. The first population ranges in $\delta^{18}O_{fluid}$ from +1.3 to +7.7‰. The second

population of $\delta^{18}O_{fluid}$ values ranges from -3.8 to -0.1‰, followed by a third population

of $\delta^{18}O_{fluid}$ values ranging from -7.2 to -4.0‰. The first population may represen· a

possible magmatic or highly-evolved meteoric water. The third population may represent a

meteoric water (pristine to slightly-evolved meteoric water). The second population may represent a mixture between a magmatic/highly-evolved meteoric water and a meteoric water.

The $\delta^{18}O$ data of volcanic rocks on a regional scale in the Okanagan Falls area reveal that there are two ^{18}O depletion zones with mineralization (i.e., the Vault Hydrothermal System, and the Dusty Mac Hydrothermal System) and two ^{18}O depletion zones without mineralization (i.e., the Southern Hydrothermal System, and the Northern Hydrothermal System). The ^{18}O depletion zones with mineralization are characterized by moderate depletions in ^{18}O (the lowest $\delta^{18}O_{whole-rock}$ values > -2‰) and moderate calculated water to rock ratios (1.5 to 2.5), whereas ^{18}O depletion zones without mineralization are characterized by extreme depletions in ^{18}O (the lowest $\delta^{18}O_{whole-rock}$ values < -6‰) and very high calculated water to rock ratio (up to 7.5).

The oxygen data in combination with fluid inclusion data from the Okanagan Falls area offer a mineralization model (Fig. 25) slightly different from the model largely based on data from the western United States. The main difference lies in that the detachment fault provided a major channel for meteoric water to penetrate the existing rocks in the Okanagan Falls area, whereas ring faults and cauldron craters related to volcanic activities are main channels for meteoric waters in the mineralization model based on data from the western United States.

REFERENCES

Armstrong, R.J.., 1988, Mesozoic and early Cenozoic magmatic evolution of the Canadian Cordillera. Geol. Soc. Special Paper. 218:55-92

Barton, P.B., Jr., Bethke, P.M. and Roedder, E., 1977, Environment of ore deposition in the Creede mining district, San Juan Mountains, Colorado: Part III Progress toward interpretation of the chemistry of the ore-forming fluid for the OH vein. Econ. Geol., 72:1-24

Bardoux, M., 1985a, The Kelowna detachment zone, Okanagan Valley, south-central British Columbia. In Current Research, Part A, Geological Survey of Canada, Paper 85-1A, p.333-339

Bardoux, M, 1985b, Tertiary tectonic denudation in the hinterland of the Canadian Cordillera: Initial results from Kelowna, B.C. GSA annual meeting, Cordilleran Section, Program with abstracts, vol.17, p.339

Bardoux, M. and Irving, E., 1989, Paleomagnetism of Eocene rocks of the Kelowna and Castlegar area, British Columbia: Studies in determining paleohorizontle. Can. J. Earth Sci., 26:829-844

Bethke, P.M., 1988, The Creed, Colorado ore-forming system: A summary model. U.S. Geol. Survey Open-file Rept., 88-403, 29p.

Bethke, P. M. and Rye, R.O., 1979, Environment of ore deposition in the Creede mining district, San Juan Mountains, Colorado: Part IV: Source of fluids from oxygen, hydrogen, and carbon isotope studies. Econ. Geol., 74:1832-1851

Bostock, H.S., 1941, Okanagan Falls, British Columbia, Geol. Surv. Canada, Map 627A

Brown, R.L., Journeay, J. and Murray, J., 1985, A duplex model of crustal evolution, Omineca Belt, southern British Columbia. GSA annual meeting, Cordilleran Section, Program with abstracts, vol.17, p.344

Campbell, A., Rye, D.M. and Petersen, U., 1984, A hydrogen and oxygen isotope study of the San Cristobal mine, Peru: Implications of the role of water to rock ratio for the genesis of wolframite deposits. Econ. Geol., 79:1818-1832

Carr, S.D. and Brown, R.L., 1989, Crustal structure and tectonic chronology near the Lithoprobe Line in the Thor/Odin-Pinnacles-Cherryville-Vernon area, southern British Columbia: A progress report. Lithoprobe Workshop

Carr, S.D. and Brown, R.L., 1990a, Southern Cordilleran Lithoprobe Transect: Evidence for crustal thickening and collapse of the Omineca Belt, Valhalla Complex to Okanagan Valley, British Columbia. GAC-MAC Annual Meeting, Vancouver, Program with abstracts, Vol. 15, A22

Carr, S.D. and Brown, R.L., 1990b, Southern Cordillera Lithoprobe: Transect Lines 6 to 10: Crustal structure and tectonic chronology. Lithoprobe Workshop

Carr, S.D., Parrish, R.R. and Brown, R.L., 1987, Eocene structural development of the Valhalla complex, southeastern British Columbia. Tectonics, 6:175-196

Carr, S.D., Crowley, J.L., Johnson, B.J., Brown, R.L. and Coleman, V.J., 1992, Summary and implications of results from supporting geoscience field mapping and geochronology projects in the southern Cordillera adjacent to Lithoprobe profiles 4-10 and 19. Lithoprobe Work sh~p

Church, B.N., 1973, Geology of the White Lake Basin, British Columbia Department of Mines and Petroleum Resources, Bulletin 61.

Church, B.N., Ewing ,T.E. and Hora, Z.D., 1983, Volcanology, structure, coal and minera¹ resources of early Tertiary outliers in south-central British Columbia, Field Trip Guidebook, Trip 1, University of Victoria, p.15-27

Clayton, R.N. and Mayeda, T.K., 1963, The use of bromine pentafluoride in extraction of oxygen from oxides and silicates for isotopic analysis. Geochim. Cosmochim. Acta, 27:43-52

Clayton, R.N., O'Neil, J.R. and Mayeda, T.K., 1972, Oxygen isotope exchange between quartz and water. Journal of Geophysical Research, 77:3057-3067

Clayton, R.N., Goldsmith, J.R. and Mayeda, T.K., 1989, Oxygen isotope fractionation in quartz, albite, anorthite and calcite. Geochim. Cosmochim. Acta, 53:725-733

Coney, P.J. and Harms, T.A., 1984, Cordilleran metamorphic core complexes: Cenozoic extensional relics of Mesozoic compression. Geology, 12:550-554

Coney, P.J., Jones, D. and Monger, J.W.H., 1980, Cordilleran suspect terranes. Nature, 288:329-333

Cole, D.R., Ohmoto, H., and Jacobs, G.K., 1992, Isotopic exchange in mineral-fluid systems:III. Rates and mechanisms of oxygen isotope exchange in the system granite-H₂O±NaCl±KCl at hydrothermal conditions. Geochim. Cosmochim. Acta, 56:445-465

Cook, F.A., Clows, R.M., Spencer, C., Green, A.G., Kanasewich, E.R. and Kapoyis, S., 1989, The 1988 Lithoprobe Southern Cordillera reflection program. Lithoprobe Workshop.

Cook, F.A., Varsek, J., Clows, R., Kanasewich, E., Spencer, C., Brown, R., Carr, S., Parrish, R., Johnson, B., Price, R. and Moore, J., 1990, Reflection crustal structure of the southern Canadian Cordillera Interior: Omineca Crystalline Belt and Intermontane Belt. Lithoprobe Workshop

Craig, H., 1953, The geochemistry of the stable carbon isotopes. Geochim. Cosmochim. Acta, 3:53-92

Craig, H., 1961, Standards for reporting concentrations of deuterium and oxygen-18 in natural waters. Science, 133:1833-1834

Criss, R.E. and Champion, D.E., 1991, Oxygen isotope study of the fossil hydrothermal system in the Comstock Lode mining district, Nevada. In Taylor, Jr., H.P., O'Neil, J.R., Kaplan, I.R., ed., Stable Isotope Geochemistry: A Tribute to Samuel Epstein, pp.437-447. The Geological Society, Special Publication No.3.

95

Criss, R.E. and Fleck, R.J., 1987, Petrogenesis, geochronology, and hydrothermal systems of the northern Idaho batholith and adjacent areas based on $^{18}O/^{16}O$, D/H, $^{87}Sr/^{86}Sr$, K-Ar, and $^{40}Ar/^{39}Ar$ studies. U.S. Geol. Sur. Prof. Pap., 1436:95-137

Criss, R.E. and Taylor, H.P., Jr., 1986, Meteoric-hydrothermal system. In Valley, J.W., Taylor, H.P., Jr., and O'Neil, J.R., ed., Stable Isotopes in High Temperature Geological Processes, Reviews in Mineralogy, Vol. 16, 373-424, Mineral. Soc. Am.

Criss, R.E., Solomon, G.C. and Taylor, Jr., H.P., 1983, Application of $\delta^{18}O$ and δD contour maps to exploration for epithermal and porphyry mineral deposits formed in subaerial environments. Geological Society of America Abstract with Programs, 15:278

Criss, R.E. and Champion, D.E. and McIntyre, D.H., 1985, Oxygen isotope, aeromagnetic, and gravity anomalies associated with hydrothermally altered zones in the Yankee Fork Mining District, Custer County, Idaho. Econ. Geol., 80:1277-1296

Drummond, S.E. and Ohmoto, H., 1985, Chemical evolution and mineral deposition in boiling hydrothermal systems. Econ. Geol., 80:126-147

Ewing, T.E., 1980, Paleogene tectonic evolution of the Pacific Northwest. J. Geology (Chicago), 88:619-638

Gabrielse, H. and Yorath, C.J., 1989, DNAG # 4. The Cordilleran orogen in Canada. Geoscience Canada, 16:67-84

Giletti, B.J. and Yund, R.A., 1984, Oxygen diffusion in quartz. J. Geophys. Res., 89:4039-4046

Golding, S.D. and Wilson, A.F., 1983, Geochemical and stable isotope studies of the No. 4 Lode, Kalgoorlie, Western Australia. Econ. Geol., 78:438-450

Haas, J.L., Jr., 1976, Physical properties of the coexisting phase and thermochemical properties of the H2O component in boiling NaCl solutions. U.S. Geological Survey Bulletin, 1421-A, p.A25-A27

Heald, P. Foley, N.K. and Hayba, D.O., 1987, Comparative anatomy of volcanic-hosted epithermal deposits: Acid-sulfate and adularia-sericite types. Econ. Geol., 82:1-26

Hedenquist, J.W. and Aoki, M., 1991, Meteoric interaction with magmatic discharges in Japan and the significance for mineralization. Geology, 19:1041-1044

Hedenquist, J.W. and Henley, R.W., 1985, The importance of CO_2 freezing point measurement of fluid inclusions: evidence from active geothermal systems and implications for epithermal ore deposition. Econ. Geol., 80:1379-1406

Henley, R.W., 1991, Epithermal gold deposits in volcanic terranes. In Foster, R.P., ed., Gold Metallogeny and Exploration, Blackie, Glasgow and London

Hollister, L.S., Crawford, M.L., Roedder, E., Burruss, R.C., Spooner, E.T.C., and Touret, J., 1981, Practical aspect of microthermometry. In Fluid Inclusions: Applications to Petrology, Hollister, L.S. and Crawford, M.L., ed., MAC short course vol.6, pp.278-301

Ivosevic, S.W., 1984, Gold and silver handbook. Published by the author himself, printed in Denver, Colorado

Journeay, M. and Brown, R., 1987, Major tectonic boundaries of the Omineca Belt in southern British Columbia: a progress report. In Current Research, Part A, Geological Survey of Canada, Paper 86-1A, 81-88

Klein, T.L. and Criss, R.E., 1988, An oxygen isotope and geochemical study of meteoric-hydrothermal systems at Pilot Mountain and selected other localities, Carolina slate belt. Econ. Geol., 83:801-821

Larson, P.B. and Zimmerman, B.S., 1991, Variations in $\delta^{18}O$ values, water/rock ratios, and water flux in the Rico paleothermal anomaly, Colorado. In Taylor, Jr., H.P., O'Neil, J.R., Kaplan, I.R., ed., Stable Isotope Geochemistry: A Tribute to Samuel Epstein, pp.463-469. The Geological Society, Special Publication No.3.

Little, H.W., 1961, Kettle River (west half), British Columbia. Canada Geological Survey Prelim. Ser. Map 15-1961

Lynch, J.V.G., 1989, Hydrothermal zoning in the Keno Hill Ag-Pb-Zn vein system: A study in structural geology, mineralogy, fluid inclusions, and stable isotope geochemistry. Unpublished Ph.D. thesis, Department of Geology, University of Alberta

Magaritz, M. and Taylor, Jr., H.P., 1986, Oxygen 18/oxygen 16 and D/H studies of plutonic granitic and metamorphic rock across the Cordilleran batholiths of southern British Columbia. Journal of Geophysical Research, 91:2193-2217

Matsuhisa, Y., Goldsmith, J.R. and Clayton, R.N., 1979, Oxygen isotope fractionation in divalent metal carbonates. J.Chem. Physics, 51:5547-5558

Mathews, W.H., 1981, Early Cenozoic resetting of potassium-argon dates and geothermal history of north Okanagan area, British Columbia. Can. J. Earth Sci., 18:1310-1319

McCrea, J.M., 1950, On the isotopic chemistry of carbonates and a paleotemperature scale. J. Chm. Phys., 18:849-857

Medford, G.A., 1975, K-Ar and fission track geochemistry of an Eocene thermal event in the Kettle River (West Half) map area, southern British Columbia. Can. J. Earth Sci., 12:836-843

Meyer, C. and Hemley, J.J., 1967, Wallrock alteration. In Barnes, H.L., ed., Geochemistry of hydrothermal ore deposits. New York, Holt, Rinehart and Wilson, p.166-235

Meyers, R.E., 1989, Preliminary economic geology of the Vault gold deposit. Exploration in B.C. 1988, B.C. ministry of energy, mines and petroleum, B5-B19

Meyers, R.E. and Hubner, T.B, 1991, Overview of exploration activities in south central district. In Exploration in British Columbia 1990, pp.55. B.C. Ministry of Energy, Mines and Petroleum Resources.

Minister of Mines and Petroleum Resources, British Columbia, 1975, Annual report, Chapter 3, Mineral resources statistics, p. A51-A97

Minister of Mines and Petroleum Resources, British Columbia, 1976, Annual report, Chapter 3, Mineral resources statistics, p. A61-A106

Monger, J.W.H., Price, R.A. and Tempelman-Kluit, 1982, Tectonic accretion and the origin of the two major metamorphic and plutonic welts in the Canadian Cordillera. Geology, 10:70-75

Muessig, S., 1967, Geology of the Republic quadrangle and a part of the Aeneas quadrangle, Ferry County, Washington. U.S. Geol. Survey Bull., 1216, 135p

Ohmoto, H., 1972, Systematics of sulfur and carbon isotopes in hydrothermal ore deposits. Econ. Geol., 67:551-578

Ohmoto, H., 1986, Stable isotope geochemistry of ore deposits. In Stable Isotopes in High Temperature Geological Processes, Reviews in Mineralogy, vol. 16, Mineralogical Society of America, pp.491-559

Ohmoto, H. and Rye, R.O., 1974, Hydrogen and oxygen isotopic compositions of fluid inclusions in the kuroko deposits, Japan. Econ. Geol., 69:947-953

Ohmoto, H. and Rye, R.O., 1979, Isotopes of sulfur and carbon . In Barnes, H.L., ed., Geochemistry of Hydrothermal Ore Deposits. John Willey and Sons, New York, 509-567

Ohmoto, H. and Taylor, H.P.,Jr., 1967, The oxygen isotope and cation exchange chemistry of feldspars. Am. Mineral., 52:1411-1437

O'Neil, J.R., 1987, Preservation of H, C, and O isotopic ratios in the low temperature environment. In MAC Short Course Vol. 13, Stable Isotope Geochemistry of Low Temperature Fluids, pp.85-128

O'Neil, J.R., Clayton, R.N., and Mayeda, T.K., 1969, Oxygen isotope fractionation in divalent metal carbonates. J. Chem. Phys., 51:5547-5558

O'Neil, J.R. and Taylor, H.P., Jr., 1967, The oxygen isotope and cation exchange chemistry of feldspars. Am. Mineral., 52:1414-1437

Parkinson, D., 1985, Geochronology of the western side of the Okanagan metamorphic core complex, southern B.C. GSA annual meeting, Cordilleran Section, Program with abstracts, vol. 17, p.399

Parrish, R.R., Carr, S.D. and Parkinson, D., 1988, Eocene extensional tectonics and geochronology of the southern Omineca Belt, British Columbia and Washington. Tectonics, 7:181-212

Potter, II, R.W., Clynne, M.A. and Brown, D.L., 1978, Freezing point depression of aqueous sodium chloride solutions. Econ. Geol., 73:284-285

Reed, M.H. and Spycher, N.F., 1985, Boiling, cooling, and oxidation in epithermal systems: A numerical model approach. In Berger, B.R. and Bethke, P.M., ed., Review in Economic Geology, Volume 2, Geology and Geochemistry of Epithermal Systems, Society of Economic Geologist, p.249-272

Reynolds, S.J. and Spencer, J.E., 1985, Evidence for large-scale transport on the Bullard detachment fault, west-central Arizona. Geology, 13:353-356

Robinson, B.W. and Chritie, A.B., 1980, Epithermal silver-gold mineralization, Mraatoto Mine, New Zealand: Stable isotopes and fluid inclusions. Proceedings of the Fifth Quadrennial IAGOD Symposium, E. Schweizerbaart'sche Verlagsbuchhandlung (Nagel u. Obermiller), Stuttgart, Germany, pp.719-730

Roedder, E., 1981, Origin of fluid inclusions and changes that occur after trapping. *In* Fluid Inclusions: Applications to Petrology, Hollister, L.S. and Crawford, M.L., ed., MAC short course vol.6, pp.101-137

Roedder, E., 1984, Fluid Inclusions. Reviews in Mineralogy, vol. 12, Mineralogical Society of America. 644p.

de Ronde, C.E.J. and Blattner, P., 1988, Hydrothermal alteration, stable isotopes, and fluid inclusions of the Golden Cross epithermal gold-silver deposit, Waihi, New Zealand. Econ. Geol., 83:895-917

Rye, R.O., Doe, B.R. and Wells, J.D., 1974, Stable isotope and lead isotope studies of the Cortez, Nevada, gold deposit and surrounding area. U.S. Geol. Survey Jour. Res., 2:13-23

Seal, R.R., II and Rye, R.O., 1992, Stable isotope study of water-rock interaction and ore formation, Bayhorse base and precious metal district, Idaho. Econ. Geol., 87:271-287

Schroeter, T.G., Lund, C., and Carter, G., 1989, Gold production and reserves in British Columbia. Open File 1989-22, Ministry of Energy, Mines and Petroleum Resources, B.C.

Shepherd, T.J., Rankin, A.H. and Alderton, D.H.M., 1985, A practical guide to fluid inclusion studies. Blackie, Glasgow, 239p.

Soloman, G.C. and Taylor, H.P., 1991, Oxygen isotope studies of Jurassic fossil hydrothermal systems, Majave Desert, southeastern California. *In* Taylor, Jr., H.P., O'Neil, J.R., Kaplan, I.R., ed., Stable Isotope Geochemistry: A Tribute to Samuel Epstein, pp.449-462. The Geological Society, Special Publication No.3.

Spooner, E.T.C., 1981, Fluid inclusion studies of hydrothermal ore deposits. *In* Fluid Inclusions: Applications to Petrology, Hollister, L.S. and Crawford, M.L., ed., MAC short course vol.6, pp.209-240

Taylor, H.P., Jr., 1968, The oxygen isotope geochemistry of igneous rocks. Contrib. Mineral. Petrol., 19:1-71

Taylor, H.P., Jr., 1971, Oxygen isotope evidence for large-scale interaction between meteoric ground waters and Tertiary granodiorite intrusions, western Cascade Range, Oregon. J. Geophys. Res., 76:7855-7874

Taylor, H.P., Jr., 1974, The application of oxygen and hydrogen isotope studies to problems of hydrothermal alteration and ore deposition. Econ. Geol., 69:843-883

Taylor, H.P., Jr., 1978, Oxygen and hydrogen studies of plutonic granitic rocks. Earth. Planet. Sci. Lett., 38:177-210

Taylor, H.P., Jr., 1979, Oxygen and hydrogen isotope relationships in hydrothermal mineral deposits. *In* Barnes, H.L., ed., Geochemistry of Hydrothermal Ore Deposits. John Willey and Sons, New York, 235-277

Taylor, H.P., Jr., and Magaritz, M., 1978, Oxygen and hydrogen isotope studies of the Cordiileran batholiths of western North America. *In* Robinson, B.W., ed., Stable isotopes in the earth sciences. Sciences information division, DSIR, P.O. Box 9741, Wellington

Taylor, H.P., Jr., Frechen, J. and Degens, E.T., 1967, Oxygen and carbon isotope studies of carbonatites from the three Lacher See District, West Germany, and the Lano district, Sweden. Geochim. Cosmochim. Acta, 31:407-430

Tempelman-Kluit, D., 1984, Meteoric water model for gold veins in a detached terrane. GSA annual meeting at Reno, Nevada, Program with abstracts, vol.16, 674

Tempelman-Kluit, D. and Parkinson, D., 1986, Extension across the Eocene Okanagan crustal shear in southern British Columbia. Geology, 14:318-321

Tempelman-Kluit, D.J., 1989, Geological map with mineral occurrences, fossil localities, radiometric ages and gravity field for Penticton map area, southern B.C. Geological Survey of Canada, Open File 1969

Truesdell, A.H., Nuthenson, M. and Rye, R.O., 1977, The effects of subsurface boiling and dilution on the isotopic compositions of Yellowstone thermal waters. J. Geophys. Res., 82:3694-3703

Valley, J.W., 1986, Stable isotope geochemistry of metamorphic rocks. *In* Stable Isotopes in High Temperature Geological Processes, Reviews in Mineralogy, vol. 16, Mineralogical Society of America, pp.445-490

Wernicke, B., and Burchfiel, B.C., 1982, Modes of extensional tectonics. Journal of Structural Geology, 4:105-115

Zhang, X., 1986, Fluid inclusion and stable isotope studies of the gold deposits in Okanagan Valley, British Columbia, unpublished M.Sc., University Of Alberta

Zhang, X., Nesbitt, B.E. and Muehlenbachs, K., 1989, Gold mineralization in the Okanagan Valley, southern British Columbia: Fluid inclusion and stable isotope studies. Econ. Geol., 84:410-424.

Zheng, Y.-F., 1990, Carbon-oxygen isotopic covariation in hydrothermal calcite during degassing of CO_2. Mineral. Deposita, 25:245-250

Appendix I. SAMPLE RECORD FROM THE CORES OF THE VAULT PROPERTY

| SAMPLE NUMBER	DEPTH	DESCRIPTION	CORE NUMBER	SECTION
X98-1	454.2m	trachyte	DDH38898	875E
X98-2	437.8m	lahar containing small quartz vein		
X98-3	about 434.0m	lahar		
X98-4	410.0m	ultramafic		
X98-5	410.0m	ultramafic containing small quartz vein		
X98-6	393.7m	lahar		
X98-7	386.0m	sandstone		
X98-8	about 374.8m	quartz vein containing sulfide		
X98-9	about 373.1m	breccia		
X98-10	369.2m	felsite		
X98-11	about 333.0m	mudstone		
X98-12	about 328.6m	mudstone		
X98-13	324.0m	mudstone		
X778-1	3.5m	dacite	DDH82778	350E
X778-2	12.2	"		
X778-3	18.09	mudstone		
X778-4	18.1	"		
X778-5	35.0	siltstone		
X778-6	42.3	lahar		
X778-7	about 49.6	quartz vein		
X778-8	about 53.8	quartz vein		
X778-9	about 56.4	"		
X778-10	93.6	andesite		
X778-11	108.4	"		
X778-12	about 132.0	quartz vein		
X778-13	133.5	"		
X778-14	about 134.47	"		
X778-15	141.8	andesite		
X778-16	147.76	trachyte		
X778-17	151.49	"		
X778-18	about 172.8	"		
X49-1	33.9	siltstone	DDH72449	500E
X49-2	38.4	lahar		
X49-3	41.8	conglomerate containing sulfide		
X49-4	208.75	quartz vein		
X49-5	about 213.88	quartz vein		
X49-6	about 225.25	"		
X49-7	about 226.44	"		
X49-8	about 240.1	"		
X49-9	about 253.8	"		
X49-10	about 265.2	"		
X49-11	about 263.85	"		
X49-12	about 269.6	"		
X49-13	269.8	"		

```
X49-14            275.54    lahar
X49-15    about 288.66    quartz vein
X49-16    about 290.1     lahar
X49-17    about 295.5     quartz vein
X49-18    about 305.2        "
X49-19          312.04        "
X49-20          318.9         "
X49-21    about 319.7         "
X49-22    about 326.31        "
X49-23          333.9         "
X49-24    about 339.55        "
X49-25    about 340.56        "
X49-26    about 344.8         "
X49-27    about 343.54        "
X49-28    about 352.0     lahar
X49-29    about 373.8     lahar
X49-30    about 404.6        "
X49-31    about 411.75    quartz vein
X49-32    about 412.9     trachyte
X49-33          445.16        "


X83-1           394.39    trachyte            DDH82783    800E
X83-2           417.18    quartz vein
X83-3           420.43    trachyte
X83-4           426.05        "
X83-5     about 427.05    dike
X83-6     about 432.05    dike
X83-7           437.97    trachyte
X83-8     about 444.3         "


X68-1     about 470.38    trachyte            DDH72468    950E
X68-2           469.49        "
X68-3     about 463.49        "
X68-4     about 450.55        "
X68-5           436.36    ultramafic
X68-6     about 435.15    lahar containing quartz vein
X68-7           431.42    quartz vein
X68-8           421.86        "
X68-9           415.14        "
X68-11          396.15    lahar
X68-12          386.54    dacite containing sulfide veinlet


X50-1             9.77    trachyte            DDH72450    200E
X50-2            11.79        "
X50-3            18.37        "
X50-4            31.2     quartz vein
X50-5           113.13    trachyte
X50-6           117.9     lahar
X50-7           123.95    lahar
X50-8           140.51    breccia
X50-9           143.67    quartz vein
```

```
X50-10        about 150.9    lahar containing calcite vein
X50-11              161.37   quartz vein
X50-12              164.0    andesite containing quartz veinlet
X50-13              221.21   felsite containing disseminated sulfide
X50-14              248.95   mudstone
X50-15              325.5    lahar
X50-16              349.0      "
X50-17              370.97   sandstone
X50-18              378.5    trachyte containing quartz veinlet


X34-1               637.5    andesite                 DDH72434   800E
X34-2               619.94   lahar
X34-3               609.18   andesite
X34-4               597.36   andesite
X34-5               562.82     "
X34-6        about 534.11    quartz vein
X34-7               502.64   trachyte
X34-8               490.18     "
X34-9               485.34     "
X34-10              482.63   quartz vein
X34-11              477.92     "
X34-12              460.49   felsite
X34-13              456.00   quartz vein
X34-14              435.46   lahar
X34-15              431.7    quartz vein
X34-16              430.77   lahar
X34-17              420.73   lahar
X34-18              411.85   lahar
X34-19              404.95     "
X34-20              388.62   felsite
X34-21              370.95   quartz vein
X34-22              353.04   lahar
X34-23              345.8    quartz vein
X34-24              343.9    trachyte
X34-25              332.4      "
```
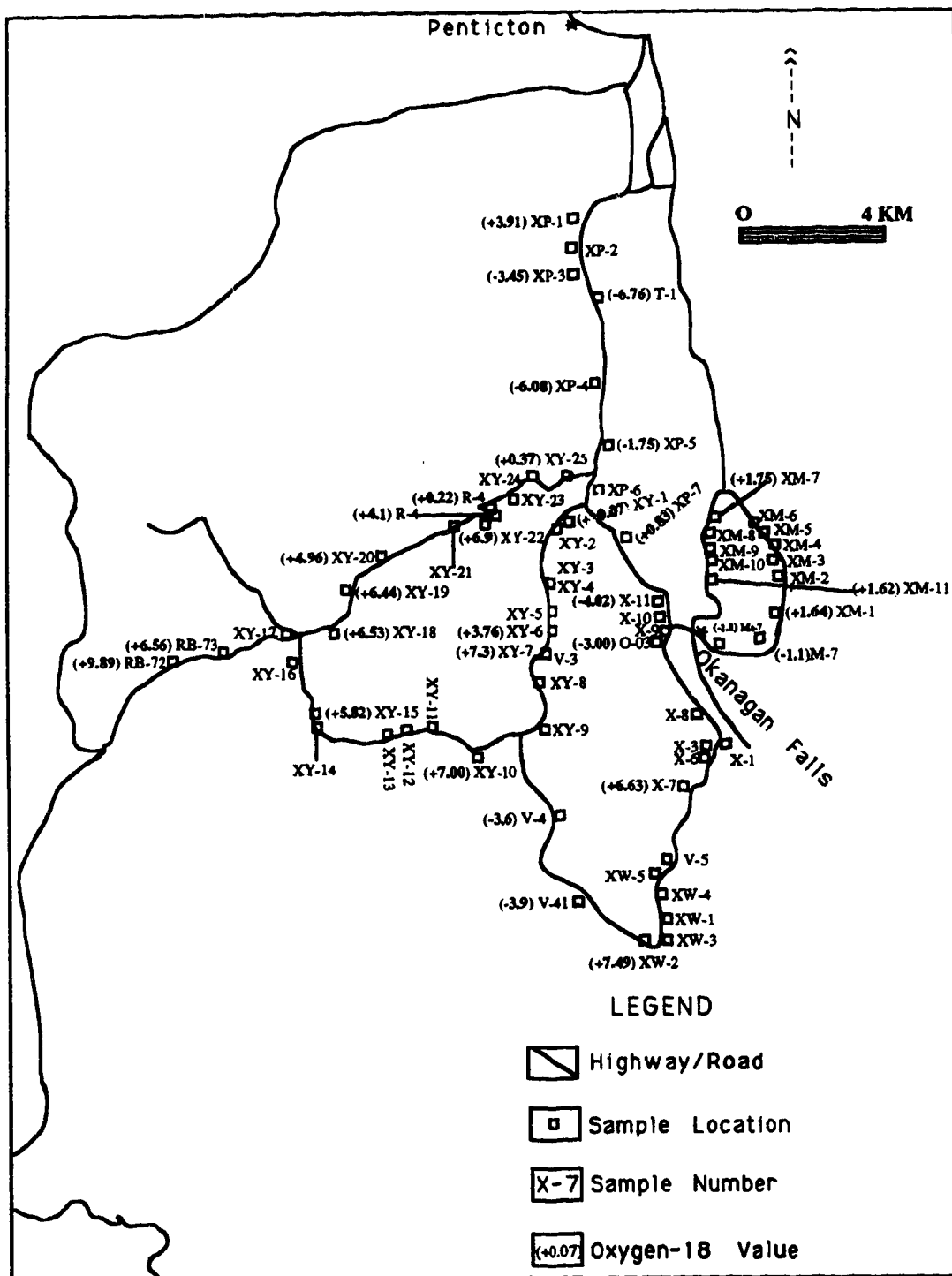
Appendix II. Whole Rock and Carbonate Sample Locations and Oxygen-18 Value for Whole Rock Samples in the Okanagan Falls Area.